

BUCKLING ANALYSIS OF STARRED ROLL
DEFECTS IN CENTER WOUND ROLLS

By

BANG-EOP LEE

Bachelor of Science in Engineering
Seoul National University
Seoul, Korea
1980

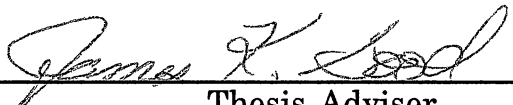
Master of Science in Engineering
Seoul National University
Seoul, Korea
1982

Submitted to the Faculty of the
Graduate College of the
Oklahoma State University
in partial fulfillment of
the requirements for
the Degree of
DOCTOR OF PHILOSOPHY
May, 1991

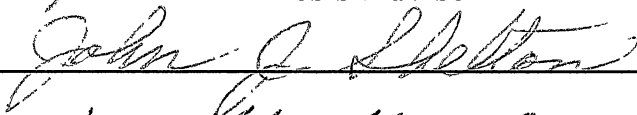
Thesis
1991D
L4776
cop. 2

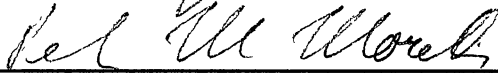
BUCKLING ANALYSIS OF STARRED ROLL
DEFECTS IN CENTER WOUND ROLLS

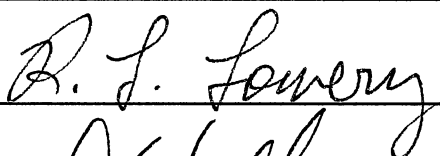
Thesis Approved:

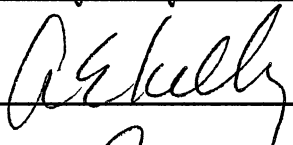



Thesis Adviser











Dean of the Graduate College

ACKNOWLEDGEMENTS

The author thanks God for His invaluable guidance and encouragement during the research period. He also expresses his deepest appreciation to his advisor, Dr. James K. Good. His guidance and patience throughout this research have been invaluable. The helpful advice of the other committee members, Dr. Richard L. Lowery, Dr. John J. Shelton, Dr. Allen E. Kelly, and Dr. Peter M. Moretti, are also gratefully appreciated.

The author greatly appreciated the School of Mechanical and Aerospace Engineering and the Web Handling Research Center for the financial support during the study.

Special gratitude is expressed to the author's parents, Seong-II Lee and Jee-Ja Kim; his loving wife, Jeong-Hee Hong; proud son, Ju-Won; and pretty daughter, Yu-Mee. Their countless sacrifices and prayers have helped him tremendously.

TABLE OF CONTENTS

Chapter	Page
I. INTRODUCTION	1
Objectives and Scope of Study	2
Major Results	4
Chapter Description	5
II. LITERATURE SURVEY	6
Wound Roll Stress and Roll Quality	6
Foundation Models	9
Elastic Stability	11
III. BUCKLING ANALYSIS OF STACKS OF PAPER	13
Finite Element Analysis	13
Introduction	13
Equivalent Thickness of A Beam	19
Radial Modulus of Elasticity	
of Reproduction Paper	20
Pfeiffer's Method	20
Polynomial Curve Fitting Method	21
Equivalent Spring Constant	22
Equivalent Modulus of Foundation	22
Classic Buckling Mode and Load	23
Finite Element Model	26
Element Types	26
Elastic Beam Element (STIF3)	26
Interface Element (STIF12)	27
Isoparametric Solid Element (STIF42) ..	28
Boundary Conditions	29
Mesh Generation	29
Nonlinear Buckling Analysis	31
Calculating Procedure	31
Pre- and Post- Processing Programs	32
Results of Finite Element Analysis	34
Stack Pressure of 1.16 psi	34
Higher Stack Pressures	39
Comparison to Classic Solutions	41

Chapter	Page
Comparison to Experimental Results.	41
Experimental Analysis	42
Radial Modulus of Reproduction Paper	42
Pfeiffer's Method	45
Polynomial Curve Fitting Method	49
Comparison of two Methods.	49
Buckling Experiments	50
Apparatus	50
Stack Pressure.	52
Experimental Procedure.	53
Results of Experimental Analysis	53
IV. BUCKLING ANALYSIS OF CENTER WOUND ROLLS	67
Finite Element Analysis	67
Introduction	67
Stress Distribution in a Center Wound Roll	67
Core stiffness	67
Hakiel's Nonlinear Winding Model	68
Winding Conditions	69
Programs for Hakiel's Model	77
Finite Element Model	77
Representation of Radial Pressure	77
Equivalent Modulus of Foundation	80
Results of Finite Element Analysis	82
Parametric Study of Calculating Conditions	82
Perturbing Load	82
Convergent Bound.	85
Parametric Study of Beam	
Geometry and Location	87
Beam Location.	87
Beam Length.	90
Beam Length with Same Effective Length	90
Beam Thickness	93
Results of Parametric Study	93
Stepped Tension Windings	95
Failure Criterion for Starred Roll Defect	102
Constant Tension Windings	105
Experimental Analysis	108
Radial Modulus of Polyester Film	108
Experimental Procedure	114
Results of Experimental Analysis	114
Stepped Tension Windings	114
Constant Tension Windings	116

Chapter	Page
V. SUMMARY AND RECOMMENDATIONS	121
Summary	121
Recommendations	123
REFERENCES	124
APPENDIX A - BUCKLING OF A BEAM UPON AN ELASTIC FOUNDATION	128
APPENDIX B - HAKIEL'S NONLINEAR WINDING MODEL	132
APPENDIX C - PROGRAMS FOR HAKIEL'S WINDING MODEL AND CLASSIC SOLUTION	137
APPENDIX D - PROGRAMS FOR NONLINEAR BUCKLING ANALYSIS	148
APPENDIX E - PROGRAM FOR PFEIFFER'S K_1 AND K_2	161

LIST OF TABLES

Table	Page
I. Material Properties of Experimental Materials	18
II. Dimension of Experimental Materials	18
III. Material Properties and Classic Solutions of Stack Tests for Each Stack Pressure	25
IV. Buckling Mode Determination of Stack Tests for Each Stack Pressure	37
V. Buckling Loads and Modes of Stack Tests for Each Stack Pressure	39
VI. Winding Conditions at 3M Splicer Winder Core I.D.=3.035", O.D.=3.445", Winding Speed=30 fpm	70
VII. Buckling Modes and Stresses for Center Wound Rolls	99
VIII. Comparison of Buckling Stresses and Circumferential Stresses for Center Windings	103
IX. Radial Modulus of Polyester Film as a Function of Pressure (Type 377/Grade 92)	113

LIST OF FIGURES

Figure	Page
1. Circumferential Stress Distribution of a Center Wound Roll . . .	14
2. Simplified Model of a Center Wound Roll	15
3. Finite Element Mesh of Simplified Model	16
4. Detailed Mesh around Beam Elements	17
5. Two Dimensional Elastic Beam Element(STIF3)	26
6. Two Dimensional Interface Element(STIF12)	27
7. Two Dimensional Isoparametric Element (STIF42).	28
8. X-directional Mesh Generation by Geometric Progression	30
9. Flow Chart of Nonlinear Buckling Analysis	33
10. Lateral Displacements according to Beam Status Stack Pressure = 1.16 psi, Buckling Mode = 8	35
11. Lateral Displacements under Axial Loads Stack Pressure = 1.40 psi, Buckling Mode = 8	36
12. Buckling Mode Determination by Finite Element Analysis of Stack Tests	38
13. Buckling Loads of Stack of Reproduction Paper for Different Stack Pressures	40
14. Apparatus for Radial Modulus Measurement	43
15. Load vs Displacement Curve for Radial Modulus Measurement of Stack of Reproduction Paper	44
16. Pressure vs Strain Curve for Radial Modulus Measurement of Stack of Reproduction Paper	46

Figure	Page
17. Determination of Constants k_1 and k_2 in Pfeiffer's Expression	47
18. Radial Modulus of Reproduction Paper	48
19. Apparatus for Buckling Test of Stacks of Paper	51
20. Calibration of Ram Pressure by Load Cell	52
21. Load vs Displacement Curve of Buckling Experiment (Loaded up to Fully Buckled State)	54
22. Beam Status in Buckling Experiment	55
23. Buckling Load Determination by the Slope Change (Loaded up to Slightly Buckled State)	56
24. Effect of Loading Rate on the Buckling Load of Buckling Experiments	58
25. Buckling Loads for Stack Pressure of 1.16 psi	60
26. Buckling Loads for Stack Pressure of 1.40 psi	61
27. Buckling Loads for Stack Pressure of 1.63 psi	62
28. Buckling Loads for Stack Pressure of 1.86 psi	63
29. Buckling Loads for Stack Pressure of 2.10 psi	64
30. Buckling Loads for Stack Pressure of 2.33 psi	65
31. Buckling Loads with Standard Deviation at Stack Pressures from 1.16 to 2.33 psi	66
32. History of Constant Winding Tensions	71
33. Radial Pressure Distribution at Constant Tension Windings ...	72
34. Circumferential Stress Distribution at Constant Tension Windings	73
35. History of Stepped Winding Tensions	74
36. Radial Pressure Distribution at Stepped Tension Windings	75

Figure	Page
37. Circumferential Stress Distribution at Stepped Tension Winding Polyester Film (Type 377/Grade 92)	76
38. Flow Chart of Programs for Hakiel's Model	78
39. Representation of Radial Pressure in Finite Element Model ...	79
40. Equivalent Spring Constant of Foundation	81
41. Lateral Displacements for Different Perturbing Loads	83
42. Effect of Perturbing Load on the Buckling Mode and Stress	84
43. Effect of Convergent Bound on the Buckling Mode and Stress.	86
44. Beam Locations in a Wound Roll	88
45. Effect of Beam Location on the Buckling Mode and Stress	89
46. Effect of Beam Length on the Buckling Mode and Stress	91
47. Buckling Modes and Stresses for Different Beam Length with Same Effective Length	92
48. Effect of Beam Thickness on the Buckling Mode and Stress	94
49. Determination of Beam Thickness from Circumferential Stress Distribution	96
50. Determination of Beam Thickness by Comparing Buckling Stress to Circumferential Stress	97
51. Classic, Numerical and Experimental Buckling Modes at Stepped Tension Windings	100
52. Classic and Numerical Buckling Stresses at Constant Tension Windings	101
53. Margin of Safety for Starred Roll Defect at Stepped Tension Windings	104
54. Classic and Numerical Buckling Modes at Constant Tension Windings	106
55. Margin of Safety for Starred Roll Defect at Constant Tension Windings	107

Figure	Page
56. Layout of 3-M Splicer Winder	109
57. Pressure vs Strain Curve of Polyester Film (Type 377/ Grade 92)	111
58. Radial Modulus of Polyester Film (Type 377/ Grade 92)	112
59. Starred Roll Defect at Stepped Tension Winding	117
60. Buckling Modes at Stepped Tension Windings (200 to 500 psi)	118
61. Buckling Modes at Stepped Tension Windings (300 to 500 psi)	119
62. Buckling Modes at Stepped Tension Windings with Standard Deviations	120
63. A Beam with Axial Load upon Elastic Foundation	128
64. Free Body Diagram of a Segment of a Ring	132

NOMENCLATURE

A	Area of the beam contacted to the foundation
A _i	Constant in Hakiel's algebraic equations
a ₁	Thickness of the inner foundation
a ₂	Thickness of the outer foundation
B _i	Constant in Hakiel's algebraic equations
C	Constant to calculate the classical buckling mode
C _i	Constant in Hakiel's algebraic equations
C _n	Coefficients of polynomial function of strain
C _n '	Coefficients of polynomial function of radial modulus
E	Young's modulus for isotropic material
E _c	Core Stiffness
E _{cm}	Young's modulus of core material
E _t	Tangential Young's modulus of a wound roll
E _r	Radial Young's modulus of a wound roll
F	Axial force
F _{cr}	Buckling load
F _{crm}	Modified classic buckling load
g ²	Ratio of moduli of wound roll (E _t /E _r)
h	Thickness of a stack
I ₁	Moment of inertia of one layer
I _{eq}	Equivalent moment of inertia of a beam
I _n	Moment of inertia of n layers

k_1	Constant in Pfeiffer's equation
k_2	Springiness factor in Pfeiffer's equation
k_g	Shear parameter of Pasternak's foundation model
k_θ	Moment parameter of the generalized foundation model
k_s	Second parameter of two parameter foundation model
k_t	Second parameter of Vlasov foundation model
L	Length of a beam
m	Buckling mode
n	Number of layers or dummy index
n_a	Number of division of the foundation in x-direction
P	Potential energy of a beam
$p(x)$	Reaction pressure from the foundation on the beam
P_i	Radial pressure at any point of a wound roll
P_o	Radial pressure at the outside of a core
P_r	Radial pressure
$q(x)$	Intensity of a distributed load
r	Radius or a multiplying factor
r_c	Inner radius of a core
r_i	Radius at any point of a wound roll
r_o	Outside radius of a core
s	Dimensionless outside diameter of a wound roll
t	Caliper of web material
T	Tension applied to the top of an elastic foundation
T_w	Winding Tension
u	x-directional displacement
u_n	x-directional displacement at node n
u_x	Lateral displacement of foundation

v	y-directional displacement
v_n	y-directional displacement at node n
w	Radial displacement
W	Width of a stack or wound roll
x	x coordinate
x_{in}	Smallest mesh size in x-direction of the solid element
y	y coordinate
α	Spring constant
β	Modulus of the foundation
δ	Lateral displacement
δP	Incremental radial pressure
δT	Incremental circumferential stress
ϵ_r	Radial strain
ϵ_t	Tangential strain
η	Normalized local coordinate
η_n	Normalized local coordinate at node n
μ	Friction coefficient
ν	Poisson's ratio
ν_c	Poisson's ratio of the core
θ	Rotational degree of freedom
σ_{cr}	Buckling stress
σ_r	Radial stress
σ_t	Circumferential stress
ω_z	Rotational angle about z-axis
ξ	Normalized local coordinate
ξ_n	Normalized local coordinate at node n

CHAPTER I

INTRODUCTION

Thin flat flexible materials such as film, foil, paper, sheet metal and textile are defined as webs. Webs are wound upon a core as a roll because the roll is a convenient form to handle, store, and to use in subsequent web processing. The core is made of fiber, plastic or steel. The winding methods may be center winding, surface winding or a combination of both.

The stress distribution in a wound roll depends upon the winding conditions and material properties. The stress in the radial direction is called the radial or interlayer pressure. The stress in the circumferential direction is called the circumferential or tangential stress. Extreme radial pressure and/or circumferential stress may cause various roll defects. Gilmore [14] collected various roll defects and defined a roll defect terminology. The roll defects concerning the radial pressure are dishing, telescoping, offset, loose core, core slippage, etc. The roll defects due to the circumferential stress are crushed core and starred roll defect. Among the roll defects, the starred roll defect, which is also called starring, is a starred pattern of a wound roll due to the buckling of the web layers.

Numerous sources [1, 7, 8, 9, 14, 20, 21, 26, 34, 35, 39, 40, 47] have reported that the circumferential stress can be negative and may cause the starred roll defect, but none had tried to calculate the buckling stress quantitatively rather than qualitatively. The buckling stress is a function of

radial pressure distribution, core stiffness, friction coefficient between the webs and material properties of the web.

Objectives and Scope of Study

The objectives of this research are:

- To develop a numerical model that can predict the buckling stress of a center wound roll.
- To set up a failure criterion of a starred roll defect.

The buckling analysis is based on the stress distribution in a wound roll. There has been a variety of research concerned with theoretical and experimental stress distributions for three decades. The winding models to date are a linear isotropic model [5], an anisotropic model [1, 31, 47] with constant radial modulus and an anisotropic nonlinear modulus model [17]. Hakiel's nonlinear model [17] is the most recently developed model. This model implemented the nonlinear radial modulus of the wound roll and included a core boundary condition.

The friction force between webs increases the buckling load of web layers, which decreases the chance of starred roll defect. The numerical models employed in this research implemented Hakiel's nonlinear model and the slippage between webs. The typical stress distribution of a center wound roll wound at constant tension exhibits a wide plateau region of radial pressure and circumferential stress. The circumferential stress is negative in the plateau region and the value depends upon the winding tension. Excessive negative circumferential stress may cause the roll to buckle. The radial stiffness of the roll tends to protect the roll from buckling and so does the friction force between the webs.

A part of a series of webs in compressive circumferential stress region was modeled as an elastic beam which has the equivalent moment of inertia as the selected webs. The surrounding wound webs were modeled as elastic foundations which act as linear springs in the radial direction. Interface elements were used between the beam and the foundations to model the slippage between the webs.

The classic solutions of the buckling problem of a beam upon elastic foundation was calculated by energy method with Winkler's foundation model [42]. Both numerical and experimental analyses were performed. For the numerical buckling analysis, the geometric nonlinear static analysis was employed using the ANSYS program [2] installed in the HARRIS 800 computer and IBM-"RT" computer. ANSYS is a general purpose structural analysis program which is based on the finite element method.

The problem of a buckling analysis of a center wound roll was studied with two simplified models. The first model assumed the radial pressure and modulus as constant throughout the roll. The second implemented variable radial pressure and corresponding modulus to represent the wound roll more accurately.

The radial modulus was obtained as a function of pressure by several stack tests using a servo-hydraulic material testing machine [22, 27]. The friction coefficient between the webs were measured using the ASTM standard [3].

The validity of the first constant modulus model was established by a number of buckling experiments with stacks of reproduction paper using the material testing machine. Several rolls were center wound using the 3M Splicer Winder in the Web Handling Research Center (WHRC) at

Oklahoma State University (OSU). Starred roll defects were generated by rotating the wound rolls upon a flat surface while pressing them down.

Major Results

A numerical model was developed which can predict the buckling stress of a center wound roll. A margin of safety of a starred roll defect was defined as an indicator of the starring of a wound roll.

The numerical buckling loads for the buckling experiments of stacks of reproduction paper were at the lower limits of the experimental values including one standard deviation. The buckling modes of the numerical and experimental analyses were almost the same for the different stack pressures tested. The conclusion was drawn that the finite element model can be used to predict the initial buckling stress of stacks of reproduction paper.

The numerical buckling modes for stepped tension windings showed reasonable agreement to that of winding experiments. The numerical values were within one standard deviation of the experimental values.

The classic buckling load was modified by adding the friction force between the beam and the foundation due to the radial pressure and the friction coefficient between webs. The friction involved classic buckling loads were smaller than that of the finite element analyses, but not more than 25 % for all the cases. The finite element analysis for one winding condition required tens of hours of computing time using the IBM-"RT" computer, but a few minutes were enough to calculate the classic solutions. Considering the computing time, the classic solution may be a useful tool to

roughly predict the numerical solutions and the starred roll defect for a given winding condition.

A margin of safety of a starred roll defect was defined as the difference of the maximum compressive circumferential stress from the buckling stress in absolute value divided by the maximum compressive circumferential stress or buckling stress. If the margin of safety is positive, the denominator will be the maximum circumferential stress. If the margin of safety is negative, the denominator will be the buckling stress. The larger the margin of safety is, the safer the roll is from starring. If it is around zero, the roll may be buckled by a small perturbing load. When it is negative, the larger the absolute value is, the more easily the starred roll defect may occur.

Chapter Description

In Chapter II, a literature survey is presented which covers winding models, roll quality, foundation models, and elastic stability .

In Chapter III, the buckling analyses of stacks of paper are presented. The finite element analyses for the nonlinear buckling problems and the buckling experiments of stacks of paper using material testing machine are described.

In Chapter IV, the buckling analyses of center wound rolls are presented. The finite element analyses and the winding experiments using 3M Splicer Winder are described.

In Chapter V, a summary of the conclusions which can be drawn from the classic, numerical and experimental results and suggests future research.

CHAPTER II

LITERATURE SURVEY

Wound Roll Stress and Roll Quality

Wound roll stress analysis has been a very important topic for web handling industries, as roll quality is dependent on the stress distribution in a wound roll. The winding models to date have been formulated based on the following assumptions:

1. Rolls are wound on a center winder,
2. Rolls are homogeneous, linear or nonlinear elastic solids,
3. Web caliper is constant through the winding,
4. The body force of the roll is ignored,
5. The air entrainment during winding is ignored,
6. The web is a perfect annulus,
7. There is no slippage between the web layers.

In 1966, Pfeiffer, J.D. [31] described a method for calculating the internal pressure distribution in a roll of paper by measuring sound wave velocity. The radial pressure was suggested as an exponential function of strain and the radial modulus was derived as a linear function of radial pressure. The original pressure function was shown in Equation (2.1). In 1968, the pressure function was updated to enforce the pressure to be zero at zero strain as shown in Equation (2.2). [32] The modulus function was

derived by differentiating the pressure with respect to strain as shown in Equation (2.3).

$$P_r = k_1 \exp(k_2 \epsilon_r) \quad (2.1)$$

$$P_r = -k_1 + k_1 \exp(k_2 \epsilon_r) \quad (2.2)$$

$$E_r = \frac{dP_r}{d\epsilon_r} = k_1 k_2 + k_2 P_r \quad (2.3)$$

In 1967, Frye, K.G. [12] reported controllable winding variables by the machine and the operator, and all their effects on roll quality and roll hardness. Roll structure can be controlled by unwind, nip pressure, rider roll, core shaft, drive-torque, and web tension.

Daly, D.A. [7] divided roll defects into five categories and discussed them in detail. These categories are operational, web control, nonuniform nip, roll structure, and specific roll defects.

In 1968, Altman, H.C. [1] assumed the roll as a linear orthotropic thick wall cylinder, i.e., the radial modulus is constant but different from the tangential modulus. Closed formula for radial pressure and circumferential stress were derived as a function of winding tension, radius ratio of any point to the outside radius, and some elastic parameters of the roll.

Hussain, S.M. [21] et al. measured the circumferential stress within a roll of paper by splicing a specially made strain gauge directly into the webs of paper. In 1977 [20], an instrumented steel core was developed to measure the accurate pressures at the core surface.

In 1973, Ericksson, L.G. and Rand, T. [9] analyzed the stresses in large newsprint rolls during winding. The circumferential stress was measured using a strain gage glued to the web. The interlayer pressure

was calculated by drilling the roll to the core radially and measuring the difference of the hole size before and after winding. Paper roll density was calculated by measuring the paper thickness variations in a later paper [8].

In 1975, Monk, D.W. [26] et al. calculated the internal stresses within rolls of cellophane by integrating the relations given by Altmann. Various factors that caused the roll defects were studied. It was found that a roll at a constant tension winding had the most negative circumferential stress which usually caused the starring. It was also found that a roll wound at a constant torque had the least negative circumferential stresses. ✓

In 1979, Pfeiffer [34] applied an energy balanced principle to calculate the roll stresses. The tensile strain energy given by the wound-in tension provided the compressive energy of the layers underneath. The pressure and modulus functions obtained by the compression tests of stack of roll materials were used to derive the stresses.

In 1980, Yagoda, H.P. [47] developed an accurate series solutions and clarified the stress behavior near the core. An explicit analytic solution was derived using hypergeometric functions for the radial and circumferential stresses. It was emphasized that the stresses near the core should be considered to design an appropriate core.

In 1987, Hakiel, Z. [17] implemented a finite difference method to solve the nonlinear second order differential equations based on the nonlinear material property in radial direction and an accurate core boundary condition. This nonlinear model is the most recently developed model.

Pfeiffer, J.D. [36] updated his winding model by changing the expression of the slope term in the equilibrium equation.

Roisum, D.R. [39] summarized the stress history of paper stresses: before, during and after winding. In 1988, the measurement methods of the

roll quality were summarized and the statistics were emphasized to analyze the data correctly. [40]

In 1988, Willett, M.S. and Poesch, W.L. [44] calculated the stress distributions in wound reels of magnetic tape using a nonlinear finite difference approach. The governing equation included the thermal expansion term. A procedure to measure the Poisson's ratio in the radial direction using laser beam was presented.

In 1990, Roisum, D.R. [41] reviewed all the winding models to date and developed a new boundary condition at the outside of the roll by measuring the radial displacement during winding.

Fikes, M. [10] measured the radial pressures of center wound rolls by FSR films. It was showed that FSR film can be a good tool to measure the radial pressure after winding.

Foundation Models

In 1867, Winkler [45] assumed the foundation as closely spaced elastic supports. The reaction force of the foundation is directly proportional to the beam deflection. The deflections and stresses of a beam upon elastic supports were calculated. The force vs deflection relation is shown in Equation (2.4) and the governing equation is shown in Equation (2.5).

$$p(x) = k w(x) \quad (2.4)$$

$$EI \frac{d^2w(x)}{dx^2} + k w(x) = q(x) \quad (2.5)$$

In 1945, Hetenyi [18] derived the deflections, stresses and buckling loads of beams upon elastic foundations with various boundary conditions.

The modulus of the foundation was defined as the spring constant for unit length of the beam.

In 1964, Kerr, A.D. [24] reviewed various elastic and visco-elastic foundation models. The presented models were Pasternak's model [29], Filonenko-Borodich's model [11], Hetenyi's model [18, 19], Ressner's model [37] and a generalized foundation model [13].

In 1983, Zhaohua, F. and Cook, R.D. [48] divided the foundation models into one and two parameter models. The first parameter represents the linear response of the foundation on the beam. The second parameter has several different physical meanings depending upon the assumption a model has made on the second order differential term.

Filonenko-Borodich's model [11] assumed that top ends of the springs were connected to an elastic membrane that was stretched by a constant tension T .

$$p(x) = k w(x) - T \frac{d^2 w(x)}{dx^2} \quad (2.6)$$

Pasternak's model [29] considered the shear interactions between the springs.

$$p(x) = k w(x) - k_g \frac{d^2 w(x)}{dx^2} \quad (2.7)$$

The generalized foundation [13] includes the moments at each points of contact.

$$p(x) = k w(x) - k_g \frac{d^2 w(x)}{dx^2} \quad (2.8)$$

Vlasov's model [23, 43] regarded the foundation as a semi-infinite elastic medium.

$$p(x) = k w(x) - k_t \frac{d^2 w(x)}{dx^2} \quad (2.9)$$

All these two parameter models are mathematically the same if the constants of the second order terms were substituted by k_s . The force vs deflection relation and the governing differential equation for these models are shown in Equations (2.10) and (2.11).

$$p(x) = k w(x) - k_s \frac{d^2 w(x)}{dx^2} \quad (2.10)$$

$$EI \frac{d^2 w(x)}{dx^2} - k_s \frac{d^2 w(x)}{dx^2} + k w(x) = q(x) \quad (2.11)$$

Neglecting the second term in Equation (2.11) gives the governing equation of Winkler's foundation in Equation (2.5). Because the constants in the second parameter were unknown and very difficult to calculate, the Winkler's foundation model was used to calculate the classic solutions in this research.

Elastic Stability

In 1961, Timoshenko [42] wrote a representative reference for buckling analysis. It includes various theoretical solutions of elastic or inelastic buckling problems of bars, frames, beams, rings, arches, curved bars, plates, shells, etc. It also describes the energy method to solve the buckling problem of a beam upon Winkler's foundation. The classic solution of this research referred this energy method.

Because the buckling problem of a wound roll includes the interlayer friction and the radial pressure, it is not a linear buckling or eigenvalue problem but a nonlinear buckling problem.

In 1977, Zienkiewicz [49] discussed the geometric nonlinear problems in detail. It was mentioned that the nonlinear buckling problem should be solved by considering it as a geometric nonlinear static problem.

The analytic methods of geometric nonlinear structural problems can be divided into two classes: One class is incremental and does not necessarily satisfy the equilibrium conditions. The other class is self-correcting and satisfies the equilibrium conditions.

The first class includes the incremental stiffness procedure [25, 28] and the Newton-Raphson methods [28]. The incremental procedure is easy to apply but is not accurate. A very fine load step should be used to get an accurate solution.

The second class includes the iteration method combined with the systematic relaxation [30], the perturbation method [6], the self-correction incremental forms [15], the incremental procedure combined with Newton-Raphson iteration [46], the initial value formulation [6, 30], and the self-correcting initial value formulation [16].

The ANSYS program [2] is a general purpose structural analysis program based on the finite element method. It can solve linear and nonlinear buckling problems: The linear buckling problems use the eigenvalue technique and the nonlinear buckling problems use the geometric nonlinear static analysis by the large deflection option. It also has interface elements to model the slippages between materials. To perform the geometric nonlinear static analyses using the ANSYS program, the full Newton-Raphson option was used, which updates the stiffness matrix every iteration.

CHAPTER III

BUCKLING ANALYSIS OF STACKS OF PAPER

Finite Element Analysis

Introduction

Several assumptions were made for the finite element model as follows:

1. One quarter of the circumference of the roll was modeled in rectangular coordinates rather than polar coordinates,
2. The plane stress condition was assumed,
3. Stresses from Hakiel's model are accurate,
4. An element has constant radial pressure and modulus,
5. Gaps exist only between the beam and the foundations,
6. Core deformations were neglected,
7. Poisson's ratio of the web material was assumed as zero.

Figure 1 shows a wide range of compressive circumferential stress distribution in a center wound roll. A part of the compressive stress region was modeled as two dimensional elastic beam elements with an equivalent moment of inertia as the selected webs as shown in Figure 2. The surrounding materials were modeled as two dimensional isoparametric solid elements. Because a steel core was used throughout the experiments the core was modeled as rigid support as shown in Figure 3. The gaps

between the beam and the foundation were modeled as two dimensional interface elements that act like linear springs when compressed and have no rigidity when stretched as shown in Figure 4. The material properties and dimensions were shown in Tables I and II.

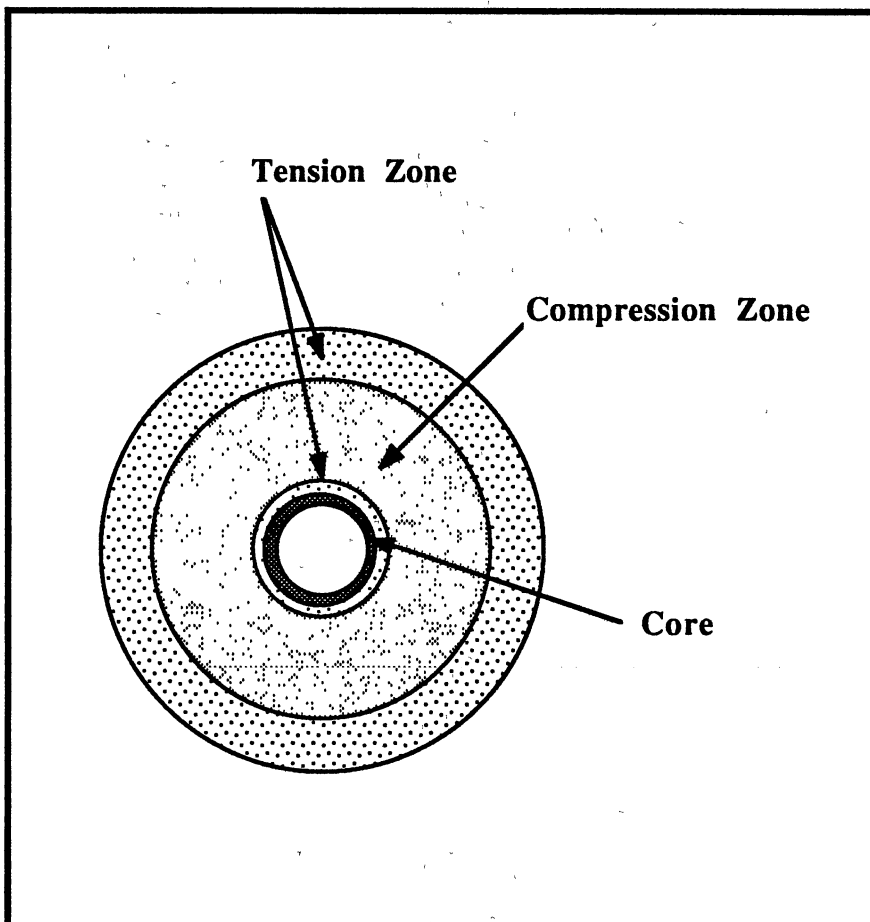


Figure 1. Circumferential Stress Distribution of a Center Wound Roll

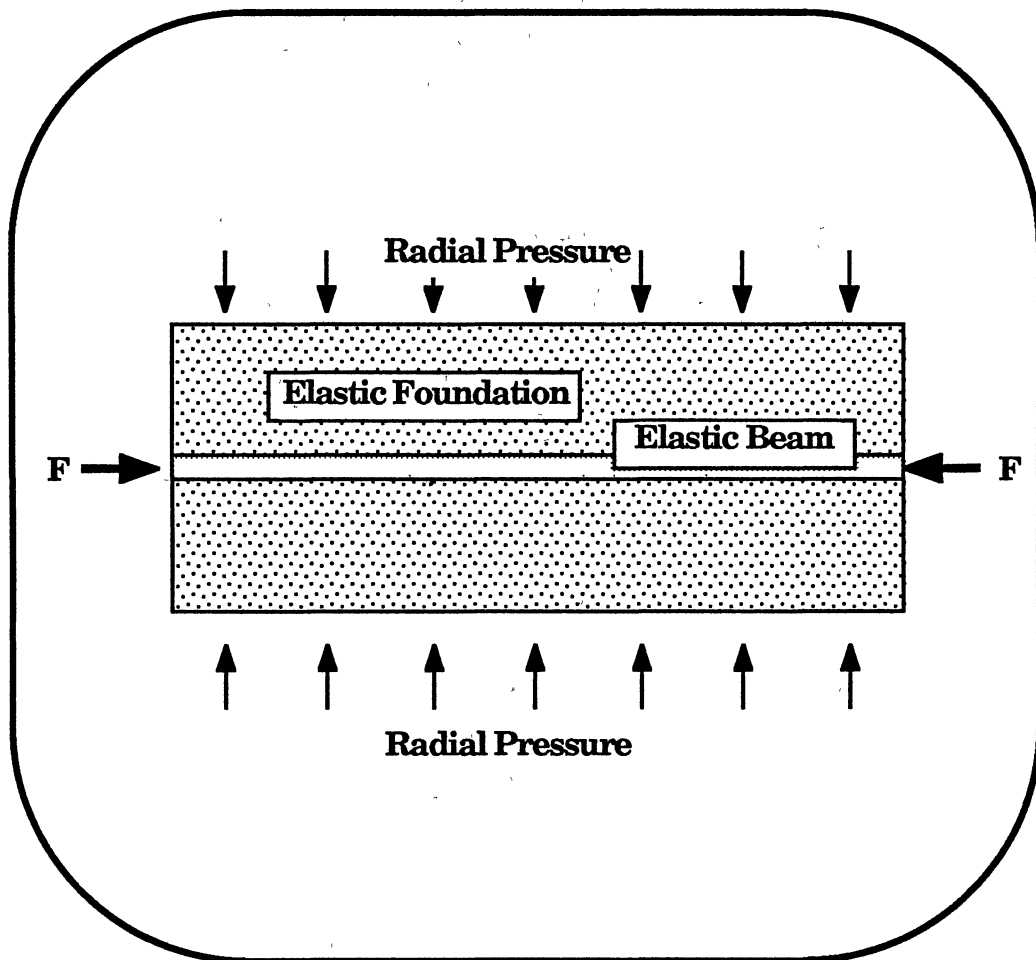


Figure 2. Simplified Model of a Center Wound Roll

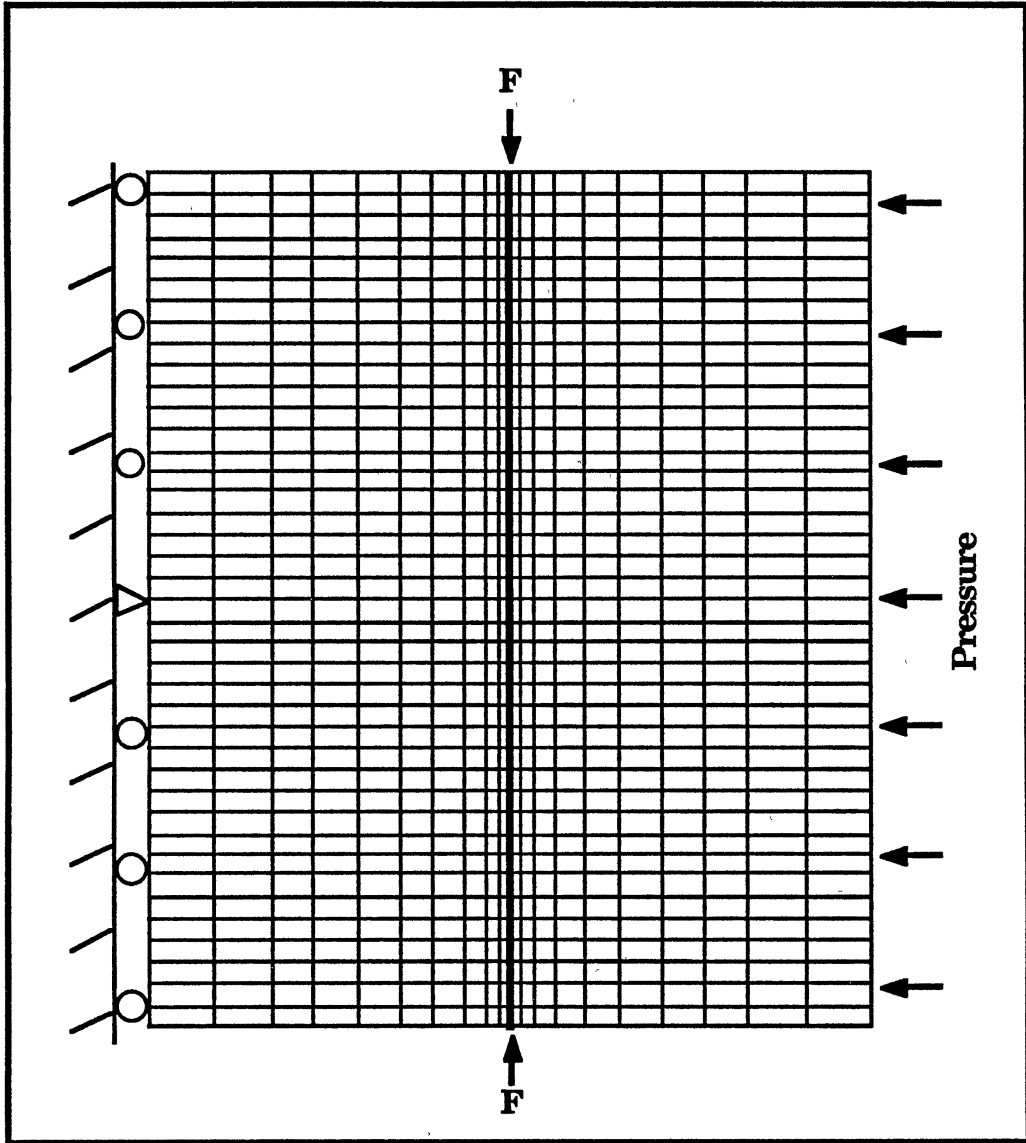


Figure 3. Finite Element Mesh of Simplified Model

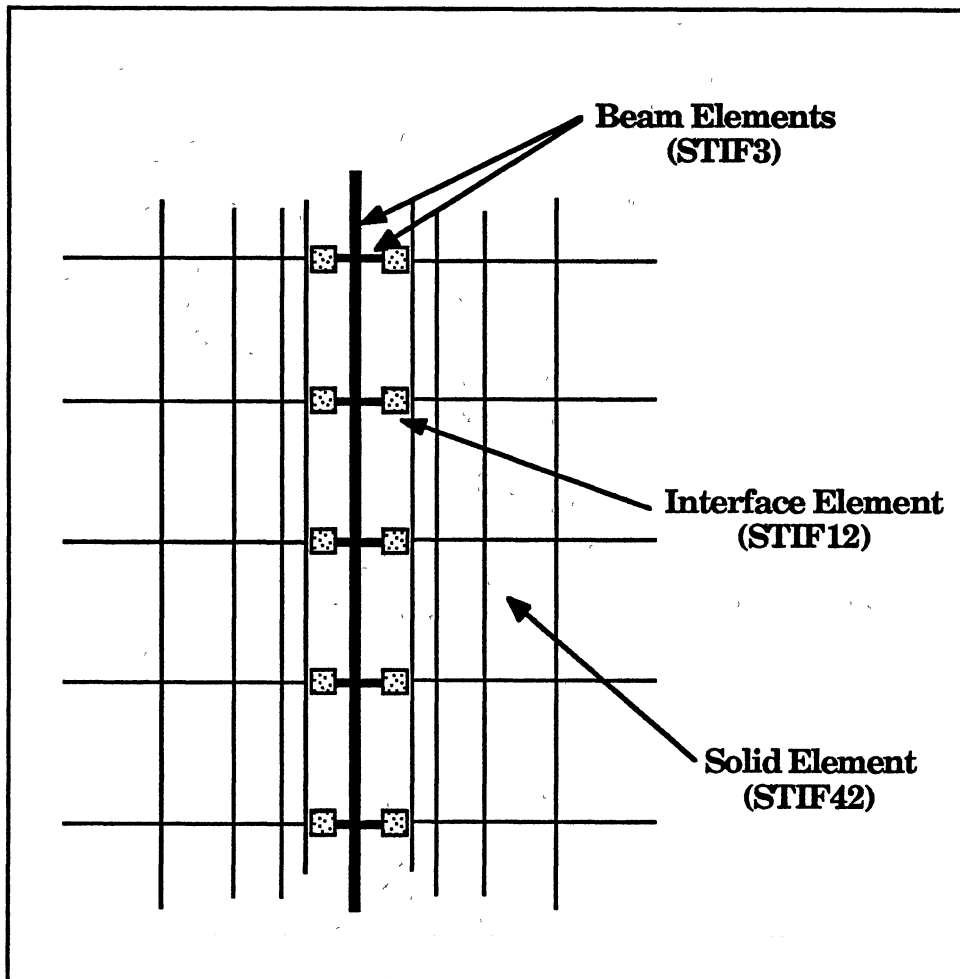


Figure 4. Detailed Mesh around Beam Elements

TABLE I
MATERIAL PROPERTIES OF EXPERIMENTAL MATERIALS

Property	Reproduction Paper	Polypropylene	Polyester Film	Steel Core
Young's Modulus(ksi)	600	450	653.4	30,000
Poisson's Ratio	0.0	0.0	0.0	0.3
Friction Coefficient	0.35	0.97	0.28	---
Core Stiffness(ksi)	---	---	---	3930

TABLE II
DIMENSION OF EXPERIMENTAL MATERIALS

Material	Caliper	Width	Thickness of Stack	Length
Stack of Beam	0.004225"	4.25"	0.4"	8.375"
Stack of Foundation	0.004225"	4.25"	3.86"	8.5"
Aluminum Block	---	4.25"	0.4"	1.25"
Aluminum Spacer	---	1.0"	0.25"	3.0"
Polypropylene	0.001"	6.0"	---	---
Polyester Film	0.00092"	6.0"	---	---

Equivalent Thickness of A Beam

The buckling stress of a beam is directly related to the moment of inertia. If the selected webs do not slip upon each other, the individual moment of inertia can be summed to get the equivalent moment of inertia of the modeled beam. The modeled beam thickness was calculated by equating the total moment of inertia of selected webs to the equivalent moment of inertia of the modeled beam. The moment of inertia of one layer and of n layers are

$$I_1 = \frac{Wt^3}{12} \quad (3.1)$$

and

$$I_n = \frac{Wt^3n}{12} \quad (3.2)$$

The equivalent moment of inertia of a beam is

$$I_{eq} = \frac{Wt_{eq}^3}{12} \quad (3.3)$$

Equating Equations (3.2) and (3.3) yields:

$$\frac{Wt^3n}{12} = \frac{Wt_{eq}^3}{12} \quad (3.4)$$

The equivalent thickness of a beam can be expressed as:

$$t_{eq} = t n^{1/3} \quad (3.5)$$

The number of layers (n) can be determined by the web caliper (t) and the beam thickness (h) such as

$$n = \frac{h}{t} \quad (3.6)$$

Substituting Equation (3.6) into (3.5) gives

$$t_{eq} = t^{2/3} h^{1/3} \quad (3.7)$$

Radial Modulus of Elasticity
of Reproduction Paper

The radial modulus of a stack of paper or web material is not a constant but a function of pressure: A stack behaves like a soft spring under low pressure and a stiffer spring under high pressure. The radial modulus was obtained as a function of pressure by compression tests of a stack of paper.

Pfeiffer's Method. Pfeiffer [33, 35] suggested an exponential relationship between pressure and strain, and derived the radial modulus as a linear function of pressure.

$$P_r = -k_1 + k_1 \exp(k_2 \epsilon_r) \quad (3.8)$$

The physical significance of the constants k_1 and k_2 is: k_1 enforces the pressure to be zero at zero strain, k_2 is called a springiness factor and shows the hardness of the material. For soft materials k_2 is low, for hard materials k_2 is high. Arranging Equation (3.8) and taking the logarithm gives:

$$\log(P_r + k_1) = \log(k_1) + k_2 \epsilon_r \quad (3.9)$$

The procedure to calculate the constants k_1 and k_2 is as follows;

1. Take the logarithm of the pressure P_r ;
2. Perform least-squares curve fitting to obtain k_1 and k_2 .
3. Add previous k_1 to the pressure P_r ;
4. Iterate procedure 1 to 3 until old k_1 and new k_1 are reasonably close.

Differentiating Equation (3.8) with respect to the strain gives the radial modulus as a linear function of pressure:

$$E_r = \frac{dP_r}{d\epsilon_r} = k_1 k_2 + k_2 P_r \quad (3.10)$$

Polynomial Curve Fitting Method. Pfeiffer's method has a very good physical meaning and in many cases will fit the data well but sometimes this method does not represent the data accurately. A polynomial curve fitting method was developed. This method represented the data very well. The pressure vs strain data was curve fitted by higher order polynomial function.

$$P_r = \sum_{n=0}^N C_n \epsilon_r^n \quad (3.11)$$

The radial modulus is the derivative of the pressure.

$$E_r = \frac{dP_r}{d\epsilon_r} = \sum_{n=1}^N n C_n \epsilon_r^{n-1} \quad (3.12)$$

Using Equations (3.11) and (3.12), the radial modulus and the pressure were tabulated according to the strain. By least-squares curve fitting of the modulus vs pressure data, the radial modulus was expressed as a polynomial function of pressure

$$E_r = \sum_{n=0}^N C_n' P_r^n \quad (3.13)$$

The calculations of the radial modulus of web material will be shown in the experimental analysis section.

Equivalent Spring Constant

The spring constant of the foundation was expressed by the radial modulus and the foundation dimension using Hooke's law. The interface element needs this spring constant as an input data.

The spring constant of an interface element can be calculated by Hooke's law.

$$\sigma_r = E_r \epsilon_r \quad (3.14)$$

The stress and the strain developed by the applied force F are:

$$\sigma_r = \frac{F}{WL} \quad \text{and} \quad \epsilon_r = \frac{\delta}{L_f} \quad (3.15)$$

Substituting Equation (3.15) into (3.14) gives:

$$\frac{F}{WL} = E_r \frac{\delta}{L_f} \quad (3.16)$$

By definition of the spring constant, we get:

$$\alpha = \frac{F}{\delta} = \frac{WLE_r}{L_f} \quad (3.17)$$

The equivalent spring constant of the stack of paper in the buckling experiment was:

$$\alpha = \frac{(4.25)(8.375)E_r}{3.86} = 9.2212 E_r \quad (3.18)$$

Equivalent Modulus of Foundation

The modulus of foundation was defined as a spring constant corresponding to unit length [42]. It is the key parameter of the classic buckling mode and load.

$$\beta = \frac{\alpha}{L} \quad (3.19)$$

Substituting Equation (3.17) into (3.19) gives:

$$\beta = \frac{WE_r}{L_f} \quad (3.20)$$

The equivalent modulus of foundation of the stack of paper in the buckling experiment was:

$$\beta = \frac{4.25E_r}{3.86} = 1.101 E_r \quad (3.21)$$

Classic Buckling Mode and Load

The buckling mode and load were predicted by the classic solutions of an eigenvalue buckling problem of a beam upon elastic foundation. The theory and the program were shown in Appendix A and C. The buckling mode is the minimum integer that satisfies Equation (3.22) and the corresponding buckling load can be obtained by Equation (3.23).

$$\frac{\beta L^4}{\pi^4 E_t I_{eq}} \leq m^2(m+1)^2 \quad (3.22)$$

$$F_{cr} = \frac{\pi^2 E_t I_{eq}}{L^2} \left(m^2 + \frac{\beta L^4}{m^2 \pi^4 E_t I_{eq}} \right) \quad (3.23)$$

The classic solution did not consider the friction force between the beam and the foundations. In the numerical model, the axial loads were applied at both sides of the beam. Because the friction forces were divided equally between the upper and lower axial loads, half of the area of the foundation was multiplied by the friction coefficient and the radial

pressure. The modified classic buckling loads were obtained by adding the friction forces to the classic buckling loads as follows:

$$F_{crm} = F_{cr} + \mu P_r A/2 \quad (3.24)$$

The material properties and dimensions are in Tables I and II. The illustrative procedure to find the classic buckling mode and load for the buckling experiment at stack pressure of 1.16 psi was as follows;

The equivalent thickness of the beam was:

$$t_{eq} = t n^{1/3} = 0.004255^{2/3} 0.4^{1/3} = 0.01935'' \quad (3.25)$$

The equivalent moment of inertia of the beam was :

$$I_{eq} = \frac{W t_{eq}^3}{12} = \frac{(4.25)(0.01935)^3}{12} = 2.566E-6 \text{ in}^4 \quad (3.26)$$

The equivalent spring constant of the foundation was :

$$\alpha = \frac{W L E_r}{L_f} = \frac{(4.25)(8.375)(148.24)}{3.86} = 1366.90 \text{ lb/in} \quad (3.27)$$

The equivalent modulus of foundation was :

$$\beta = \frac{W E_r}{L_f} = \frac{(4.25)(148.24)}{3.86} = 163.21 \text{ lb/in}^2 \quad (3.28)$$

When the stack pressure was 1.1654 psi, the buckling mode was obtained as 9 by the minimum integer that satisfied Equation (3.29):

$$\left[\frac{(163.21)(8.375)^4}{\pi^4 (6E5)(2.566E-6)} = \frac{\beta L^4}{\pi^4 E_t I_{eq}} \right] \leq m^2(m+1)^2 \quad (3.29)$$

The corresponding buckling load was obtained as:

$$F_{cr} = \frac{\pi^2 E_t I_{eq}}{L^2} \left(m^2 + \frac{\beta L^4}{m^2 \pi^4 E_t I_{eq}} \right) = 31.86 \text{ lb} \quad (3.30)$$

The modified classic solution was:

$$F_{crm} = F_{cr} + \mu P_r A / 2 = 31.86 + (0.35)(1.165)(35.594) / 2 = 39.12 \text{ lb} \quad (3.31)$$

The calculation for each stack pressure was shown in Table III.

TABLE III
MATERIAL PROPERTIES AND CLASSIC SOLUTIONS
OF STACK TESTS FOR EACH STACK PRESSURE

Stack Pressure (psi)	Spring Constant (lb/in)	Modulus of Foundation (lb/in ²)	C	Classic Solutions		
				Mode	Buckling Load(lb)	
				$\mu=0$	$\mu>0$	
1.16	1366.90	163.21	5354.0	9	31.86	39.12
1.40	1555.79	185.77	6093.9	9	33.84	42.54
1.63	1742.27	208.03	6824.3	9	35.79	45.94
1.86	1926.32	230.01	7545.2	9	37.72	49.32
2.10	2107.87	251.69	8256.3	10	39.54	52.60
2.33	2286.90	273.06	8957.5	10	41.06	55.57

where
$$C = \frac{\beta L^4}{\pi^4 E_t I_{eq}}$$

Finite Element Model

The finite element modeling was accomplished using ANSYS commercial finite element code. The version 4.4 is resident upon an IBM-RT computer.

Element Types

Elastic Beam Element (STIF3). The elastic beam element was shown in Figure 5.

Number of nodes (2) : i, j

Degrees of freedom per node (3): u, v, ω_z

Real constants : area, moment of inertia, height, shear deflection constant, initial strain

Material properties : Young's modulus, coefficient of thermal expansion, Poisson's ratio, density

Shape functions :

$$\begin{aligned} u &= c_1 + c_2 x \\ v &= c_3 + c_4 x + c_5 x^2 + c_6 x^3 \\ \omega_z &= \frac{dv}{dx} = c_4 + 2c_5 x + 3c_6 x^2 \end{aligned} \quad (3.32)$$

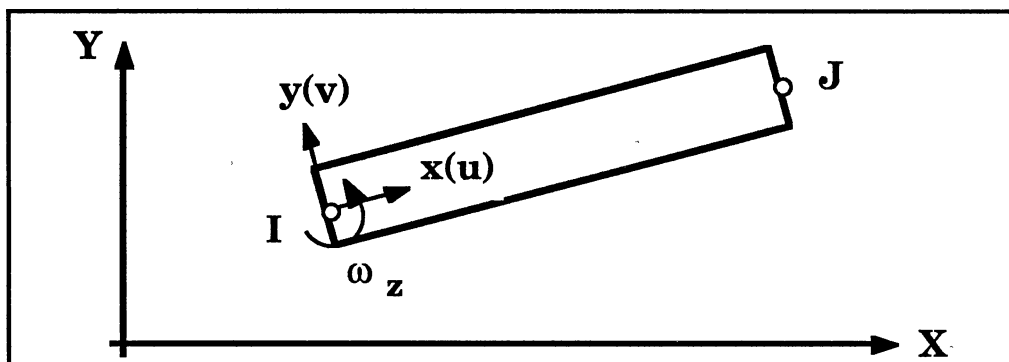


Figure 5. Two Dimensional Elastic Beam Element (STIF3)

Interface Element (STIF12). The interface element was shown in

Figure 6.

Number of nodes (2) : i,j

Degrees of freedom per node (2): u,v

Real constants (4): angle from global x-axis, normal stiffness, initial interference, initial gap status, shearing stiffness.

Material properties : Friction coefficient

Shape function : None

Operation

1. If the interface is open,
no stiffness is associated with this element.
2. If the interface is closed and sticking,
The normal stiffness is used for the gap resistance,
The shearing stiffness is used for sliding resistance.
3. If the interface is closed but sliding,
The normal stiffness is used for the gap resistance.
The constant friction force is used for the sliding resistance.

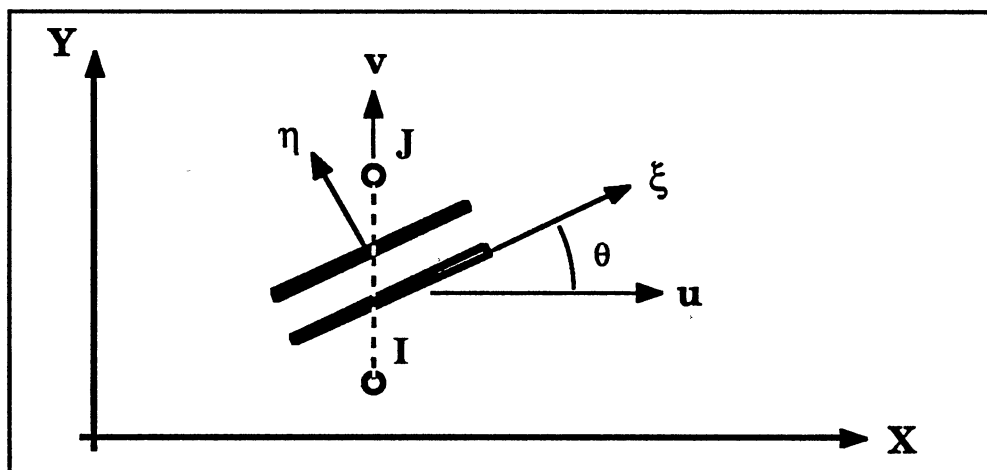


Figure 6. Two Dimensional Interface Element (STIF12)

Isoparametric Solid Element (STIF42). The isoparametric solid element was shown in Figure 7.

Number of nodes (4) : i, j, k, l

Degrees of freedom per node (2): u,v

Real constant : Thickness

Material properties : Young's modulus (x,y), Poisson's ratio, coefficient of thermal expansion (x,y), density, shear modulus

Shape functions :

$$\begin{aligned} u &= \frac{1}{4}u_n(1+\xi_n\xi)(1+\eta_n\eta) \\ v &= \frac{1}{4}v_n(1+\xi_n\xi)(1+\eta_n\eta) \end{aligned} \quad (3.33)$$

where $n = i, j, k, l$

$$\begin{aligned} \xi_i &= \xi_l = -1, \quad \xi_j = \xi_k = 1 \\ \eta_i &= \eta_j = -1, \quad \eta_k = \eta_l = 1 \end{aligned} \quad (3.34)$$

u_n, v_n : displacements at node n

ξ, η : local element coordinates

$$(-1 \leq \xi \leq 1, -1 \leq \eta \leq 1) \quad (3.35)$$

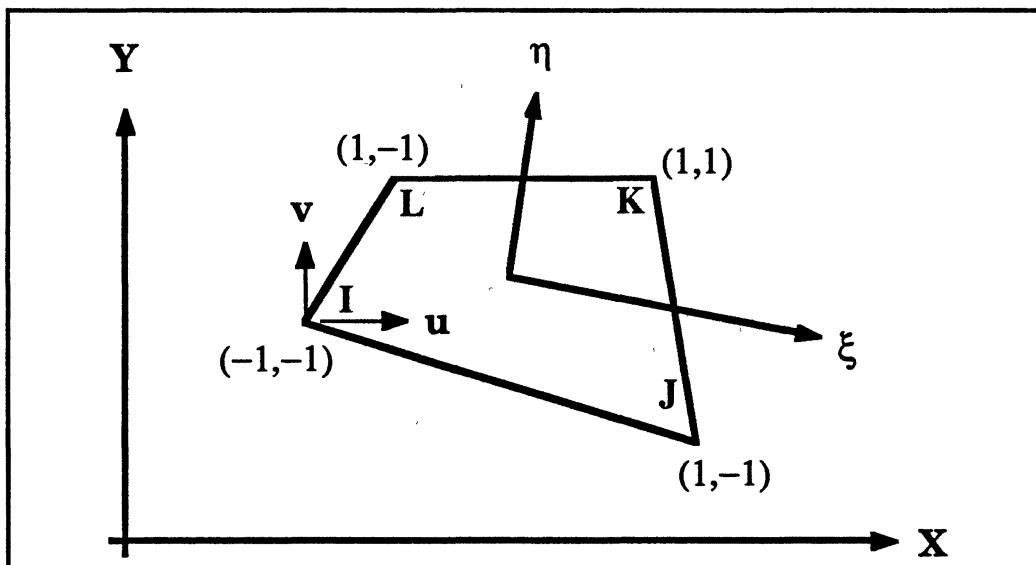


Figure 7. Two Dimensional Isoparametric Element (STIF42)

Boundary Conditions

In Figure 3, the x-directional displacements of the left boundary were fixed. The center of left boundary was simply supported to prevent vertical rigid body translation. The lateral pressure was applied to the right boundary as x-directional forces. The nodal points of the assumed buckling mode of the beam were constrained together by constraint equations. The CE command in ANSYS program can cause the nodal points to deflect together with simple constraint equations.

Mesh Generation

The y-directional mesh was determined to let one half-sine wave of a buckling mode have four elements. If assumed buckling mode was 10, the number of elements in y-direction was 40. The x-directional size and the number of division of the foundation part were determined by the geometric progression so that the mesh size increases gradually as shown in Figure 8.

$$t_{eq}(1+r^1+r^2+ \dots +r^{n_a-1}) = a_1 \quad (3.36)$$

$$n_a = \log\left(\frac{a_1(r-1)}{t_{eq}} + 1\right) / \log(r) \quad (3.37)$$

Then the x-coordinates were calculated as follows:

$$x_{in} = \frac{a_1(r-1)}{r^{n_a-1}} \text{ and } x_{i+1} = x_i + x_{in} r^i \quad (i=0, n_a-1) \quad (3.38)$$

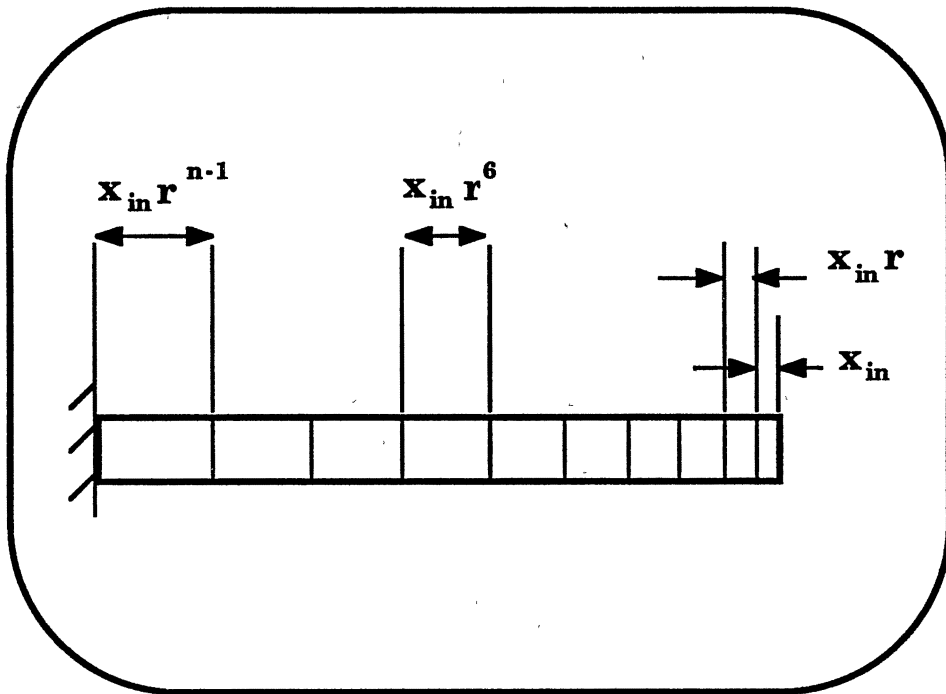


Figure 8. X-directional Mesh Generation by Geometric Progression

Nonlinear Buckling Analysis

If the structural stability depends only on the initial geometry and stress state, it is a linear or an eigenvalue buckling problem. The eigenvalue represents the buckling load and the eigenvector represents the buckling mode.

The simplified model of a center wound roll includes a beam upon an elastic foundation, radial pressure and slippages between webs. The structural stability of this model not only depends on the original geometry but also on the updated geometry, material properties and the status of the interface elements. It is a nonlinear buckling problem. The geometric nonlinear static analyses must be employed to solve this nonlinear buckling problem.

Calculating Procedure. The buckling load is defined as a transition point below which the structure recovers its original geometry and above which it deforms more. The procedure to find the buckling mode and load by nonlinear static analysis is as follows:

1. Apply boundary conditions corresponding to the assumed buckling mode: (Lateral pressure, Specified displacements, Constraint equation of nodal points for assumed buckling mode);
2. Apply small perturbing loads to the centers between the nodal points of assumed buckling mode and save the ANSYS files "file03.dat" and "file16.dat" for restart run;
3. Remove the perturbing loads and apply assumed buckling load;
4. Check the lateral displacement at the center of the beam whether it decreases or increases. If it decreases it is below the buckling load, and if it increases it is above the buckling load.;
5. If it is not buckled yet, restart the ANSYS run from the procedure 2 by increasing the load slightly until you get the buckling load;

6. If the buckling load for assumed buckling mode was found, try another buckling modes and find the mode that has the smallest buckling load.

Pre- and Post-processing Programs. For each stack pressure and buckling mode, we must modify the input data to the ANSYS program frequently. One pre- and two post-processing programs for ANSYS program were developed in C-language and were attached to Appendix C. A flow chart for these programs were shown in Figure 9.

The program "MAIN.C" reads data files 'ANSD.INP' and 'FINP' and modifies the loading range in 'ANSD.INP' according to the data in 'FINP'. To find the buckling load for assumed buckling mode, "MAIN.C" controls the individual programs "ANSD.C", "ANSP.C" and "ANSQ.C" in closed loop.

The pre-processing program "ANSD.C" generates the input data to the ANSYS program. The header file "VARIABLE.H" declares global variables and transports them between the individual programs. It also reads or writes the problem information from or to the data file 'ANSD.INP'. This data file contains the problem identification, the calculating conditions, the dimensions of the beam and the foundation, the material properties, and the lower and upper limits of the buckling loads.

The post-processing program "ANSP.C" picks several nodal displacements from the ANSYS output file 'ANS.OUT' and prints them to a file 'ANSP.O'. The program "ANSQ.C" reads the file 'ANSP.O' and checks the displacements whether the beam is buckled or not. It writes the buckling status and accuracy of the buckling load to the file 'ANSD.INP' so that the "MAIN.C" program can control the programs.

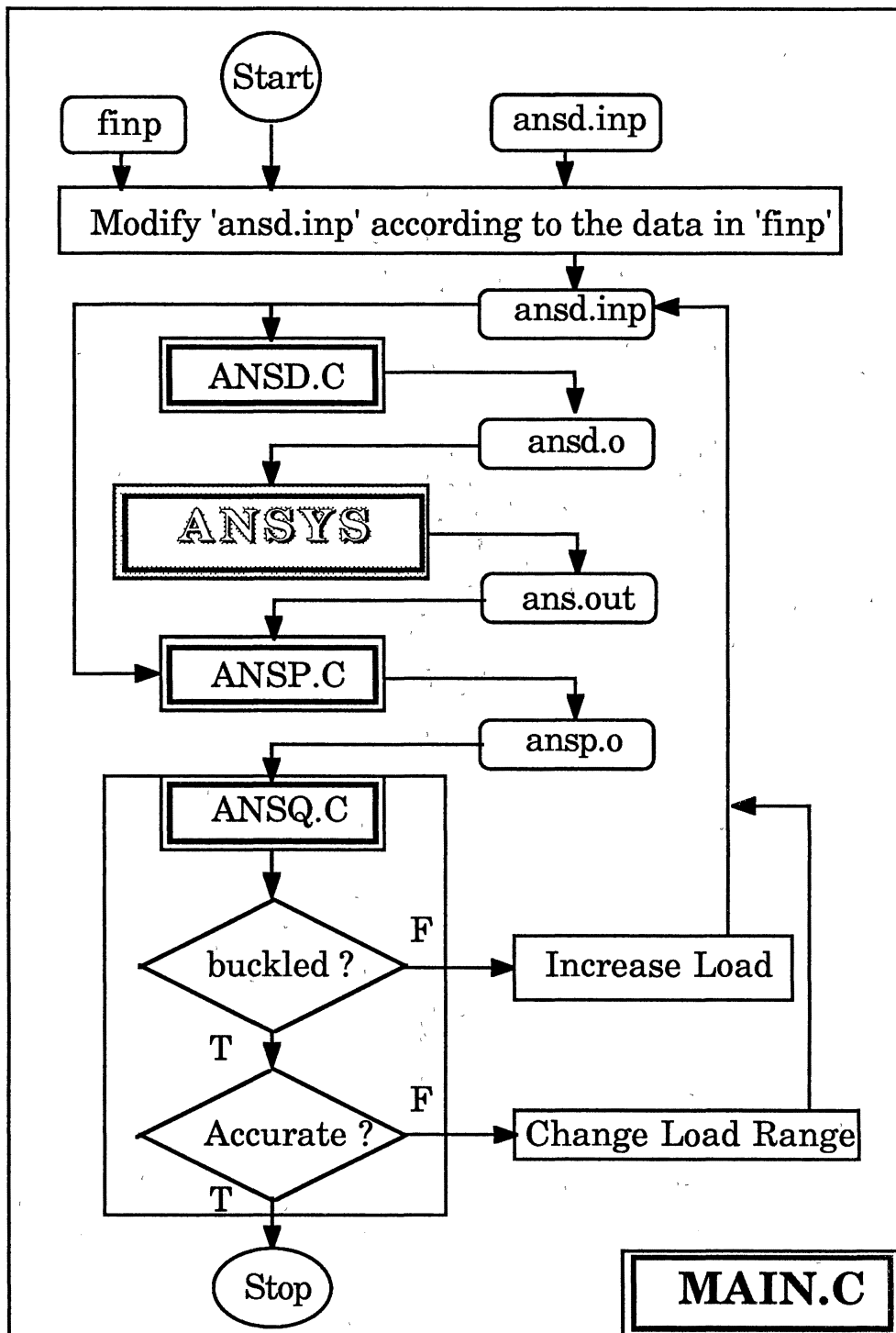


Figure 9. Flow Chart of Nonlinear Buckling Analysis

Results of Finite Element Analysis

Finite element computation of buckling loads requires some input. The calculating conditions such as a large displacement convergent bound, a perturbing load, and an iteration number were carefully chosen to give reasonable results. A detailed discussion of these effects on the numerical solutions was discussed at the section of center wound roll in Chapter IV.

Stack Pressure of 1.16 psi. As shown in Table III, the classic buckling mode was 9 and the buckling load was 39.12 lb. The buckling loads for the buckling modes from 8 to 11 were calculated and compared. The buckling mode associated with the smallest buckling load is the tabulated buckling mode.

Figure 10 shows the history of the lateral displacement at the center of the beam where the perturbing load was applied. δ_0 is the initial displacement when the radial pressure and the perturbing load were applied. $\delta_1, \dots, \delta_i, \delta_j, \dots, \delta_n$ are the displacements at assumed buckling loads. At 53 lb, the lateral displacement δ_1 was smaller than δ_0 , i.e., the beam went back to its original geometry. At 59 lb, δ_n was larger than δ_0 , i.e., the beam deformed more. δ_i was slightly smaller than δ_0 at 57.4 lb, i.e., the load was slightly below the buckling load. δ_j was slightly larger than δ_0 at 57.8 lb, i.e., the load was slightly above the buckling load. The buckling load at the buckling mode 8 was found to be between 57.4 and 57.8 lbs.

The horizontal line in Figure 11 represented the perturbed displacement δ_0 . The circled points represent the lateral displacements at assumed buckling loads. As the load increased, the lateral displacements

δ_i and δ_j approached the δ_0 . The load at δ_i was the lower bound and the load at δ_j was the upper bound of the buckling load.

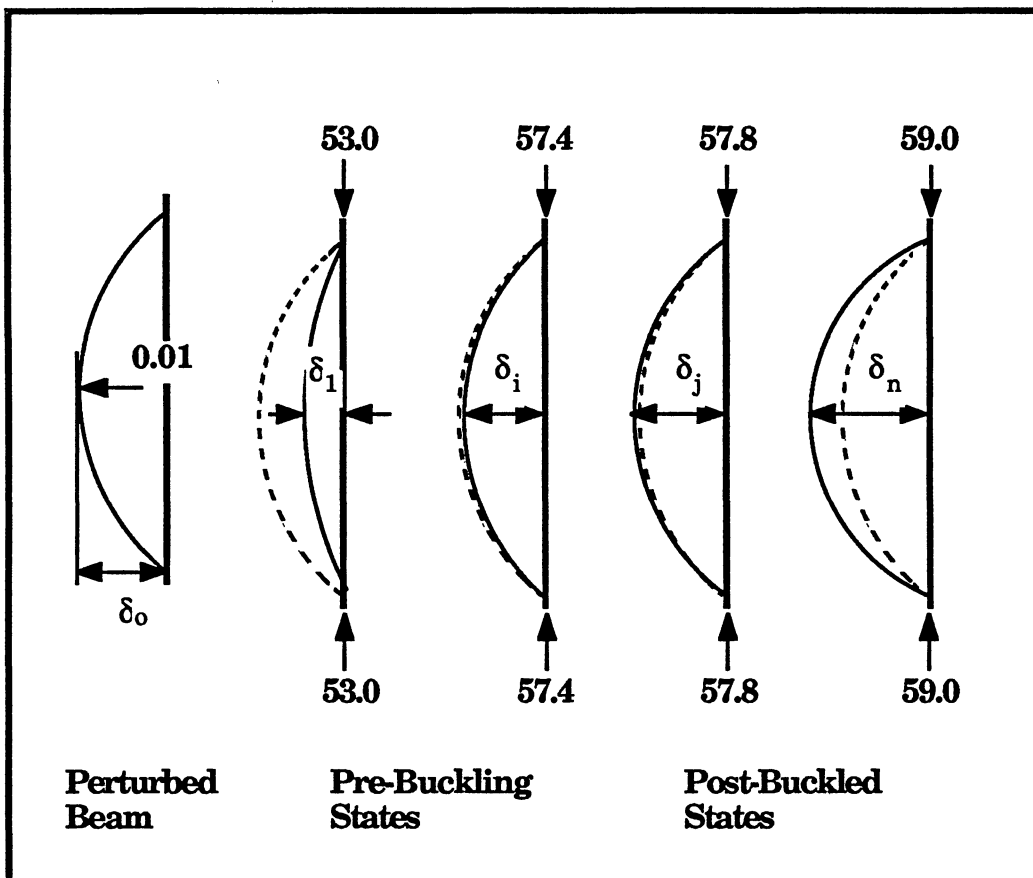


Figure 10. Lateral Displacements according to Beam Status
Stack Pressure = 1.16 psi, Buckling Mode = 8

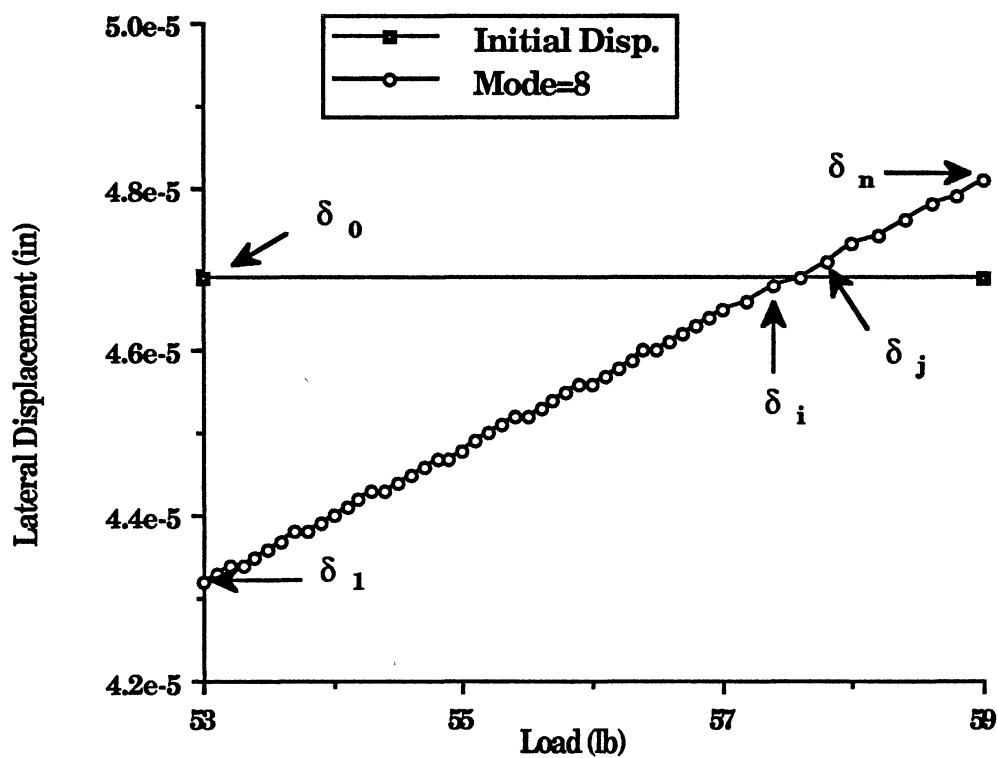


Figure 11. Lateral Displacements under Axial Loads
Stack Pressure = 1.40 psi, Buckling Mode = 8

Using the same procedure, the buckling loads for the buckling modes 9 to 11 were calculated as shown in Table IV and Figure 12. Because the buckling load for the buckling mode 10 was the smallest, the buckling mode was 10 and the corresponding buckling load was 51.90 lb.

TABLE IV
BUCKLING MODE DETERMINATION OF STACK TESTS
FOR EACH STACK PRESSURE

Buckling Mode	Stack Pressure (psi)					
	1.16	1.40	1.63	1.86	2.10	2.33
8	57.55	---	---	---	---	---
9	54.50	59.60	63.40	68.5	---	---
10	51.90	55.95	59.95	63.10	67.25	71.25
11	53.75	57.05	60.85	63.20	66.80	70.25
12	---	---	---	63.50	66.50	69.25
13	---	---	---	---	69.25	72.25

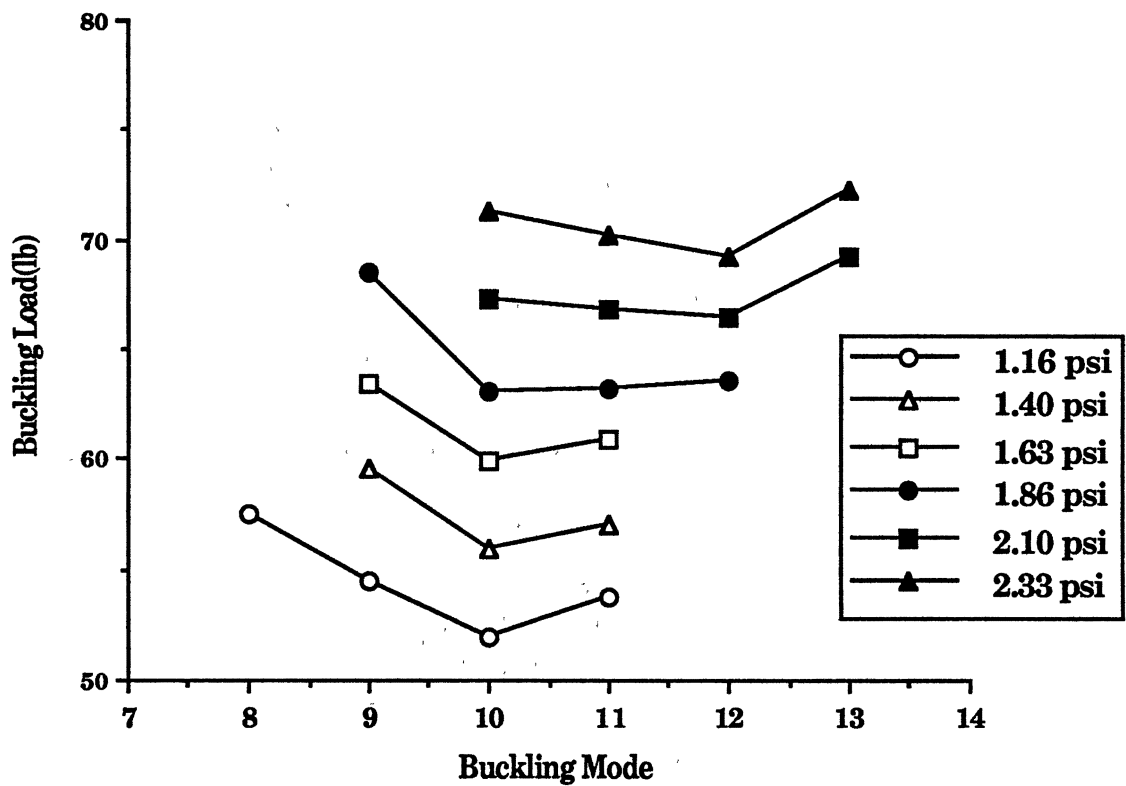


Figure 12. Buckling Mode Determination by Finite Element Analysis of Stack Tests

Higher Stack Pressures. For the higher stack pressures, the buckling loads for the buckling modes 9 to 13 were calculated and shown in Table IV and Figure 12. The buckling mode associated with the minimum buckling load represented the buckling mode for each stack pressure. The buckling modes and loads for each stack pressure are shown in Table V and Figure 13 in conjunction with the classic solutions and the experimental results.

TABLE V
BUCKLING LOADS AND MODES
OF STACK TESTS FOR EACH STACK PRESSURE

Stack Pressure (psi)	<u>Classic</u>		Mode	<u>Numerical</u>		No. of Tests	<u>Experimental</u>	
	<u>Buckling Load</u>	$\mu > 0$ %error		<u>Buckling Load</u>	%error		<u>Buckling Load</u>	STD
1.16	39.12	24.6	10	51.90	6.0	19	55.57	7.06
1.40	42.54	24.0	10	55.95	22.1	39	71.82	10.11
1.63	45.94	23.4	10	59.95	18.2	23	73.29	15.17
1.86	49.32	21.8	10	63.10	19.3	23	78.22	12.45
2.10	52.60	20.9	12	66.50	27.3	19	91.53	22.55
2.33	55.57	19.8	12	69.25	32.9	19	103.16	16.52

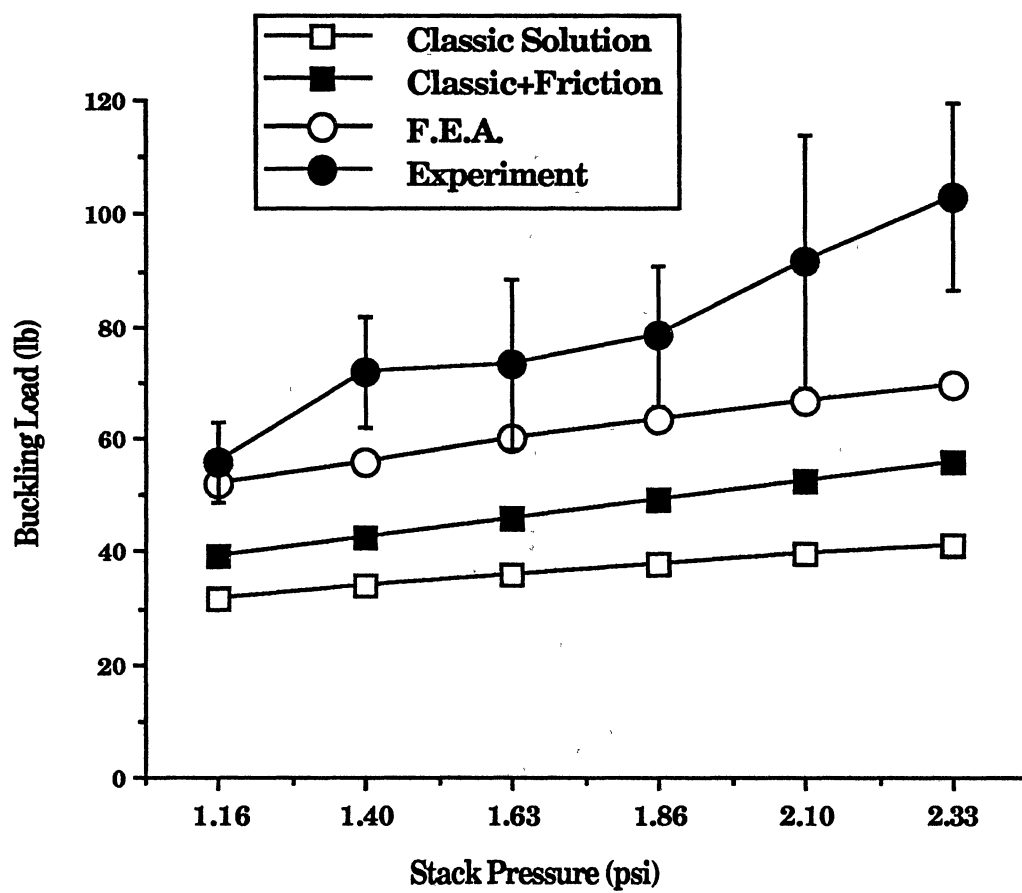


Figure 13. Buckling Loads of Stack of Reproduction Paper for Different Stack Pressures

Comparison to Classic Solutions. In Table V and Figure 13, the classic buckling loads were smaller than those computed by finite element analyses. The modified classic buckling loads included the friction forces between the beam and the foundations. The percentage errors of them relative to the numerical ones were within 25 %. Considering the computing time, the classic solution can be a useful tool to roughly predict the numerical solution and the starting of a wound roll for a given winding condition.

Comparison to Experimental Results. The experimental results were the averages of many tests. The number of tests were shown in Table V. The error bars were standard deviations of the experimental buckling loads. In experiments, the buckling loads were determined by the slope change in load vs displacement curves. Although the beam began to buckle, it could not change the slope immediately. The noticeable change in slope occurred at a slightly post-buckled state. The experimental buckling loads represented the loads at slightly post-buckled states.

The numerical results were smaller than the experimental ones for all the stack pressures, for they represented loads which were almost initial buckling loads. At the stack pressures of 2.10 psi and 2.33 psi, the difference between the numerical and experimental buckling loads was larger than at the lower stack pressures. The reason was that the friction force at the higher stack pressure was so large that the local buckling usually occurred at the loading area. The percentage errors of the numerical buckling loads relative to the averaged experimental ones were within 33 %.

These comparisons of the finite element and experimental results have shown that the finite element model was able to predict the initial buckling loads and modes of stacks of reproduction paper for various stack pressures. If the radial pressure of a wound roll is assumed to be constant, the starred roll defect of the wound roll can be predicted using this model.

Experimental Analysis

The buckling experiments were performed, which used stacks of reproduction paper as a beam and foundations, to verify the constant radial modulus model. The buckling modes were measured for a few stacks of paper and only the buckling loads were measured for most cases because an extreme load usually caused a permanent deformation of the stack of paper.

Radial Modulus of Reproduction Paper

The MTS machine [27] was used in conjunction with a one thousand pound load cell to apply compressive force on the stack. The output signals were converted to the loads and the displacements through DASH-16/16F A/D converter board and the LABTECH Notebook software which was installed in an IBM-AT compatible personal computer. The experimental equipment is shown in Figure 14.

A specimen of the stack of reproduction paper for the radial modulus measurement had an area of 3" by 4.25" and a height of 3.65". Because the strain was very large at low pressure ranges, the load was applied by stroke control in the MTS machine. A stack was tested several times by examining the effect of loading rate on the load vs displacement curve. A

loading rate that was slow enough to yield a consistent curve was used to measure the radial modulus. The up-loading curves were chosen because the buckling experiments were performed by up-loading. Figure 15 shows a load vs displacement curve for several up-loading cases. The radial modulus was measured from a stiffened specimen, because the stack of paper of buckling experiments will become more stiff by experimenting several times.

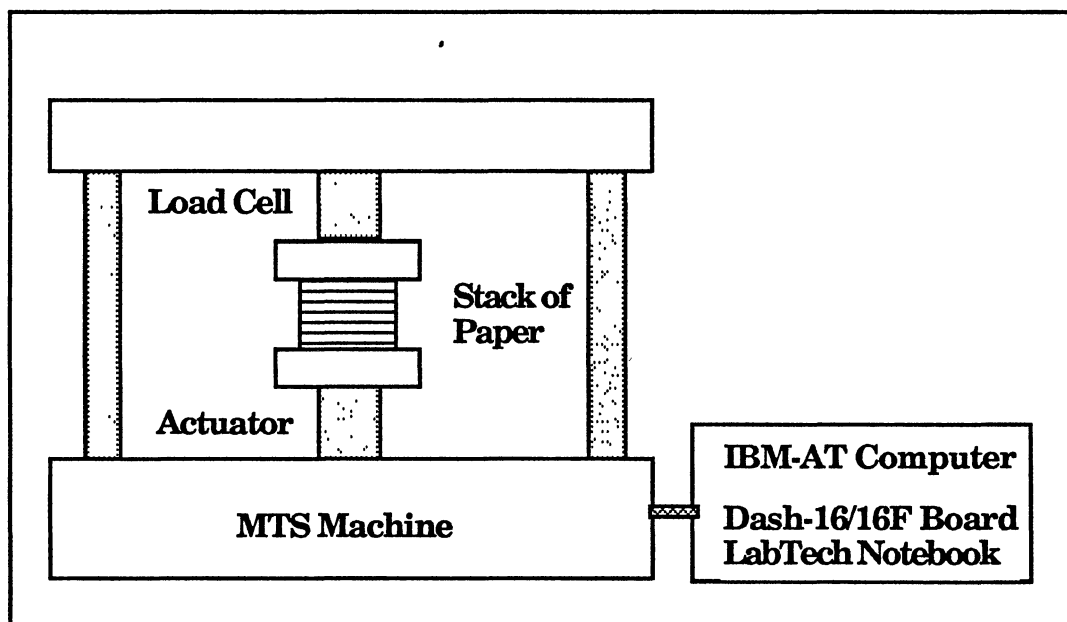


Figure 14. Apparatus for Radial Modulus Measurement

Specimen Area = 3.00" by 4.25"
Stack Height = 3.65"

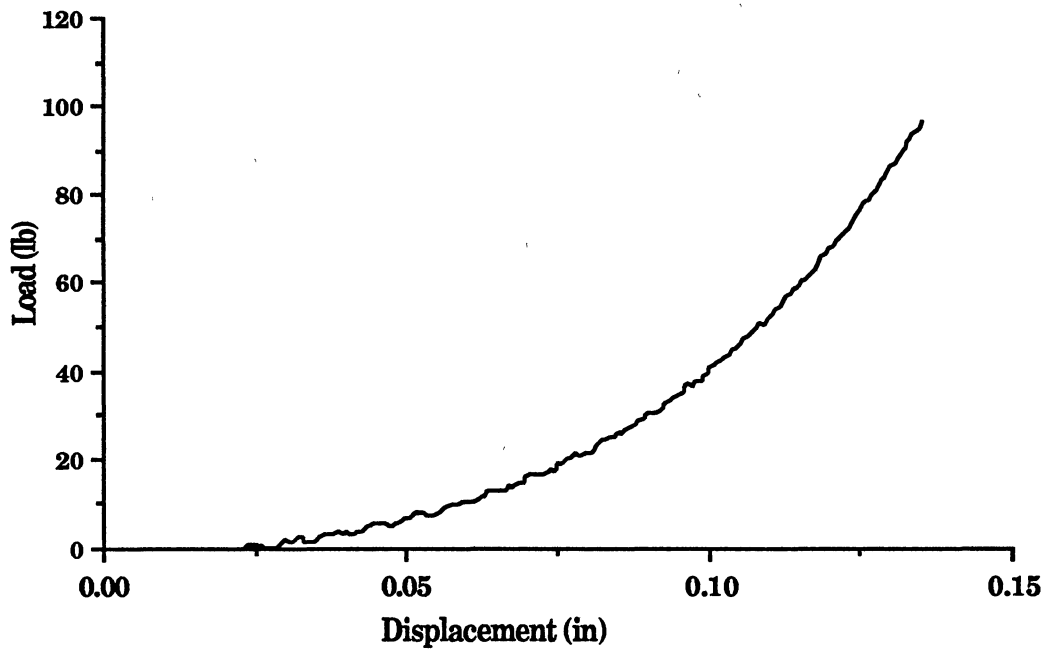


Figure 15. Load vs Displacement Curve for Radial Modulus Measurement of Stack of Reproduction Paper

Pfeiffer's Method. [35] The pressure vs strain curve was obtained in Figure 16 by dividing the compressive force by the specimen area and the displacement by the original stack height. The pressure and radial modulus functions were shown in Equations (3.9) and (3.11). The constants k_1 and k_2 were obtained by taking the logarithms and least-squares curve fittings of the pressures as shown in Equation (3.10). The constant k_1 was added to the pressures and logarithms were taken of the modified pressures. A simple program to calculate the constants k_1 and k_2 was made and presented in Appendix E.

Figure 17 shows the iterations of the curve fittings to find the converged k_1 within the error of $1.0E-5$. After 19th and 20th iterations, the constants were as follows:

$$k_1^{(19)} = 0.31047, k_1^{(20)} = 0.31048 \text{ and } k_2^{(20)} = 96.678 \quad (3.39)$$

The k_1 values from 19th and 20th iterations were close enough to decide that the pressure function fitted the data well. The pressure and radial modulus functions were obtained by substituting the constants k_1 and k_2 into Equations (3.9) and (3.11) respectively:

$$P_r = 0.3105 [\exp(96.678\epsilon_r) - 1] \quad (3.40)$$

$$E_r = 30.017 + 96.678 P_r \quad (3.41)$$

The pressure function was overlapped with the experimental data in Figure 16. The modulus function was overlapped with that of the least-squares curve fitting method in Figure 18.

1. Pfeiffer's Pressure function

$$P_r = 0.3105 [\exp(96.678\epsilon_r) - 1]$$

2. Third order polynomial function

$$P_r = -0.16195 + 68.764\epsilon_r - 2036.1\epsilon_r^2 + 1.9099e5\epsilon_r^3$$

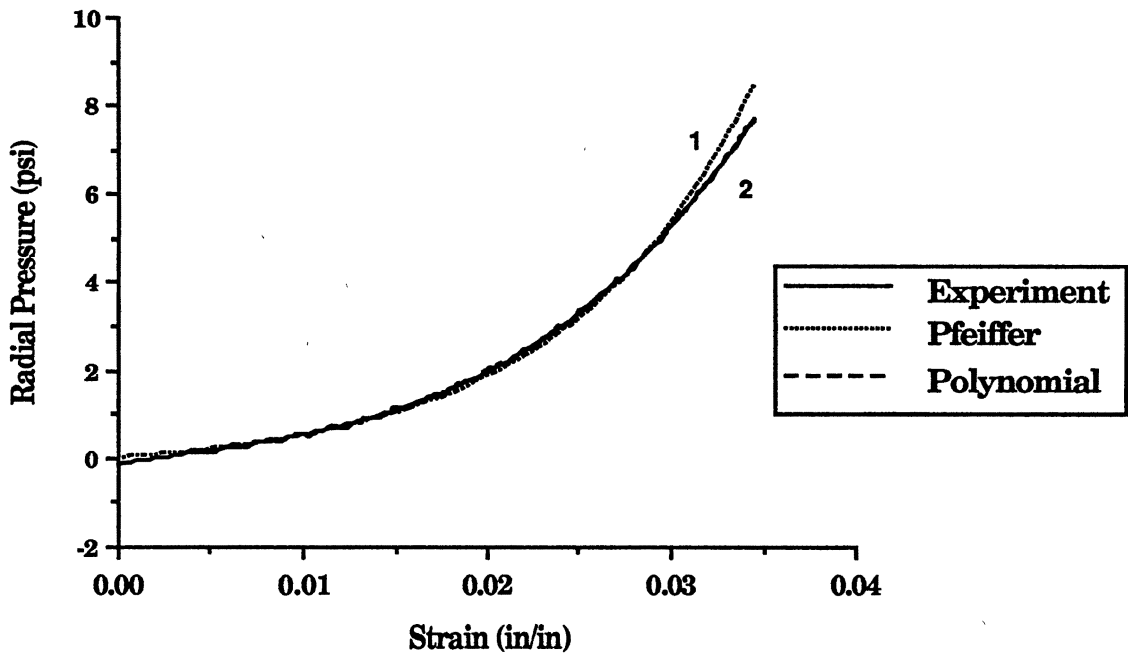


Figure 16. Pressure vs Strain Curve for Radial Modulus Measurement of Stack of Reproduction Paper

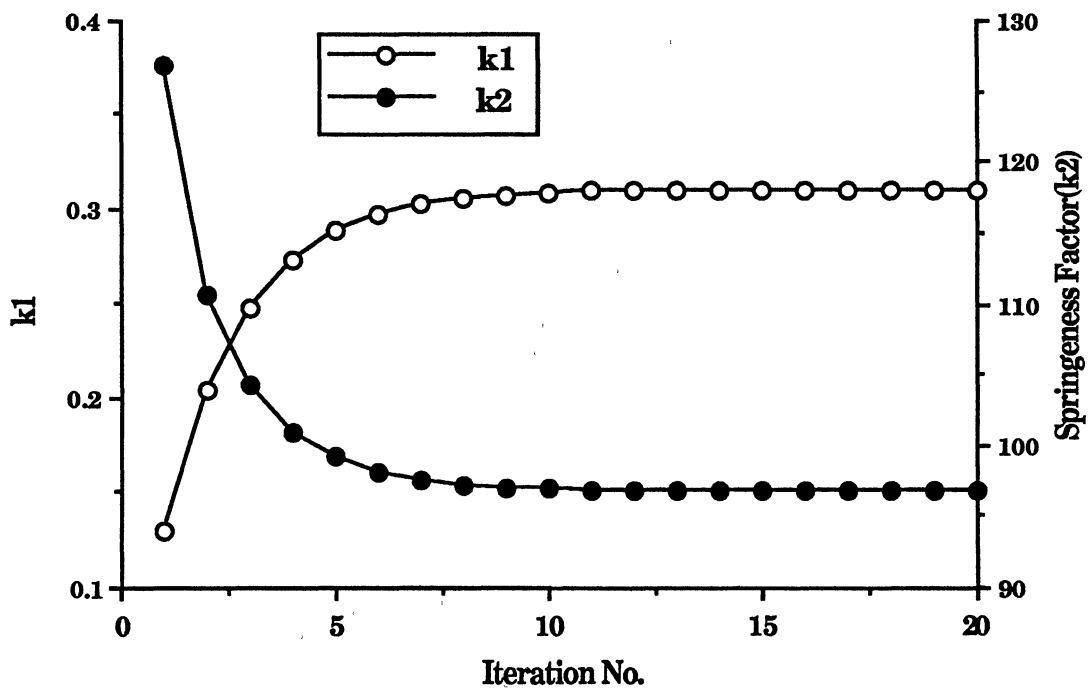


Figure 17. Determination of Constants k_1 and k_2
in Pfeiffer's Expression
 $(\log(P_r+k_1) = \log(k_1) + k_2\epsilon_r)$

1. Pfeiffer's modulus function

$$E_r = 30.017 + 96.678 P_r$$

2. Third order polynomial function

$$E_r = 42.081 + 93.729P_r - 2.1338P_r^2 - 0.06307P_r^3$$

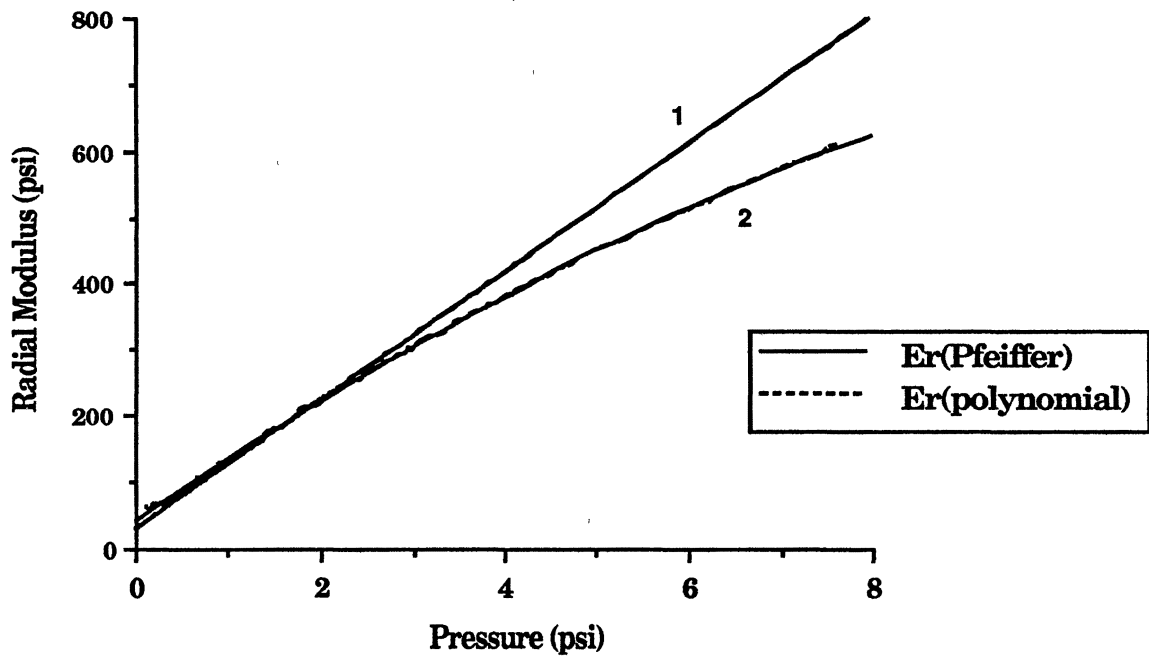


Figure 18. Radial Modulus of Reproduction Paper

Polynomial Curve Fitting Method. A third order polynomial function was obtained by a least-squares curve fitting of the pressure versus strain curve as shown in Figure 16. The radial modulus was obtained by differentiating the polynomial pressure function.

$$P_r = -0.16195 + 68.764\varepsilon_r - 2036.1\varepsilon_r^2 + 1.9099e5\varepsilon_r^3 \quad (3.42)$$

$$E_r = 68.764 - 4072.2\varepsilon_r + 5.7297\varepsilon_r^2 \quad (3.43)$$

The pressures and the moduli were tabulated versus the original strain data. The radial modulus function was then obtained as a function of pressure by a least-squares curve fitting as shown in Figure 18.

$$E_r = 42.081 + 93.729P_r - 2.1338P_r^2 - 0.06307P_r^3 \quad (3.44)$$

In Figure 16, the data below 0.2 psi were scattered so much that they were discarded in the curve fitting. The curve fitted function did not represent the pressure well around the upper edge of the data, i.e., 7.5 psi. The valid range of the polynomial function of the radial modulus was between 0.2 psi and 7.0 psi.

Comparison of Two Methods. Figure 16 shows that both Pfeiffer's and polynomial pressure functions represented the experimental pressure very well for the low pressure range below 4 psi. At the pressure range above 4 psi, Pfeiffer's pressure data were higher than the experimental ones. In Figure 18, the linear radial moduli of Pfeiffer's method were similar to that of the polynomial function at lower pressure range, but those were larger than these at higher range.

Because Pfeiffer's method assumed the radial modulus as a linear function of pressure, it could not represent the experimental data

accurately. The higher order polynomial function represented the radial modulus more accurately than Pfeiffer's linear function. The coefficients of the polynomial function do not have any physical meaning but Pfeiffer's constants do. ✓

Buckling Experiment

Apparatus. The experimental equipment was the same as the one used in the radial modulus measurement. A fixture was made for the buckling experiments of stacks of reproduction paper as shown in Figure 19 and attached to the MTS machine. A bottom plate, three vertical plates, and two loading units were made of aluminum. A hydraulic cylinder stack and a hydraulic hand pump were used to supply lateral pressure on the stacks of paper. A pressure gage was calibrated by a dead weight gage and connected to a hydraulic hand pump. Four steel rods were used to guide the movement of the vertical plate to maintain its vertical angle. Two aluminum blocks were used at the loading area to supply a good contact on the paper beam. Four thin aluminum spacers were placed below the foundation to maintain a horizontal level.

The loading area of the paper beam was carefully cut to obtain a flat surface. The upper and lower parts of the beam and the foundations were glued to be easily handled. The material properties and the dimensions of the reproduction paper and the aluminum are shown in Table I.

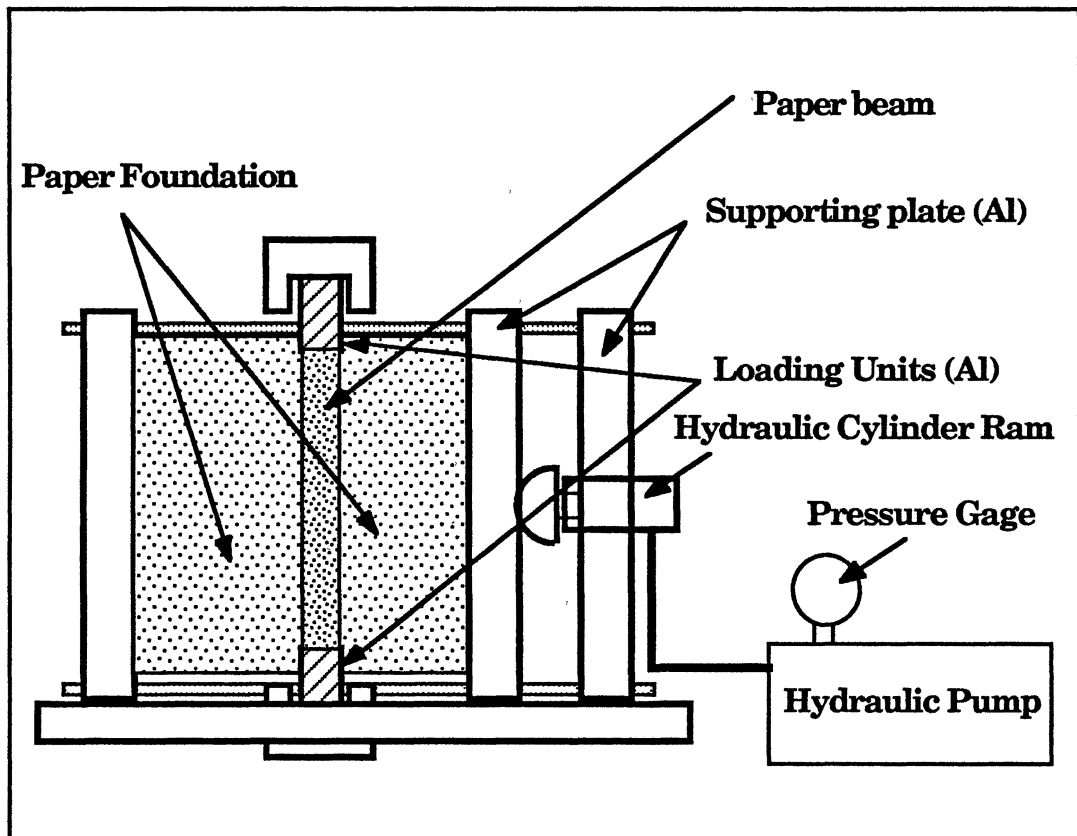


Figure 19. Apparatus for Buckling Test of Stacks of Paper

Stack Pressure. The forces corresponding to the ram pressures were measured by the load cell and least-squares curve fitted by a linear function as shown in Figure 20.

$$F = - 14.899 + 1.6578 P_{\text{ram}} \quad (3.45)$$

The constant term was due to the weight of the loading part of the ram. A converting constant from the ram pressure to the stack pressure was obtained by dividing the slope by the area of the beam which was 8.375" by 4.25".

$$P_{\text{stack}} = 0.04658 P_{\text{ram}} \quad (3.46)$$

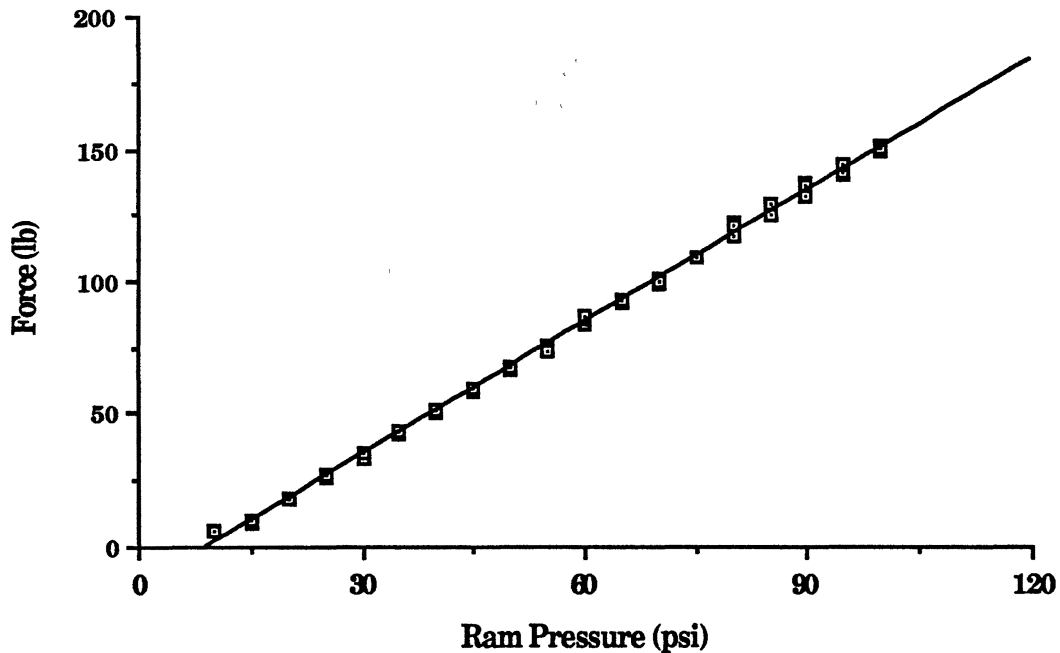


Figure 20. Calibration of Ram Pressure by Load Cell

Experimental Procedure. The loading procedure was very important.

When the vertical loading units and/or the lateral pressing units were misaligned, the paper beam was distorted and local buckling occurred at the edges of the beam. The experimental procedure was as follows;

1. Mount the foundations upon spacers, the lower aluminum block, and the beam;
2. Apply small lateral pressure and align the upper loading unit to the side supporting plate;
3. Press down the beam slightly to contact the bottom completely;
4. Apply lateral pressure gradually and check the alignment of the load cell and the lower loading unit. Adjust the whole fixture if necessary;
5. If everything is aligned well, fasten all the bolts;
6. Apply vertical load gradually by seeing the load vs displacement curve on the computer and the buckling shape of the specimen;
7. If the buckled area is localized, stop loading and align the load cell and the loading units again. Repeat steps 2 through 6, if necessary.

Results of Experimental Analysis

A typical load vs displacement curve in buckling experiments was shown in Figures 21 and 23. In Figure 21, the load was applied until the beam was fully buckled and encountered bending. Figure 22 showed the status of the beam as the load was increased. In Figure 23, the load was applied until the beam began to buckle.

Beam Thickness = 0.40"
Paper Width = 4.25"
Foundation Thickness = 3.86"
Stack Pressure = 1.16 psi

I : Pre-Buckled Region
II : Post-Buckled Region
III : Bending Region

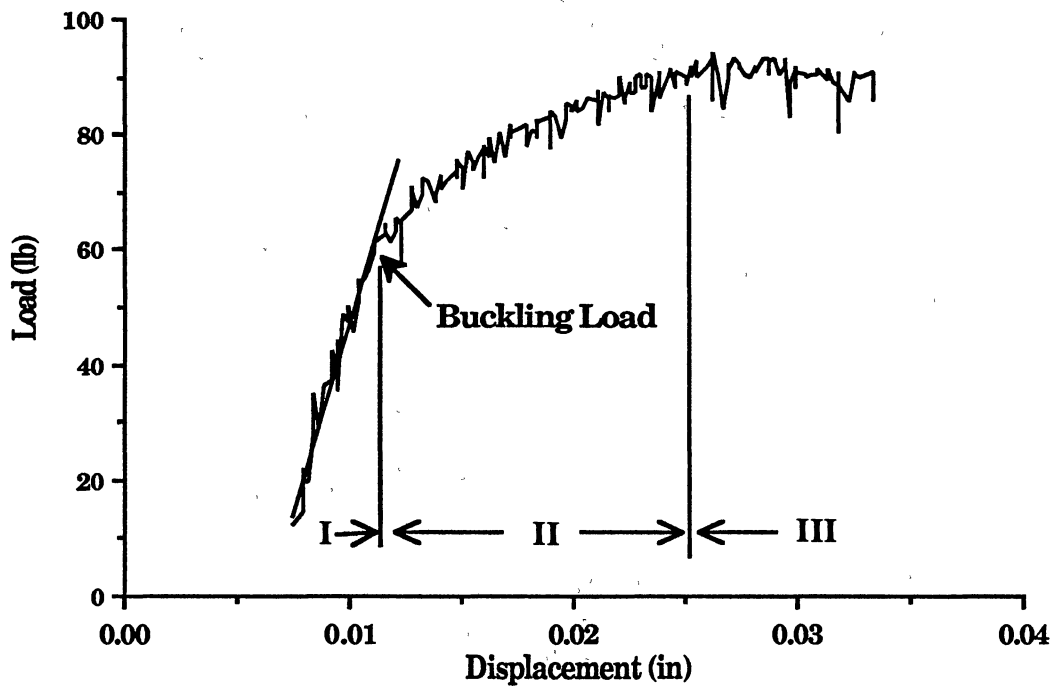


Figure 21. Load vs Displacement Curve of Buckling Experiment (Loaded up to Fully Buckled State)

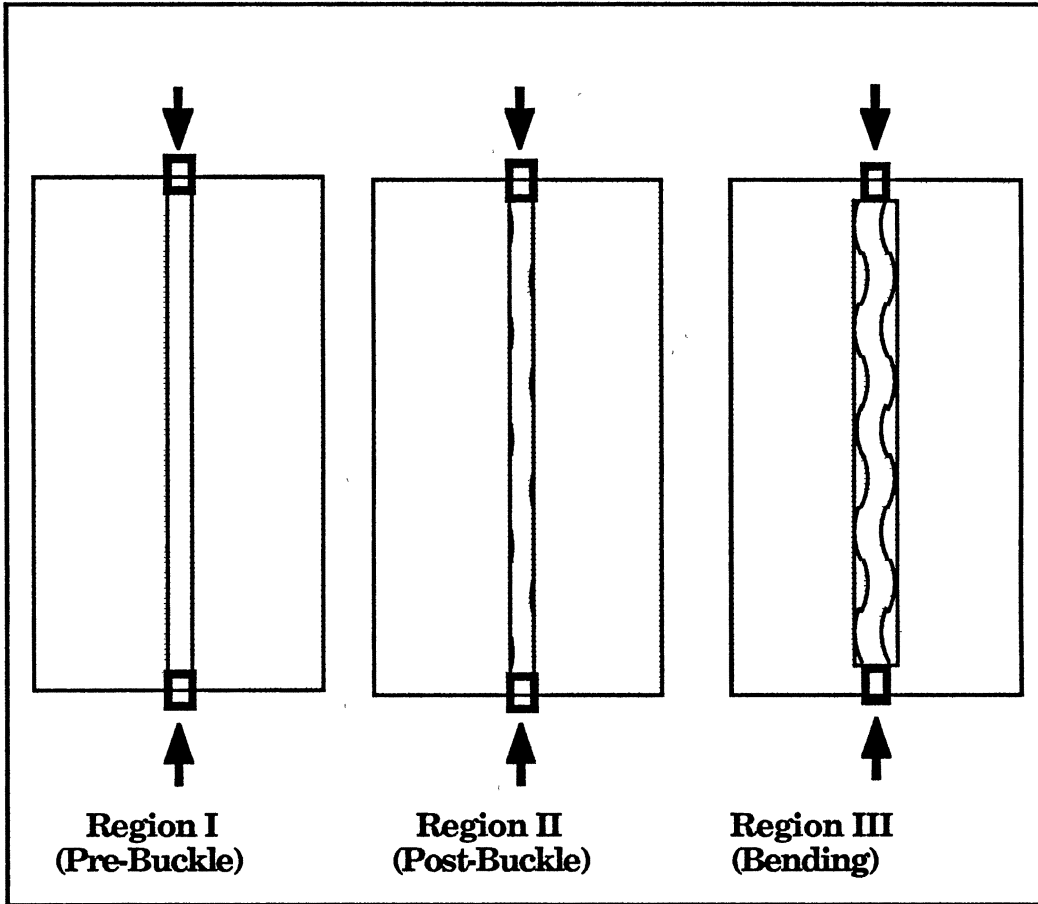


Figure 22. Beam Status in Buckling Experiment

Beam Thickness = 0.40"
Paper Width = 4.25"
Foundation Thickness = 3.86"
Stack Pressure = 1.16 psi

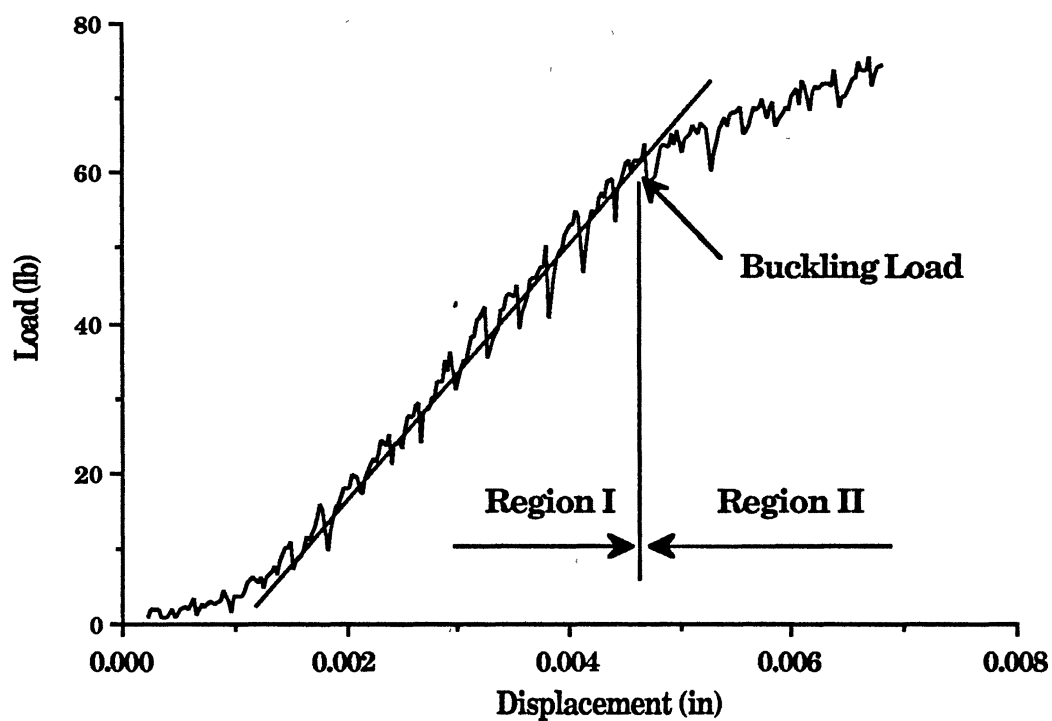


Figure 23. Buckling Load Determination by the Slope Change (Loaded up to Slightly Buckled State)

The curve in Figure 21 was divided into three regions according to the slope of the curve. In region I, the slope was almost constant and the beam was in a pre-buckled state as shown in Figure 22. In region II, the slope was decreased nonlinearly as the load was increased. The beam was encountering buckling, i.e., post-buckled state. The beam began to buckle at the transition point of the slope from region I to region II. The buckling load was obtained at this transition point. In region III, the beam was fully buckled and encountered bending, i.e., the slope was kept zero or negative although the displacement was increased. The buckling modes were clear in region III and after the middle of region II.

A few of the specimens were fully compressed up to region III to see the buckling modes. The majority of the specimens were compressed until they began to buckle, which was at the beginning part of region II as shown in Figure 23.

Determining the buckling load by the slope change from the load vs displacement curve was not easy. Occasionally the slope did not have a constant region because of the misalignment of the fixture and the load cell. Various tests were performed and analyzed statistically. The number of data obtained from the tests were 19,67,39,23,19 and 19 for stack pressures of 1.16, 1.40, 1.63, 1.86, 2.10, and 2.33 psi.

The buckling loads were measured at various loading rates to see the effect of the loading rates on the buckling loads. The buckling load was not dependent upon the loading rate at rates slower than 0.0001 in/sec as shown in Figure 24. Most of the remaining data was obtained at the loading rate of 0.0001 in/sec.

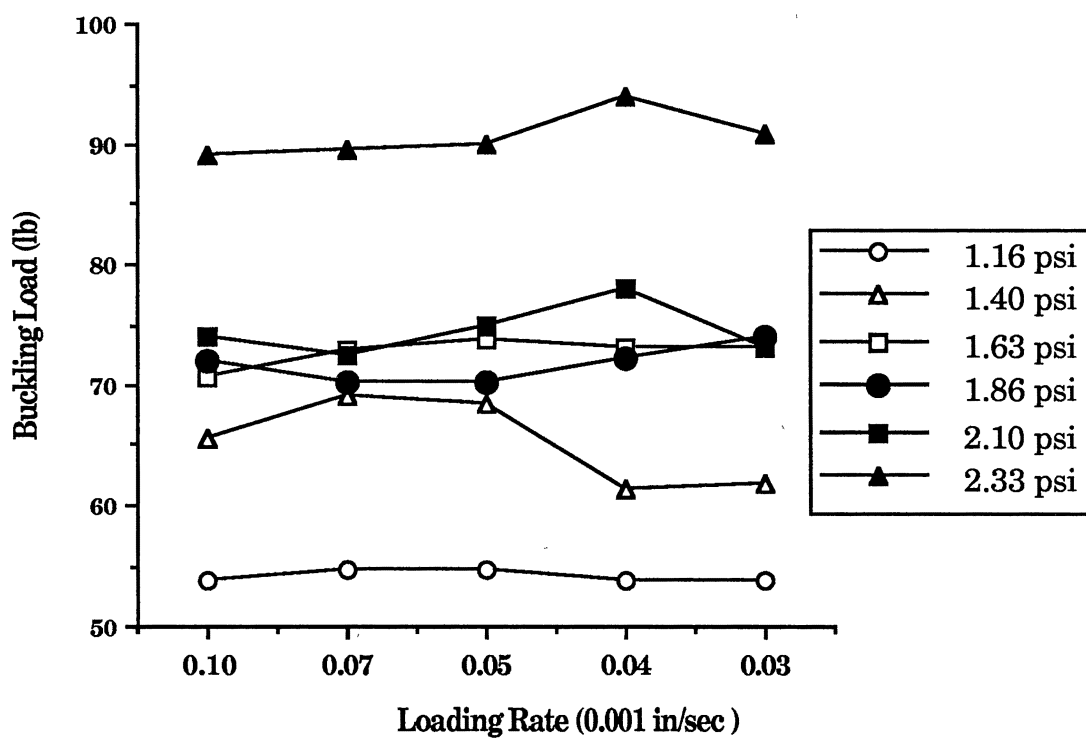


Figure 24. Effect of Loading Rate on the Buckling Load of Buckling Experiments

Figures 25 to 30 show the buckling loads for the stack pressures 1.16 to 2.33 psi. The buckling loads were scattered for all the buckling experiments. Averaged buckling loads and the standard deviations are shown in Figure 31. The standard deviations show large scattering of the buckling loads for each stack pressure. The reason for these large standard deviations was due to the misalignment of the fixture and the load cell, the initial flatness of the stacks of paper, uncertainties of the lateral pressure, the frictional behavior of the experiments and the reading error from the load vs displacement curve. The comparison of these results to the numerical solutions was discussed in the finite element analysis part and presented in Figure 13.

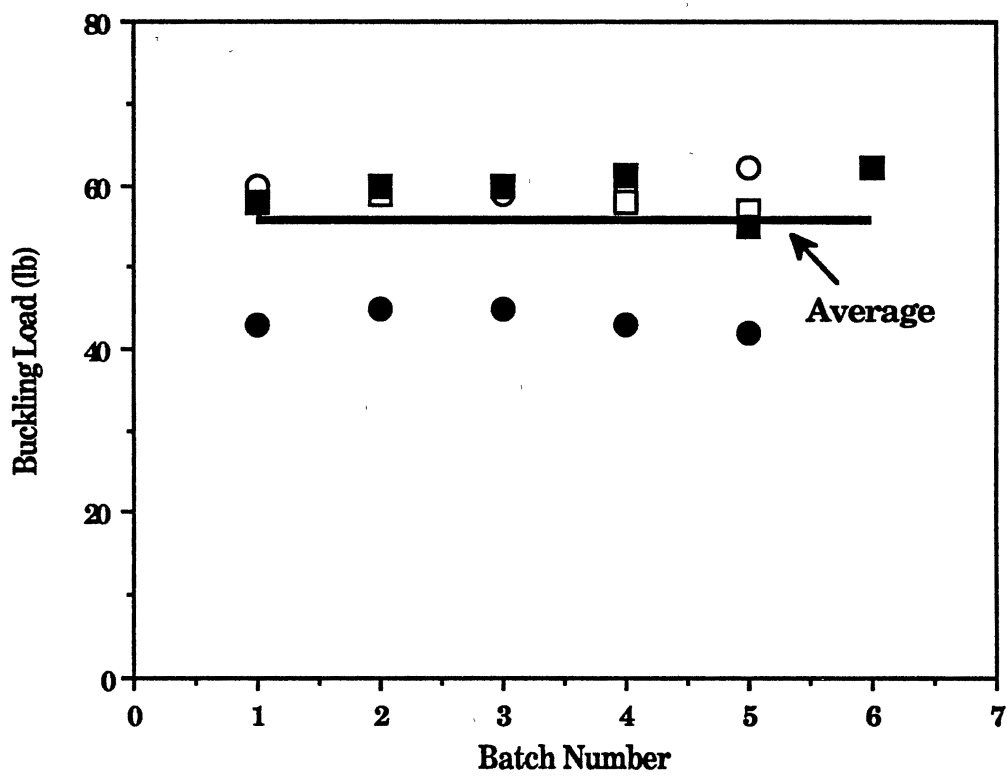


Figure 25. Buckling Loads for Stack Pressure of 1.16 psi

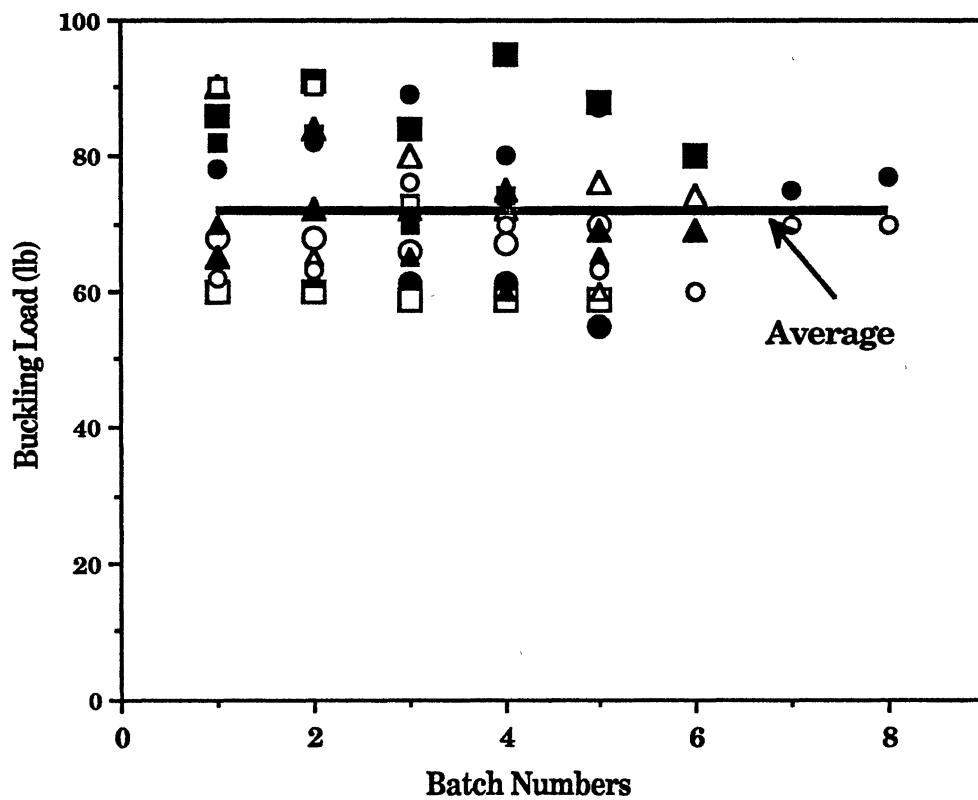


Figure 26. Buckling Loads for Stack Pressure of 1.40 psi

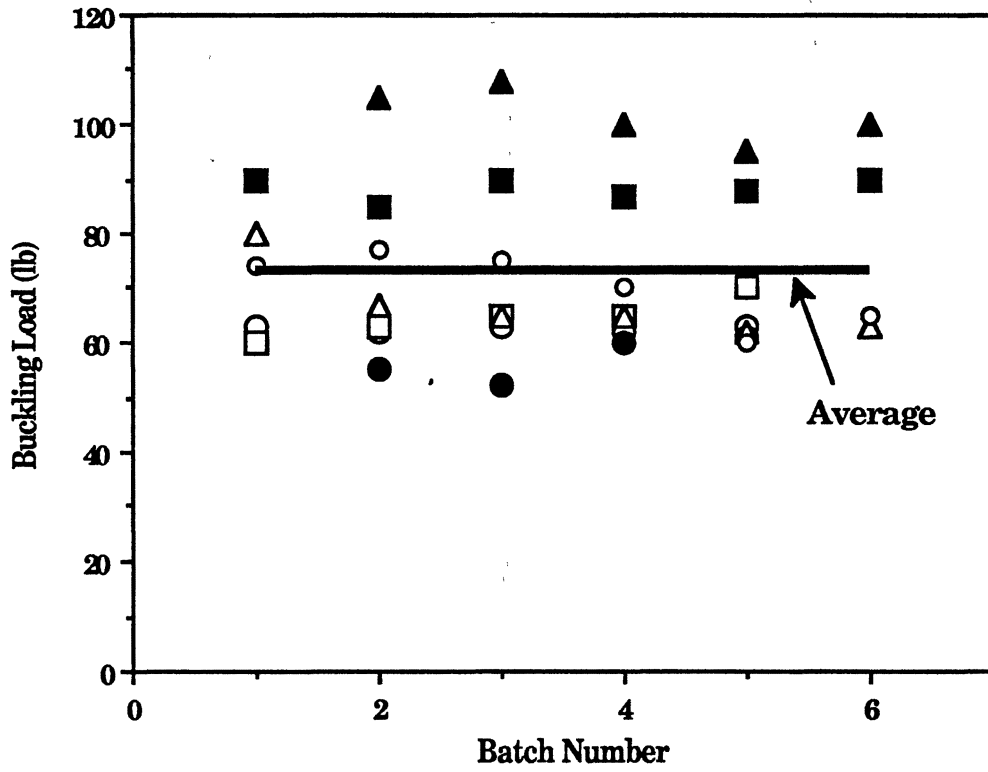


Figure 27. Buckling Loads for Stack Pressure of 1.63 psi

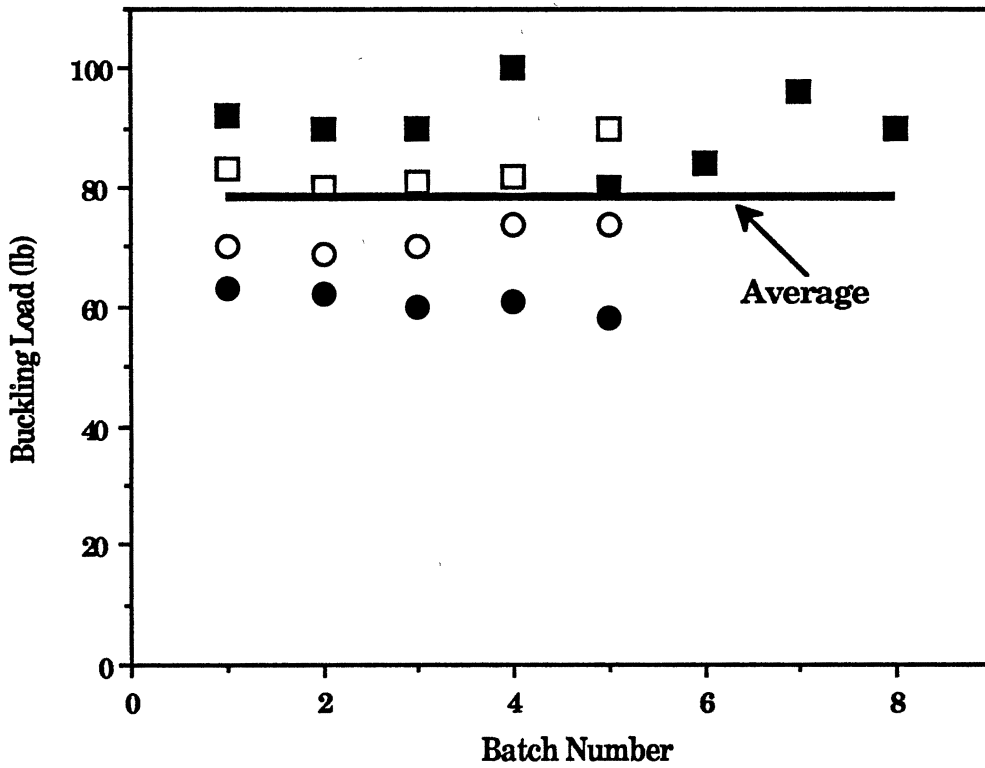


Figure 28. Buckling Loads for Stack Pressure of 1.86 psi

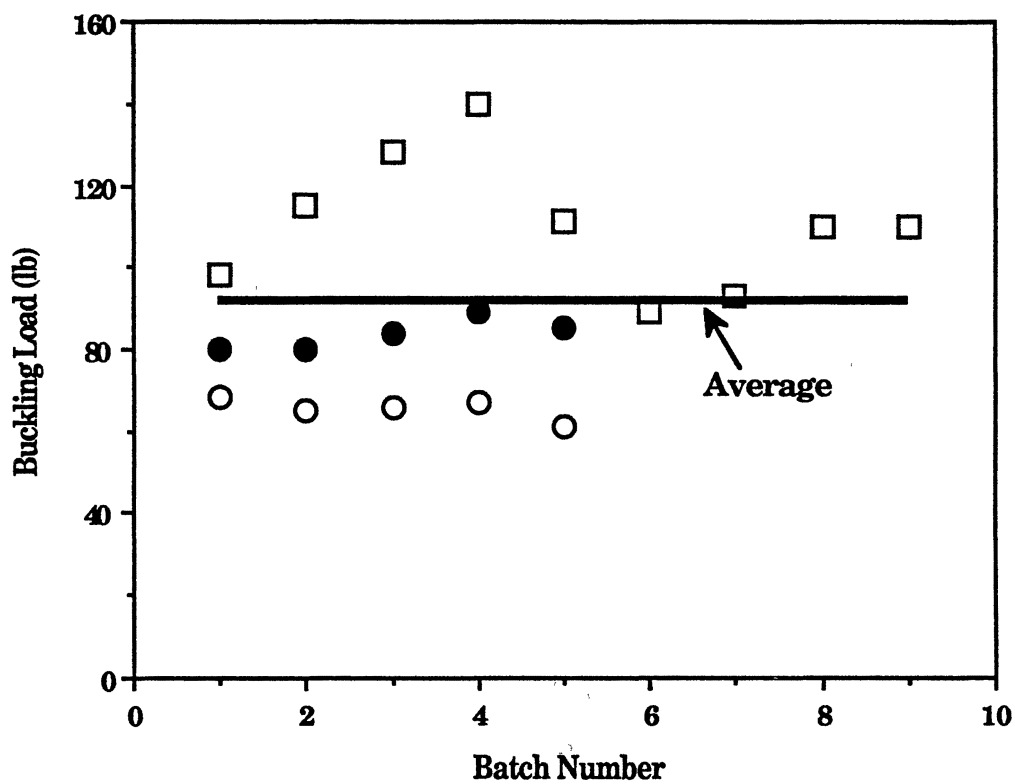


Figure 29. Buckling Loads for Stack Pressure of 2.10 psi

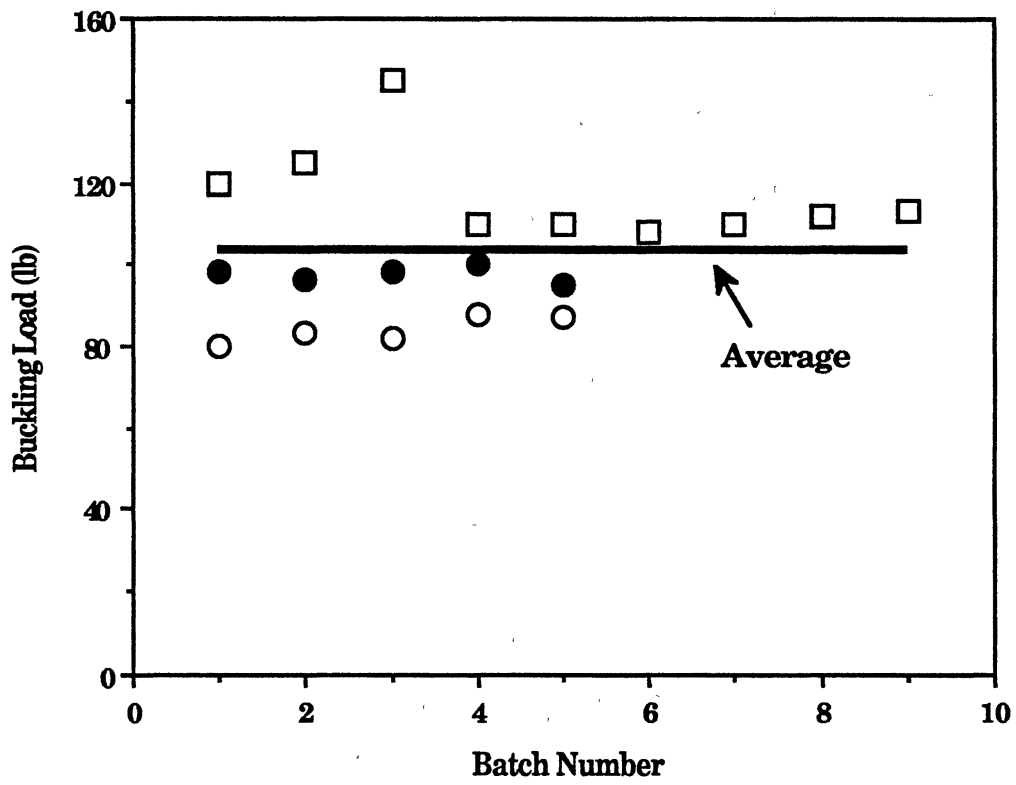


Figure 30. Buckling Loads for Stack Pressure of 2.33 psi

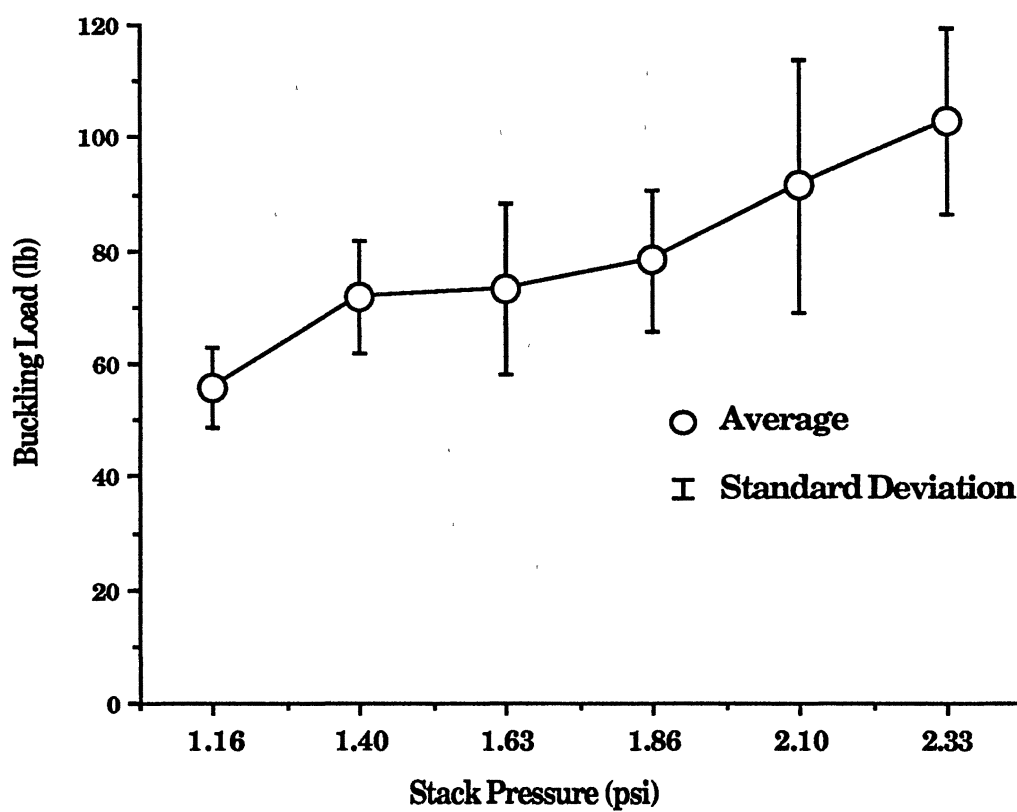


Figure 31. Buckling Loads with Standard Deviation at Stack Pressures from 1.16 to 2.33 psi

CHAPTER IV

BUCKLING ANALYSIS OF CENTER WOUND ROLLS

Finite Element Analysis

Introduction

The stress distribution of a center wound roll was calculated by Hakiel's nonlinear winding model. The variable radial pressure distribution and the corresponding radial modulus were implemented into the numerical model. The radial pressure was represented as nodal forces. The radial modulus was calculated according to the pressure by the modulus function obtained by the stack tests. The equivalent spring constant and the modulus of foundation were calculated by assuming that the springs were connected in series. The modulus of foundation is a key parameter of classic solutions.

Stress Distribution in a Center Wound Roll

Core Stiffness. A core stiffness was defined as a pressure that was necessary to strain the outside surface of the core, radially, to a value of 1 in./in. [1]. If the core is made of steel or isotropic material, the core stiffness can be derived as a function of the geometry and material properties of the core [41].

$$E_c = \frac{\sigma_r}{w/r_i} \quad \text{at } r = r_i \quad (4.1)$$

By the strain-displacement relation in a cylindrical coordinate it can be shown as:

$$E_c = \frac{\sigma_r}{\varepsilon_t} \quad \text{at } r = r_i \quad (4.2)$$

The stress-strain relation for an isotropic material is:

$$\varepsilon_t = \frac{\sigma_t - \nu\sigma_r}{E_{cm}} \quad (4.3)$$

The stresses at the outside of the core [38] are:

$$\sigma_r = -P_o \quad (4.4)$$

$$\sigma_t = -P_o \frac{r_o^2 + r_c^2}{r_o^2 - r_c^2} \quad (4.5)$$

Inserting Equations (4.3)-(4.5) into (4.2), we get:

$$E_c = E_{cm} \frac{r_o^2 - r_c^2}{r_o^2 + r_c^2 - \nu_c(r_o^2 - r_c^2)} \quad (4.6)$$

The core stiffness of the steel core in this research was:

$$E_c = (3.0E7) \frac{3.445^2 - 3.035^2}{3.445^2 + 3.035^2 - (0.3)(3.445^2 - 3.035^2)} = 3.93E6 \text{ psi} \quad (4.7)$$

Hakiel's Nonlinear Winding Model. Pfeiffer [31] regarded the radial modulus as a function of radial pressure. Yagoda [47] implemented an accurate core boundary condition into the winding model. Then Hakiel [17] implemented the finite difference method to solve the governing equations by considering the nonlinear radial modulus and the core boundary condition. The derivation of the algebraic equations from the governing

equations is shown in Appendix B. It was programmed in C-language and presented in Appendix C.

Winding Conditions. The stress distribution of a wound roll depends on the followings:

- Dimension and material properties of a core;
- Outside diameter of a roll;
- Winding speed;
- Caliper and material properties of a web;
- Winding Tension

First three parameters was fixed: Steel cores of the same size were used to avoid any effect of the core stiffness on the buckling of the roll. The outside diameter of the roll was 6", which had wide constant stress region. The winding speed of 30 feet per minute was used to reduce the air entrainment during winding.

The web material was polyester film. Constant and stepped tension windings were applied to generate the starred roll defects. Various winding conditions were presented in Table VI, Figures 32 and 35. Figure 34 shows a wide range of compressive circumferential stress distributions. Figure 37 shows large compressive circumferential stress region around the stepped area.

TABLE VI
WINDING CONDITIONS AT 3M SPLICER WINDER
 Core : I.D.=3.035", O.D.=3.445"
 Winding Speed = 30 fpm

Case Number	<u>Initial</u>		<u>Stepping</u>		<u>Final</u>	
	Radius (inch)	Tension (psi)	Radii (inch)	Tension (psi)	Radius (inch)	Tension (psi)
1	1.723	200	---	---	3.0	200
2	1.723	300	---	---	3.0	300
3	1.723	500	---	---	3.0	500
4	1.723	200	2.5 ~ 2.541	500	3.0	500
5	1.723	300	2.5 ~ 2.541	500	3.0	500

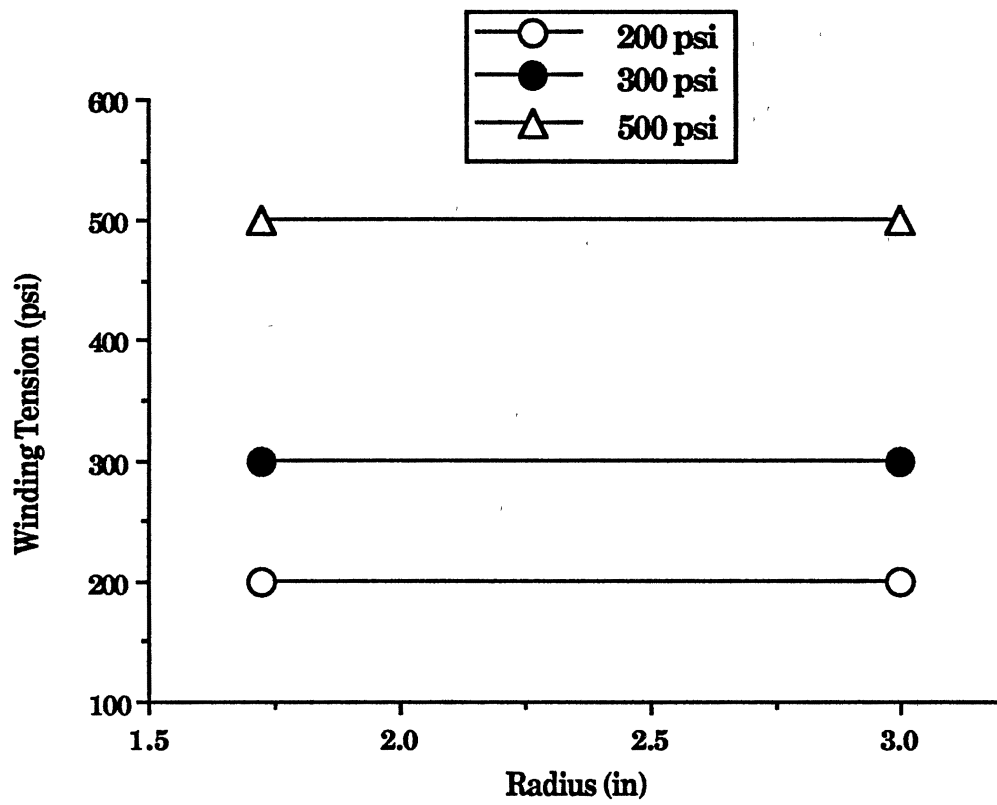


Figure 32. History of Constant Winding Tensions

Polyester Film (Type 377 / Grade 92)
Caliper = 0.00092"
Width = 6.0"
Poisson's Ratio = 0.0
Core Stiffness = 3930 ksi

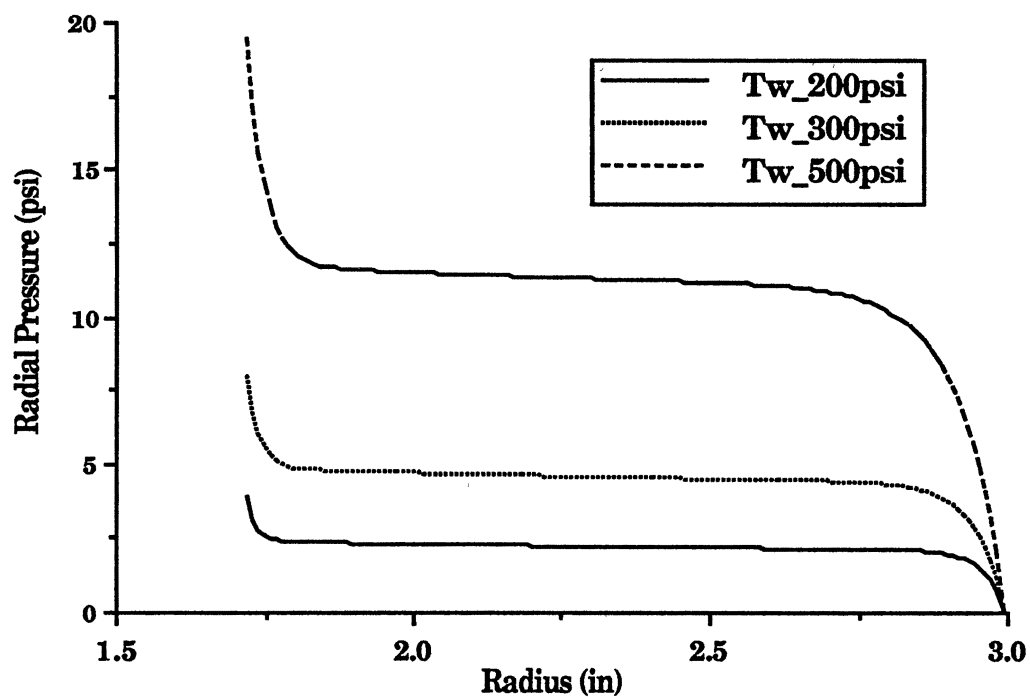


Figure 33. Radial Pressure Distribution
at Constant Tension Windings

Polyester Film (Type 377 / Grade 92)

Caliper = 0.00092"

Width = 6.0"

Poisson's Ratio = 0.0

Core Stiffness = 3930 ksi

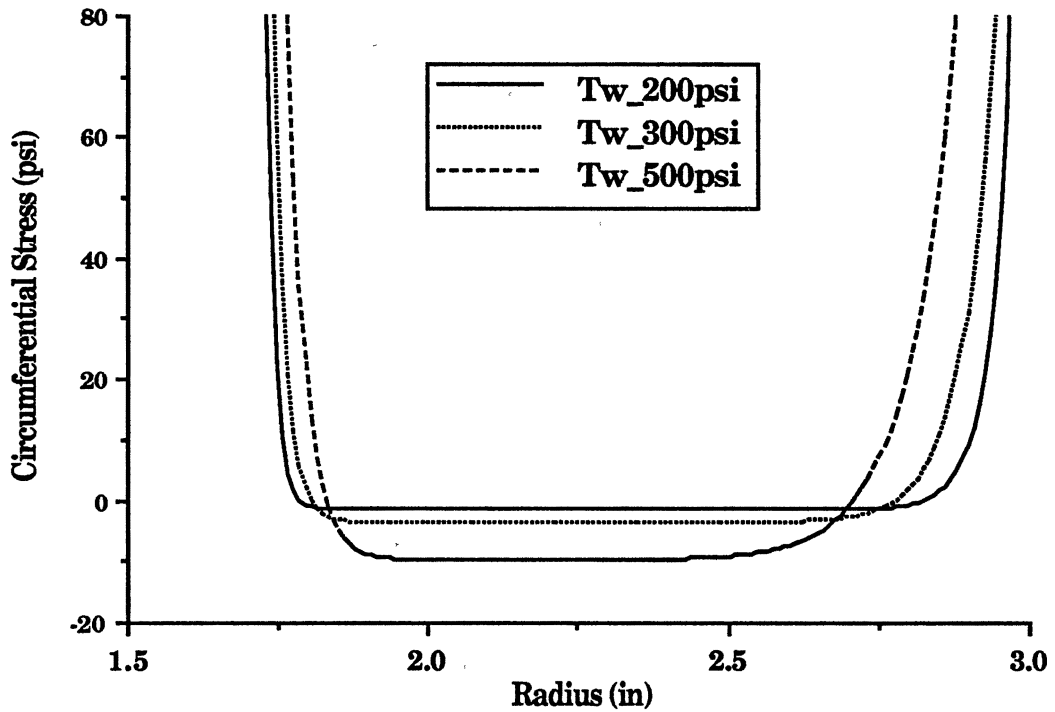


Figure 34. Circumferential Stress Distribution at Constant Tension Windings

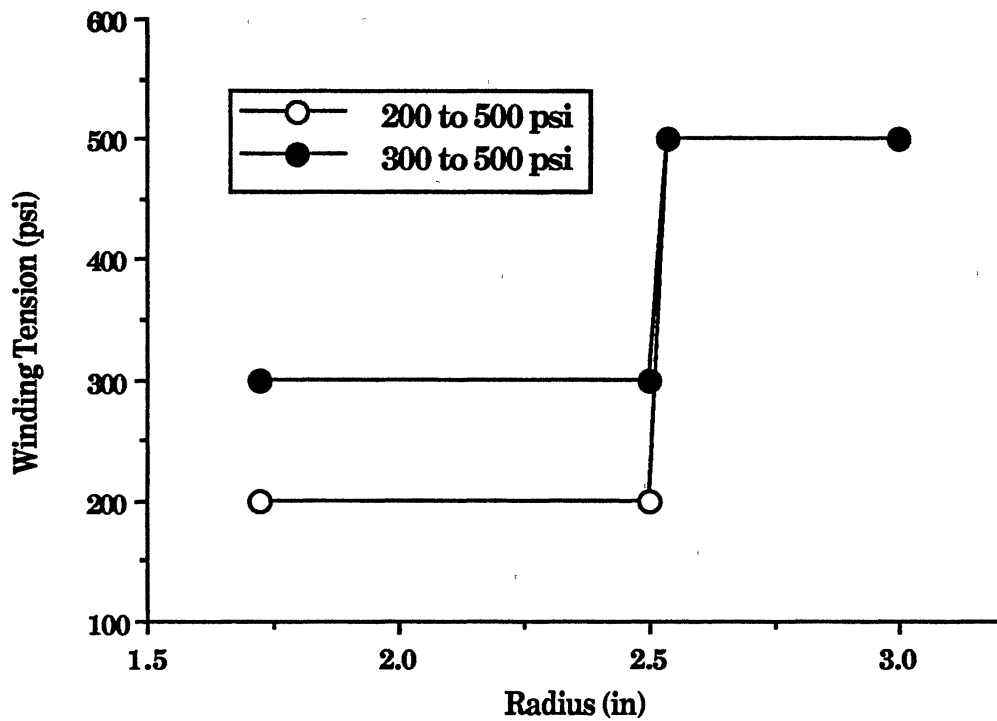


Figure 35. History of Stepped Winding Tensions

Polyester Film (Type 377 / Grade 92)
Caliper = 0.00092"
Width = 6.0"
Poisson's Ratio = 0.0
Core Stiffness = 3930 ksi

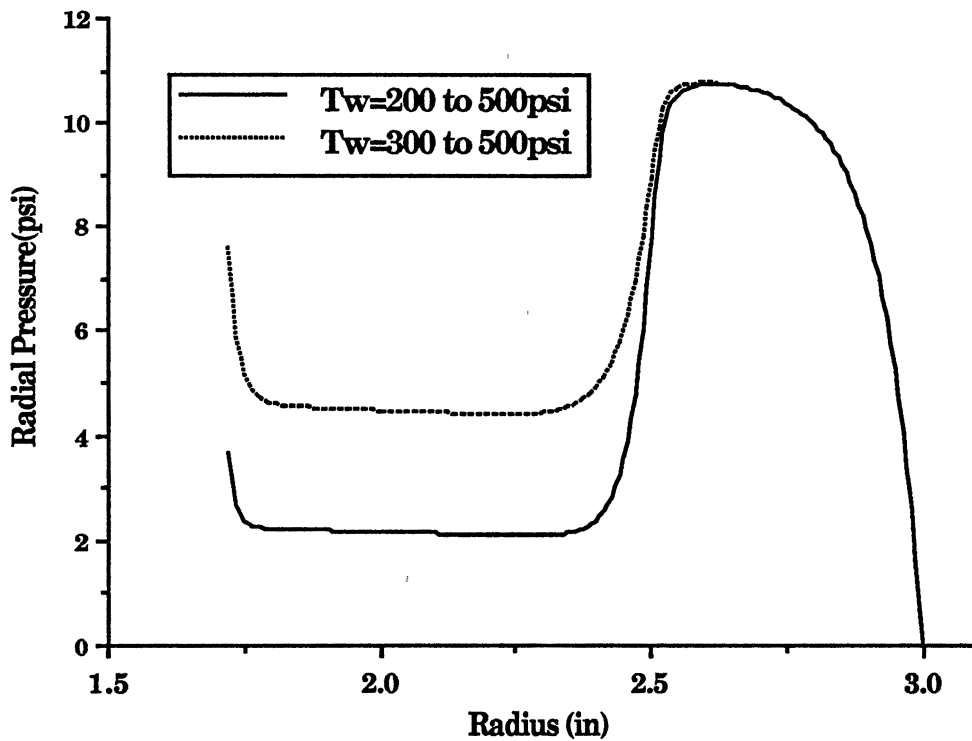


Figure 36. Radial Pressure Distribution
at Stepped Tension Windings

Polyester Film (Type 377 / Grade 92)
Caliper = 0.00092"
Width = 6"
Poisson's Ratio = 0.0
Core Stiffness = 3930 ksi

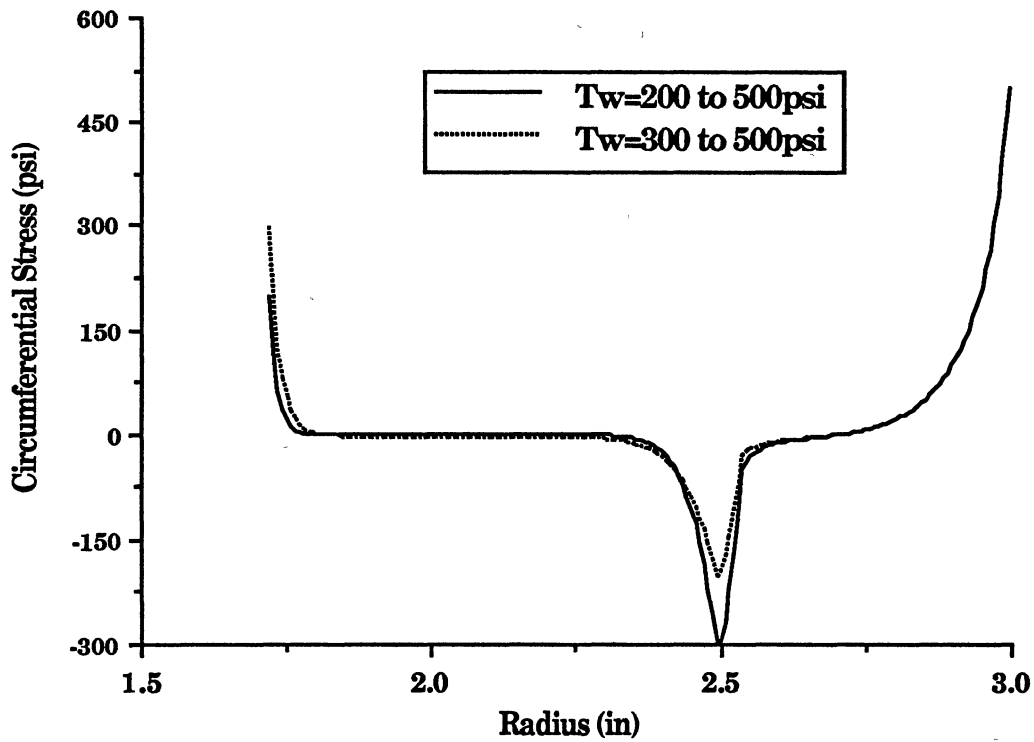


Figure 37. Circumferential Stress Distribution at Stepped Tension Windings

Programs for Hakiel's Model. The radial pressure and circumferential stress distribution in a center wound roll are calculated by the program "HAKIEL.C". The program "MESH.C" reads the output of "HAKIEL.C" and generates the radial mesh to make the input data for "ANSD.C" and "BUCKLE.C". The program "ANSD.C" generates the input data to ANSYS program as discussed in the finite element analysis section in Chapter III. The program "BUCKLE.C" calculates the classic buckling solutions and modifies the buckling load by adding the friction force due to the radial pressure. The header file "ER.H" contains the radial modulus as a function of pressure. These programs are controlled by the program "MAIN.C". A flow chart for them is shown in Figure 38.

Finite Element Model

The element types, mesh and boundary conditions for the finite element model of a center wound roll were the same as that of the stack of paper. The model of a wound roll implemented the pressure distribution in a wound roll. Only a quarter of the circumferential length of the roll was modeled as a beam length because the memory of the IBM-RT computer was limited.

Representation of Radial Pressure. A typical radial pressure distribution at a constant tension winding was shown in Figure 33. The pressure at each element was obtained by the average of the adjacent nodal pressures and was applied to the model by the incremental forces as shown in Figure 39. The total force at the right sides of the element divided by the area represents the element pressure. The radial modulus of the element was calculated according to the element pressure.

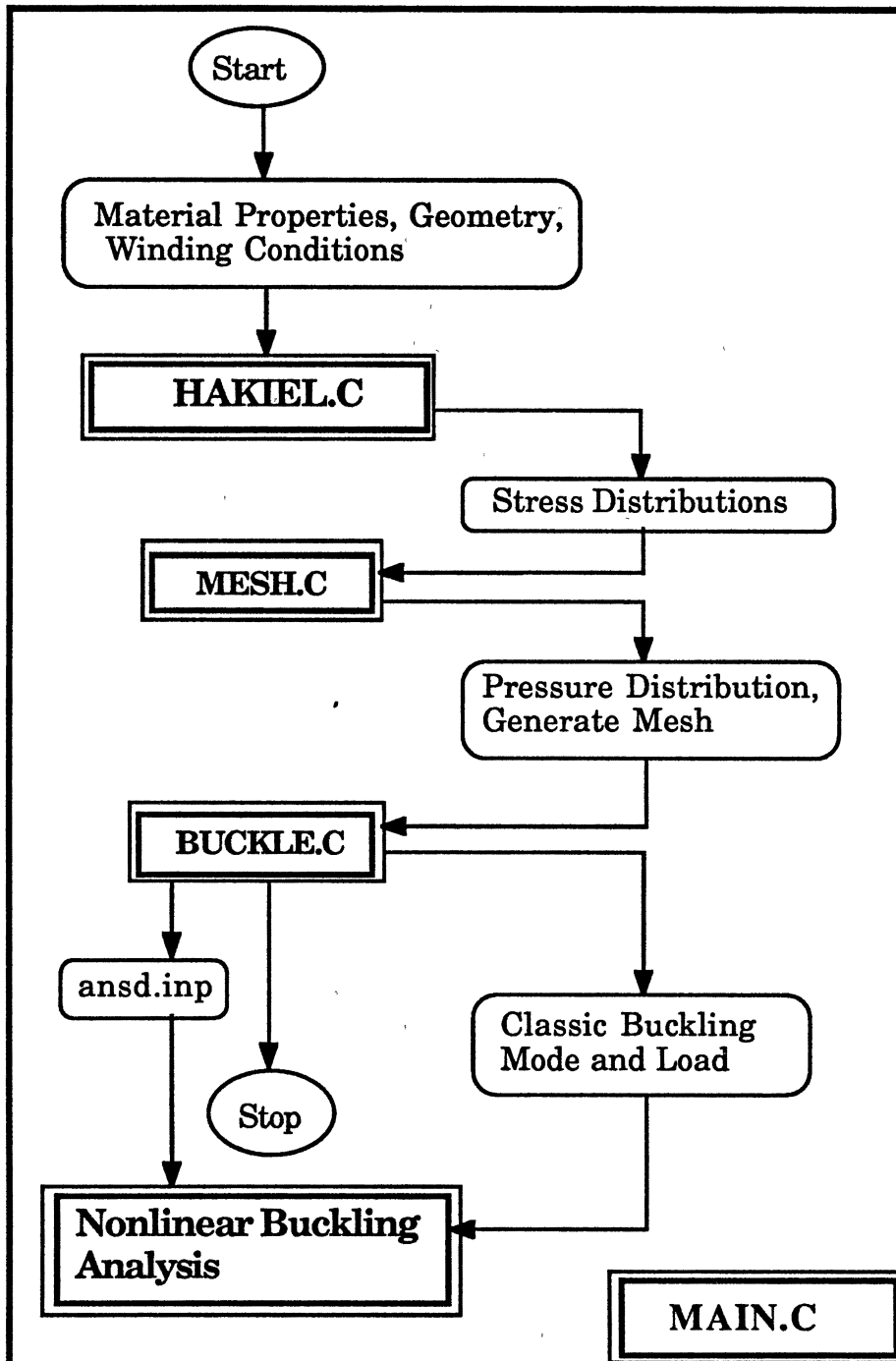


Figure 38. Flow Chart of Programs for Hakiel's Model

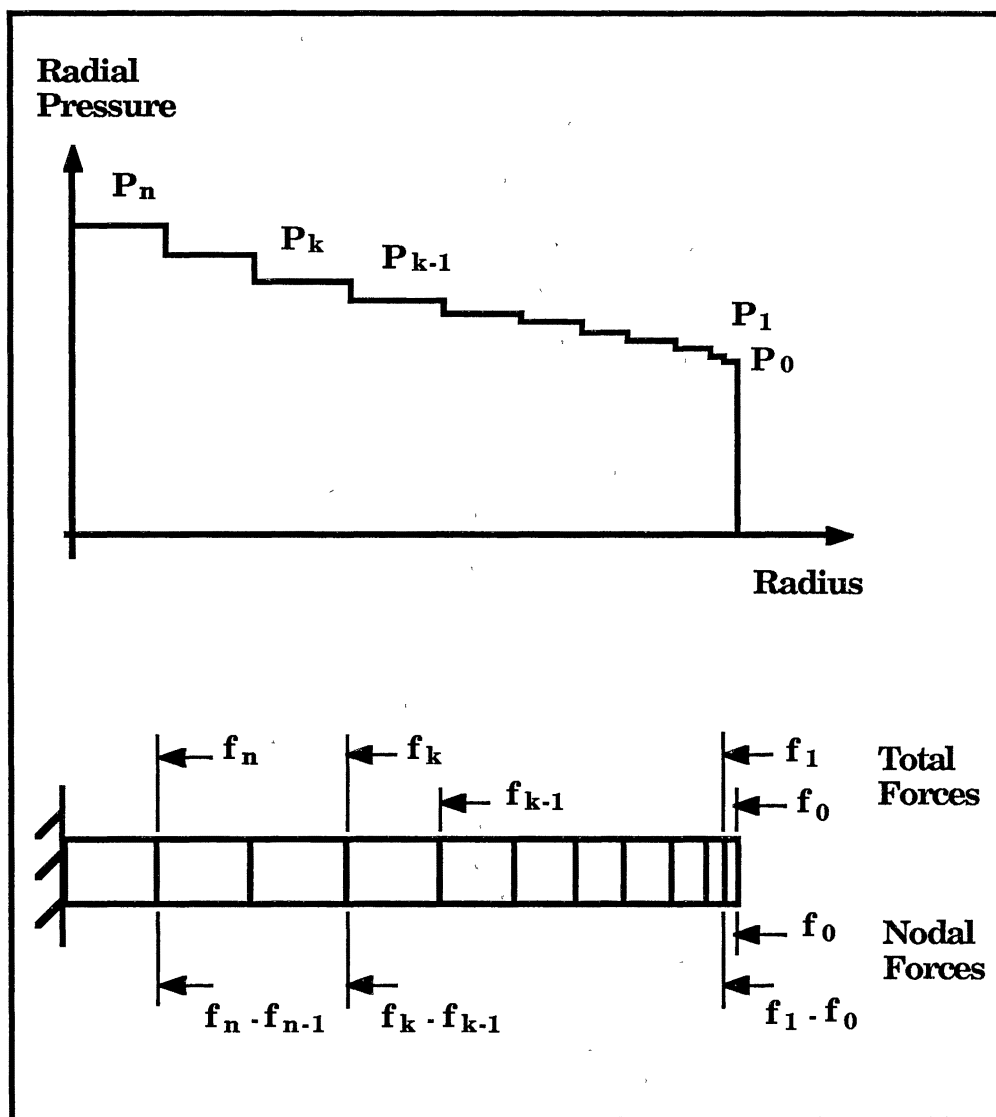


Figure 39. Representation of Radial Pressure in Finite Element Model

Equivalent Modulus of Foundation. Every element in the radial direction has a different radial modulus and size. A spring constant of the foundation was obtained by assuming that the elements were connected in a series of linear springs as shown in Figure 40. By Hooke's law, a spring constant of individual element is :

$$\alpha_i = \frac{AE_{r,i}}{L_i} \quad (4.8)$$

Total displacement under an axial force will be the summation of the individual displacements:

$$\delta = \sum_{i=1}^{na} \delta_i = \sum_{i=1}^{na} \frac{F}{\alpha_i} \quad (4.9)$$

The total displacement can be expressed by an equivalent spring constant:

$$\delta = \frac{F}{\alpha_{eq}} \quad (4.10)$$

Inserting α_i in Equation (4.8) into (4.9) and equating Equations (4.9) and (4.10) yield an equivalent spring constant as:

$$\alpha_{eq} = \left[\sum_{i=1}^{na} \frac{L_i}{AE_{r,i}} \right]^{-1} \quad (4.11)$$

The modulus of foundation can be obtained by simply dividing the spring constant by the beam length. The corresponding classic buckling mode and load can be calculated by Equations (3.22) and (3.23).

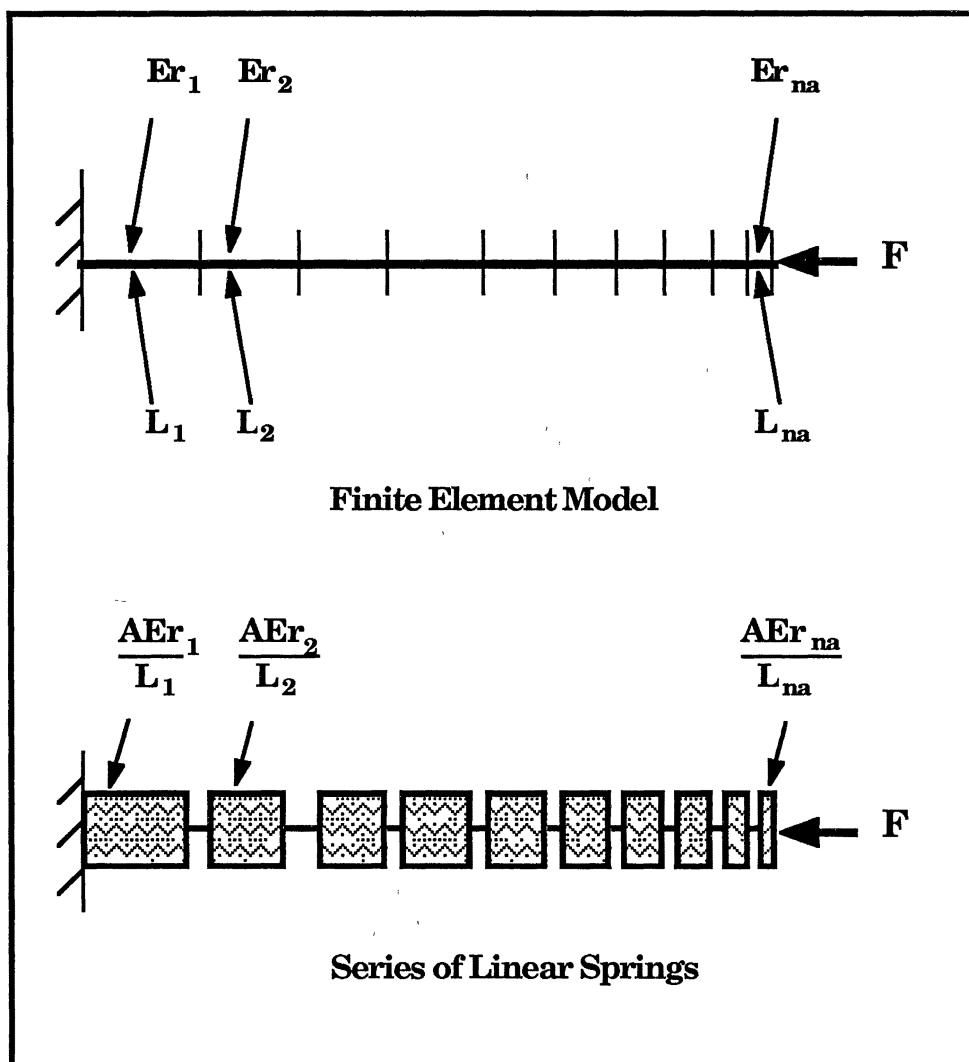


Figure 40. Equivalent Spring Constant of Foundation

Results of Finite Element Analysis

Parametric Study of Calculating Conditions

Perturbing Load. In the buckling analysis, several perturbing loads were applied at the centers of the nodal points of the beam to generate assumed buckling mode. Several perturbing loads were tested for the constant tension winding of 200 psi. The inner and outer roll radii were 1.723" and 3.00". The beam was selected between the radii 2.40" and 2.75". The beam length was calculated at the radius 2.361" which was at the middle of the wound roll. The convergent bound of large displacement was fixed at 0.005". The perturbing load was varied from 0.005 lb to 0.2 lb.

Figure 41 shows the lateral displacements for different perturbing loads. The circled points represented the perturbed displacements. The triangular and rectangular points were the displacements at the axial loads of 15 and 15.5 lb, which were lower and upper bounds of the buckling load. The displacements at these axial loads were almost the same as that due to the perturbing load, i.e., the beam maintained its original geometry.

Figure 42 shows the effect of the perturbing load on the buckling mode and stress. The buckling mode was not changed at all. The buckling stress was 12.18 psi at 0.005 lb and 12.66 psi at 0.2 lb. The error between them is only 3.8 %. The buckling load was not changed much for different perturbing loads.

The buckling load corresponding to the perturbed geometry represents the buckling load at slightly post buckled state. When the perturbing load was too small, the lateral displacement due to the perturbing load was too small to be detected because the ANSYS output

had only six significant digits. If it is too large, the buckling load may represent the load at highly post buckled state.

To calculate the buckling load, the perturbing load should be as small as possible, which can cause detectable lateral displacement.

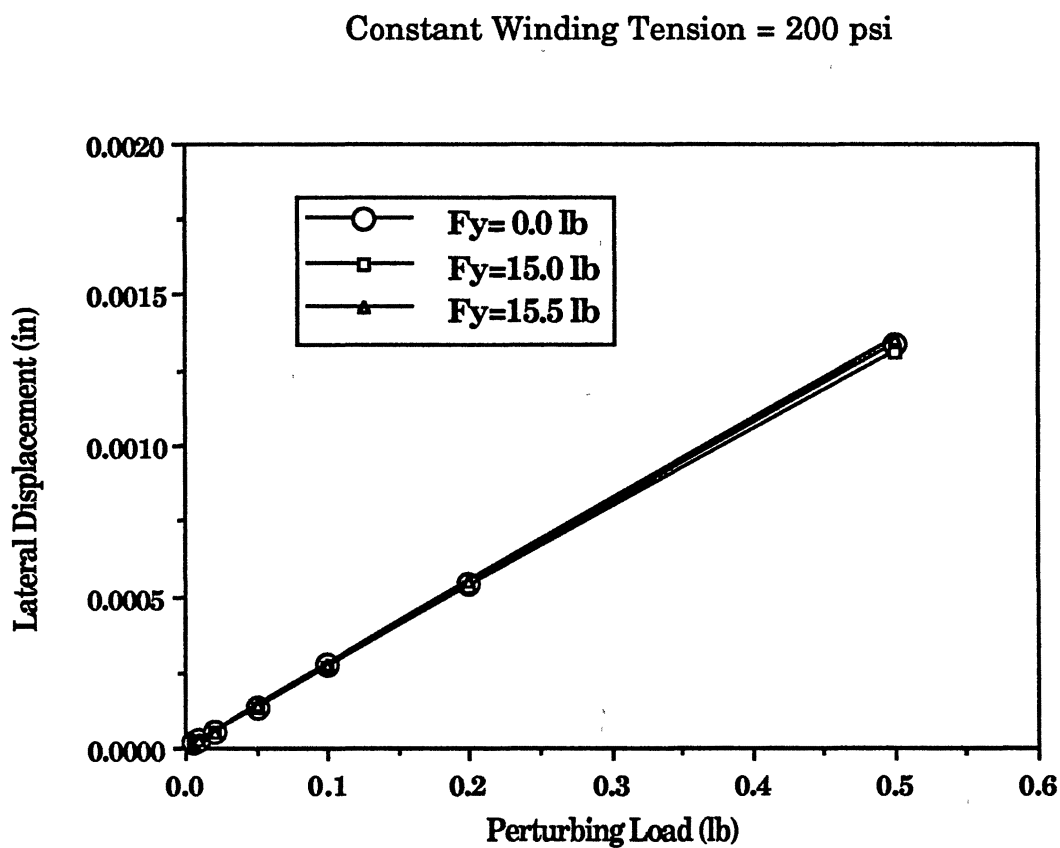


Figure 41. Lateral Displacements for Different Perturbing Loads

Calculating Conditions:

Winding Tension = 200 psi
 Inner Roll Radius = 1.723"
 Outer Roll Radius = 3.00"
 Beam Location = 2.40" to 2.75"
 Beam Length = 3.709"
 Convergent Bound = 0.005"

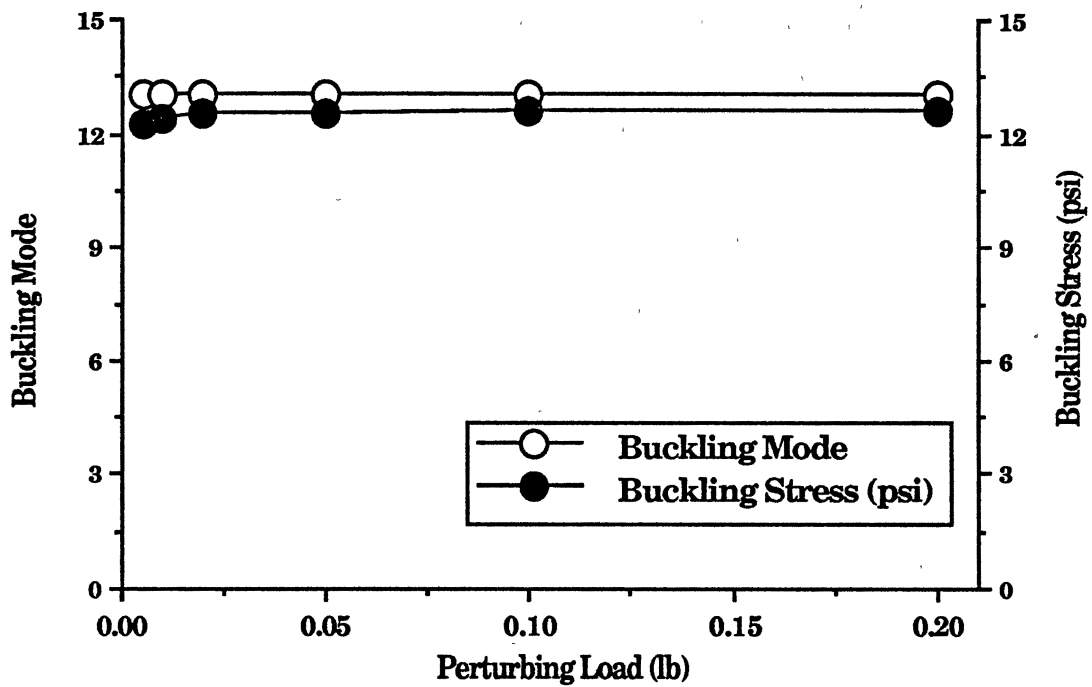


Figure 42. Effect of Perturbing Load on the Buckling Mode and Stress

Convergent Bound. To perform the geometric nonlinear static analysis by ANSYS program, the convergent bound of the displacement should be set in conjunction with the number of iterations according to the geometry, the material properties and applied load. The default value is 0.001.

Several convergent bounds were tested for the constant tension winding of 200 psi. The inner and outer roll radii were 1.723" and 3.00". The beam was selected between the radii 2.40" and 2.55". The beam length of 3.709" was calculated at the middle of the wound roll. The perturbing load was fixed at 0.05 lb. The convergent bound was varied from 0.0001" to 0.05".

When the convergent bounds were 0.0002" and 0.0001", the solutions did not converge within ten iterations. The solutions for other cases converged within two or three iterations with accurate displacement solutions. Figure 43 shows the effect of convergent bound on the buckling mode and stress. The buckling mode was not changed at all. The buckling stress was 12.46 psi at 0.0005" and 12.54 psi at 0.05". The error between them was only 0.6 %. The convergent bound did not affect the solution noticeably.

If the convergent bound is large enough that the iteration stops too early even if the solution is not accurate, the solution may not satisfy the equilibrium condition for given boundary conditions. If it is too small, the displacement may not converge at all or too many iterations may be required to get a converged solution. The convergent bound should be as small as possible to obtain the converged solution within a tolerable number of iterations.

Calculating Conditions:

Winding Tension = 200 psi
 Inner Roll Radius = 1.723"
 Outer Roll Radius = 3.00"
 Beam Location = 2.40" to 2.55"
 Beam Length = 3.709"
 Perturbing Load = 0.05 lb
 Convergent Bound = 0.001"

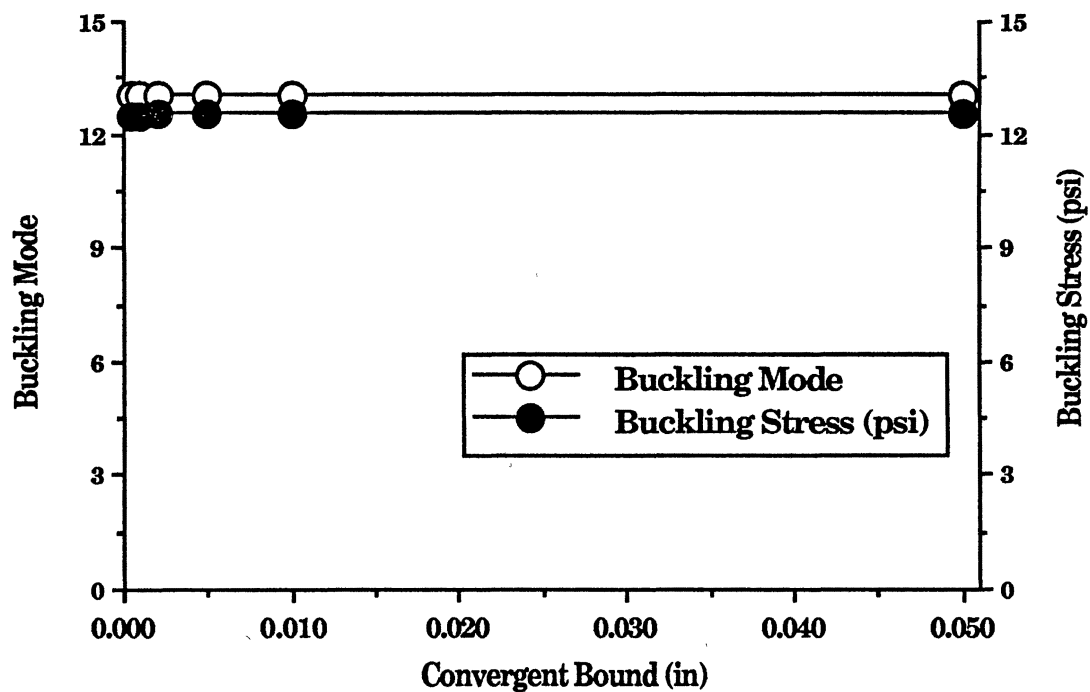


Figure 43. Effect of Convergent Bound on the Buckling Mode and Stress

Parametric Study of Beam Geometry and Location

A wound roll was modeled in rectangular coordinates rather than polar coordinates. The beam part was selected from the negative circumferential stress region. The buckling stress and mode may be affected by the selection of the length, location and thickness of the beam. Various lengths, locations and thicknesses of the beam were tested to find the effects of them on the numerical solutions and to find the best method to select the beam from the stress distribution of a wound roll.

Beam Location. The beam length was calculated by a quarter of the circumferential length of the roll at the middle of the wound roll. The beam thickness was fixed at 0.15". The perturbing load was 0.05 lb and the convergent bound was 0.001". The beam was located from inside to the outside of the roll as shown in Figure 44.

Figure 45 shows the effect of the beam location on the buckling mode and stress. When the beam was located at the radius 2.225", the buckling mode was 17 and the buckling stress was 25.16 psi. When the beam was located at the radius 2.676", the mode was 14 and the buckling stress was 17.92 psi. The buckling stress was decreased almost linearly as the beam was moved out from the core showing a sensitivity to foundation stiffness which is a function of radial pressure. The level of the circumferential stress should be considered when selecting the beam location.

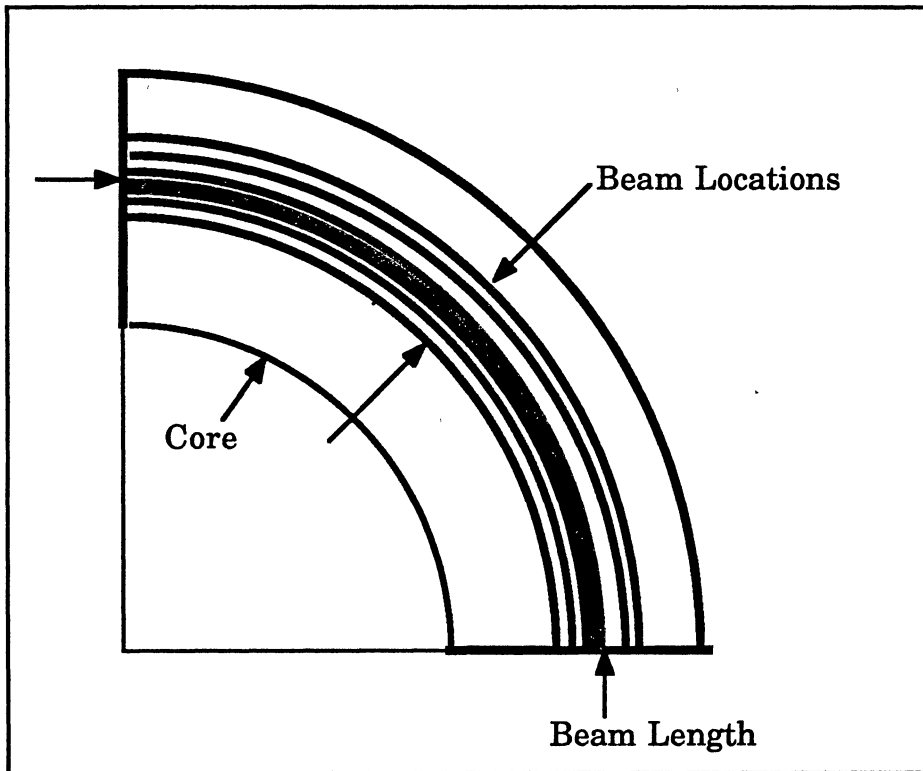


Figure 44. Beam Locations in a Wound Roll

Calculating Conditions:

Winding Tension	=	200 psi
Inner Roll Radius	=	1.723"
Outer Roll Radius	=	3.00"
Beam Thickness	=	0.15"
Beam Length	=	3.709"
Perturbing Load	=	0.05 lb
Convergent Bound	=	0.001"

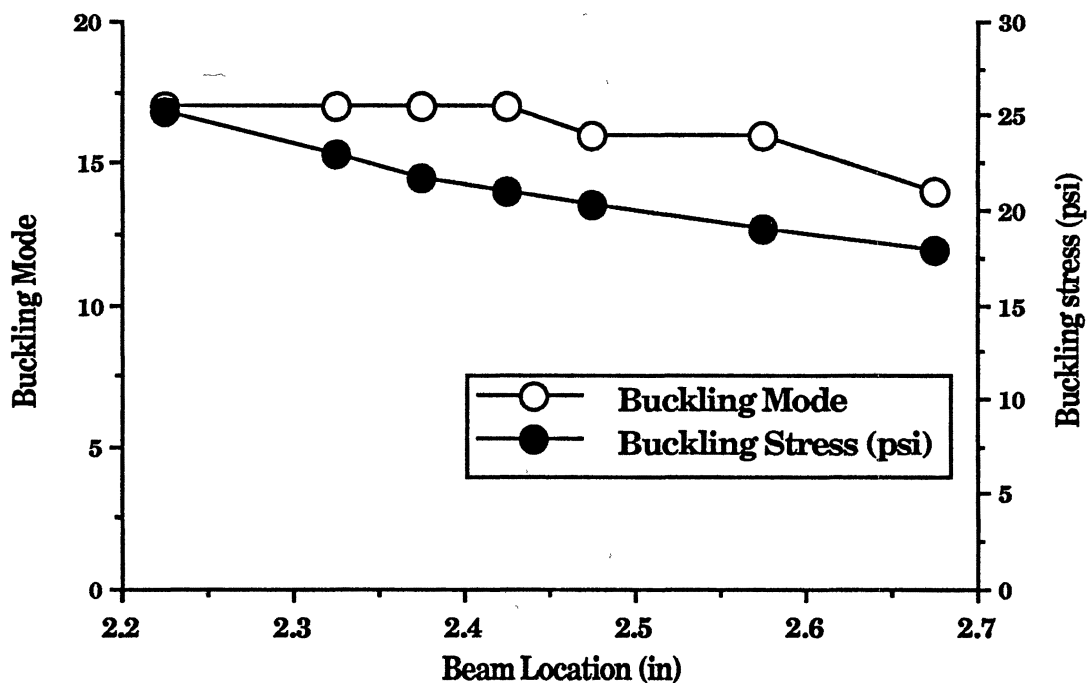


Figure 45. Effect of Beam Location on the Buckling Mode and Stress.

Beam Length. The beam was located at the middle of the roll. The beam thickness was fixed at 0.15". The perturbing load was 0.05 lb and the convergent bound was 0.001". The beam length was calculated by a quarter of the circumferential length of the roll at several locations.

Figure 46 shows the effect of the beam length on the numerical solutions. As the beam length was increased, the buckling mode was increased from 13 to 17 and the buckling stress was decreased from 20.97 psi to 18.53 psi. This shows that the beam length does not affect the buckling stress much but it affects the buckling mode considerably. It may be reasonable to calculate the beam length at the middle of the wound roll.

Beam Length with Same Effective Length. Because a quarter of the circumferential length of the roll was modeled, it should be examined whether the numerical buckling stress and mode can represent that at full circumferential length. The effective length was defined as the beam length for one buckling mode or half-sine wave. The beam length was varied so that the effective length of the beam was constant at 0.20".

Figure 47 shows the buckling stresses and modes for different beam lengths with the same effective length. When the beam length was 1.20" and the corresponding buckling mode was 6, the buckling stress was 30.64 psi. As the beam length was increased to 2.00" with the buckling mode 10, the buckling stress was decreased to 25.45 psi, i.e., the buckling stress was decreased by 17 %. When the beam length was 4.00", the buckling stress was decreased by 33 %. Even if the beams had the same effective lengths, the buckling stress was decreased as the buckling mode was increased. If this is an eigenvalue buckling problem and the effective length is the same, the buckling stress should be the same. This means that the actual

buckling stress was overestimated by the numerical model because a quarter of the roll was modeled instead of modeling the full circumferential length.

Calculating Conditions:

Winding Tension	=	200 psi
Inner Roll Radius	=	1.723"
Outer Roll Radius	=	3.00"
Beam Thickness	=	0.15"
Beam Location	=	2.30 to 2.45"
Perturbing Load	=	0.05 lb
Convergent Bound	=	0.001"

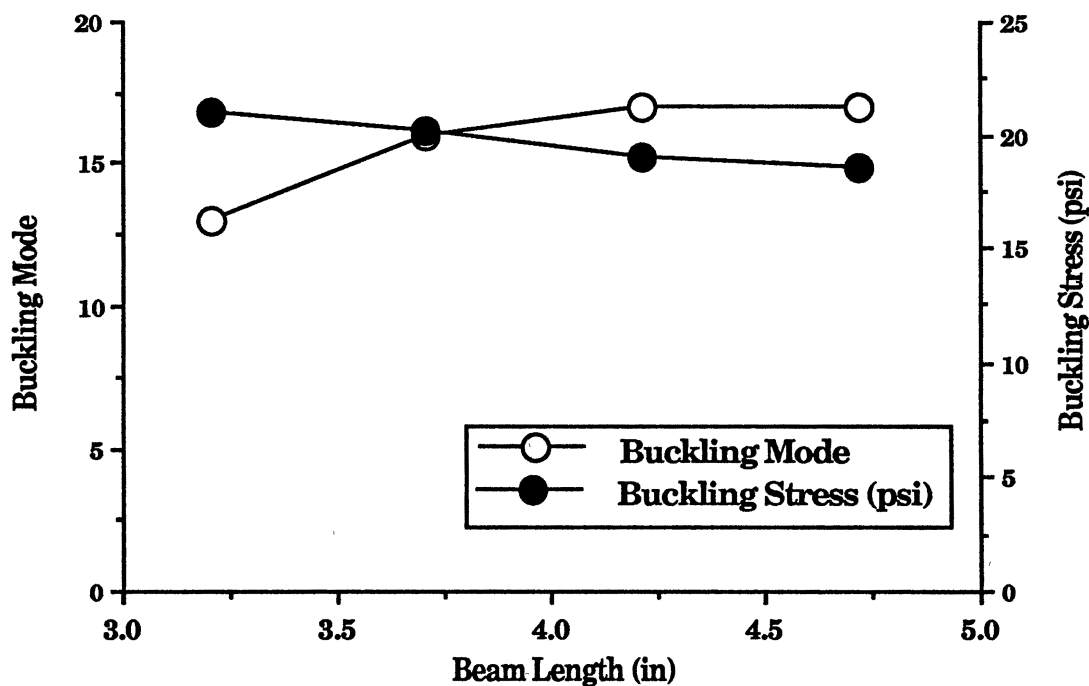


Figure 46. Effect of Beam Length on the Buckling Mode and Stress.

Calculating Conditions:

Winding Tension = 200 psi
 Inner Roll Radius = 1.723"
 Outer Roll Radius = 3.00"
 Beam Thickness = 0.15"
 Beam Location = 2.30 to 2.45"
 Perturbing Load = 0.05 lb
 Convergent Bound = 0.001"

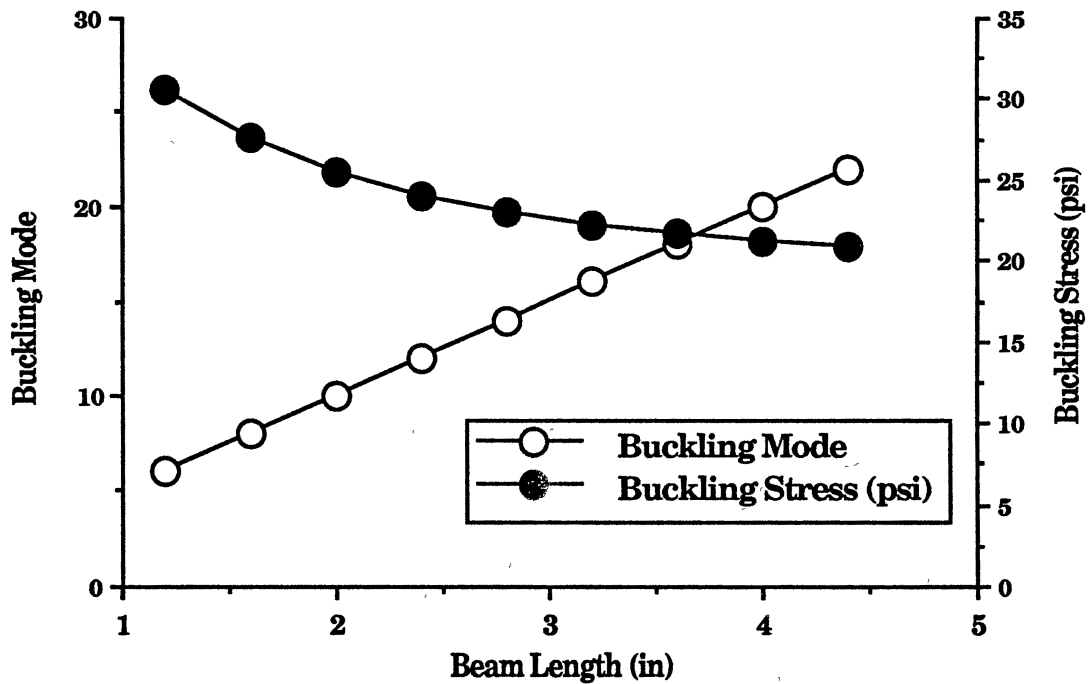


Figure 47. Buckling Modes and Stresses for Different Beam Length with Same Effective Length.

Beam Thickness. The location and the length of the beam were obtained at the middle of the roll. The perturbing load was 0.05 lb and the convergent bound was 0.001". The beam thickness was varied from 0.10" to 0.35" by an increment of 0.05".

Figure 48 shows the effect of the beam thickness on the buckling mode and stress. When the beam thickness was 0.1", the buckling mode was 17 and the buckling stress was 24.9 psi. When the beam thickness was 0.35", the buckling mode was decreased to 13 and the buckling stress was decreased to 13.1 psi, which was almost half of the buckling stress at the thickness of 0.1". The buckling stress was decreased exponentially as the beam thickness was increased.

Results of Parametric Study. From the parametric study of the effects of the location, length, and thickness of the beam, the beam thickness was found to be the most important parameter of the buckling analysis of a center wound roll. The procedure to select the beam thickness by considering the circumferential stress distribution and to calculate the corresponding buckling mode and stress was as follows:

1. Select a beam corresponding to a certain level of compressive circumferential stress. ex) $T_r > 10\%$ of $T_r(\max)$
2. Calculate the buckling mode and stress.
3. Compare the buckling stress to the circumferential stress.
 If the buckling stress is less than minimum circumferential beam stress, increase the beam thickness.
 If the buckling stress is larger than minimum circumferential beam stress, decrease the beam thickness.
4. Repeat the procedures 1 through 3 until the buckling stress and minimum circumferential beam stress are within an acceptable limit.

Calculating Conditions:

Winding Tension = 200 psi
 Inner Roll Radius = 1.723"
 Outer Roll Radius = 3.00"
 Beam Length = 3.709"
 Beam Location = 2.40 + h"
 Perturbing Load = 0.05 lb
 Convergent Bound = 0.001"

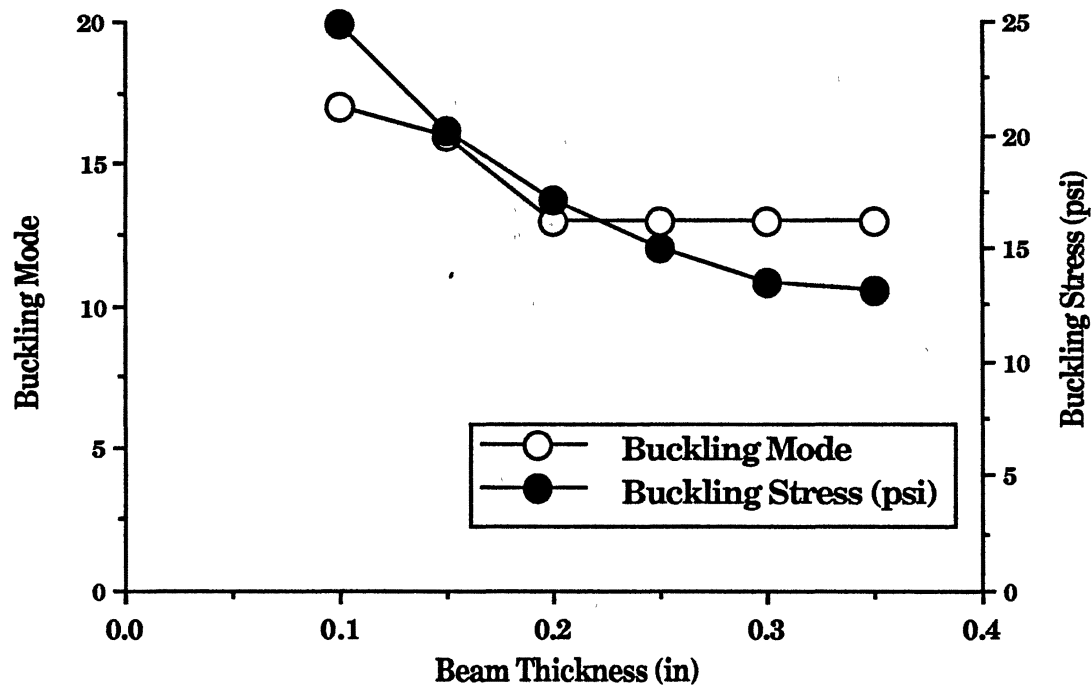


Figure 48. Effect of Beam Thickness on the Buckling Mode and Stress

Stepped Tension Windings

To generate a large compressive circumferential stress region, the winding tension was stepped from 200 to 500 psi and from 300 to 500 psi between the radii of 2.500" and 2.541" as shown in Figure 35. The inner and outer radii were 1.723" and 3.00". The radial pressure and the circumferential stress distribution are shown in Figures 36 and 37.

The results of the parametric study of the effect of the beam geometry and location on the numerical solutions were applied to the stepped tension windings.

The numerical buckling stresses for different beam selections were overlapped on the circumferential stress distribution in Figure 49. At first, the beam thickness was selected by studying the region within the wound roll in which the circumferential stresses of the roll were larger than 30.421 psi, which was 10 % of the maximum circumferential stress in absolute value. The corresponding buckling mode and stress were 17 and 19.65 psi. Because the buckling stress was less than the minimum circumferential beam stress, the beam thickness was increased by choosing 5 % of the maximum circumferential stress. The corresponding buckling mode and stress were 16 and 16.40 psi. By the iterative procedure developed in the parametric study, the beam thickness was selected so that the minimum circumferential beam stress and the buckling stress were close enough.

Figure 50 compares the buckling stresses to the minimum circumferential beam stresses at various beam thicknesses. At the fourth iteration with a beam thickness of 0.1896", the minimum circumferential beam stress of 17.04 psi was close to the buckling stress of 17.22 psi. The

corresponding buckling mode was 17. Because one quarter of the roll was modeled, the buckling mode was 68 for this stepped winding condition.

Stepped Winding Tension = 200 to 500 psi
 St = Minimum Circumferential Beam Stress
 Scr = Buckling Stress

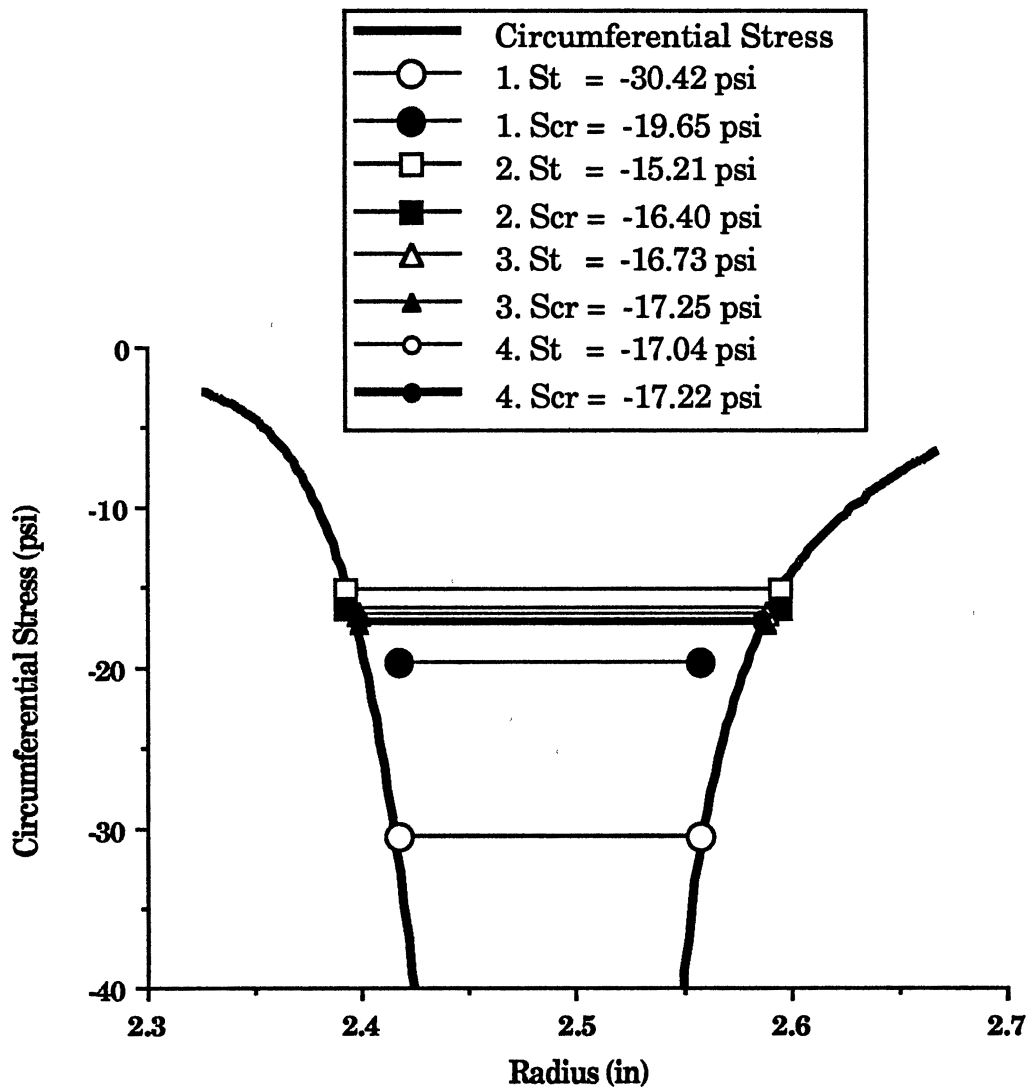


Figure 49. Determination of Beam Thickness from Circumferential Stress Distribution

Stepped Tension Winding = 200 to 500 psi

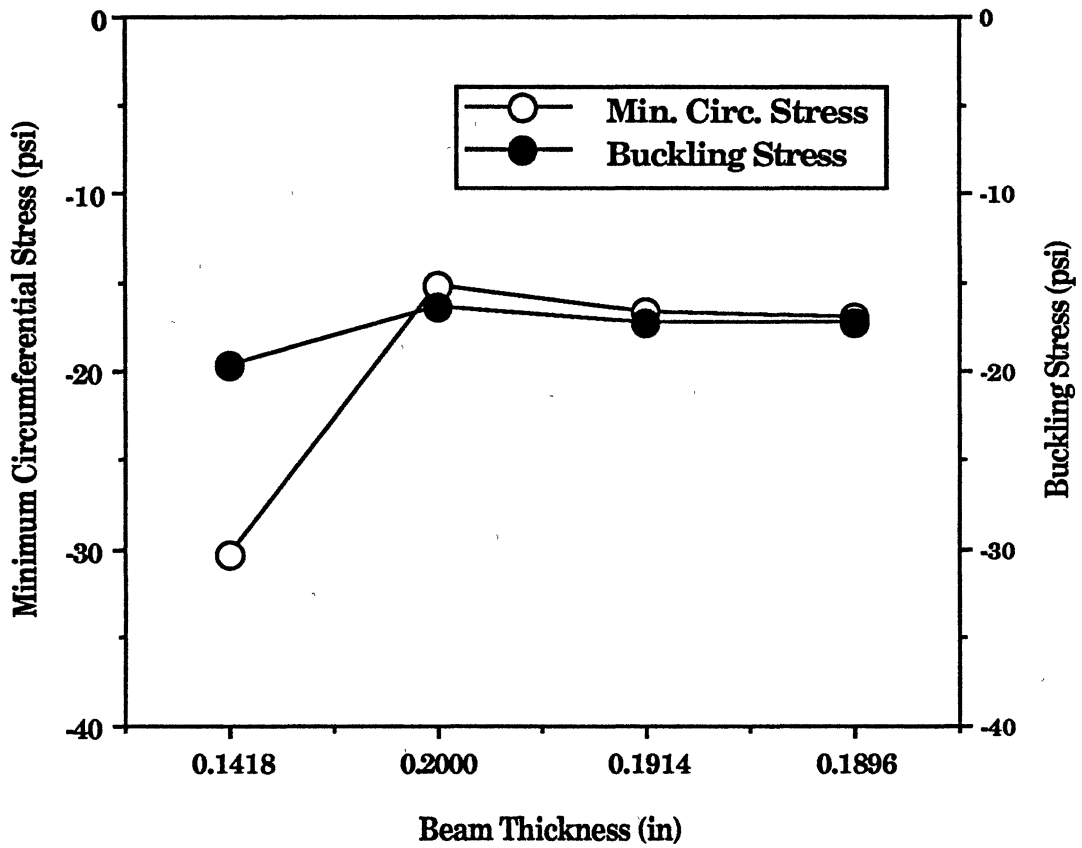


Figure 50. Determination of Beam Thickness By Comparing Buckling Stress to Circumferential Stress

With the same procedure, the buckling mode and stress were calculated for the stepped tension winding from 300 to 500 psi.

In Table VII and Figure 51, the classic buckling modes are shown to be smaller than the numerical and experimental ones within a 30 % error. The classic buckling stresses including friction force were smaller than the numerical buckling stresses within a 25 % error as shown in Table VII and Figure 52. Considering the computing time, the classic solution can be a useful tool to roughly predict the numerical solution and the starring of a wound roll for a given winding condition.

In Table VII and Figure 51, the numerical buckling mode 68 at the stepped winding tension of 200 to 500 psi was within a standard deviation 8.68 of experimental buckling mode 76. The numerical buckling mode 80 at the stepped winding tension of 300 to 500 psi was almost the same as the averaged experimental buckling mode 78.

With these comparisons of the buckling modes from the numerical and experimental analyses, the finite element model was proved to be useful to predict the buckling stress of center wound rolls.

TABLE VII
BUCKLING MODES AND STRESSES
FOR CENTER WOUND ROLLS

Winding Tension (psi)	Classic			% Error	Numerical		Experimental Buckling Mode
	Buckling Mode	Stress	Friction involved		Buckling Mode	Stress	
200~500	13(52*)	10.15	15.36	24.3	17(68*)	17.2	76 ± 8.68**
300~500	17(68*)	17.19	29.10	23.4	20(80*)	34.5	78 ± 6.90**
200	10	6.76	7.8	12.9	11	10.31	--
300	12	9.44	12.25	10.7	13	16.00	--
500	15	15.11	26.73	15.7	17	30.68	--

* Multiplied by four to compare to the experimental buckling modes

** Standard deviation of the experiments

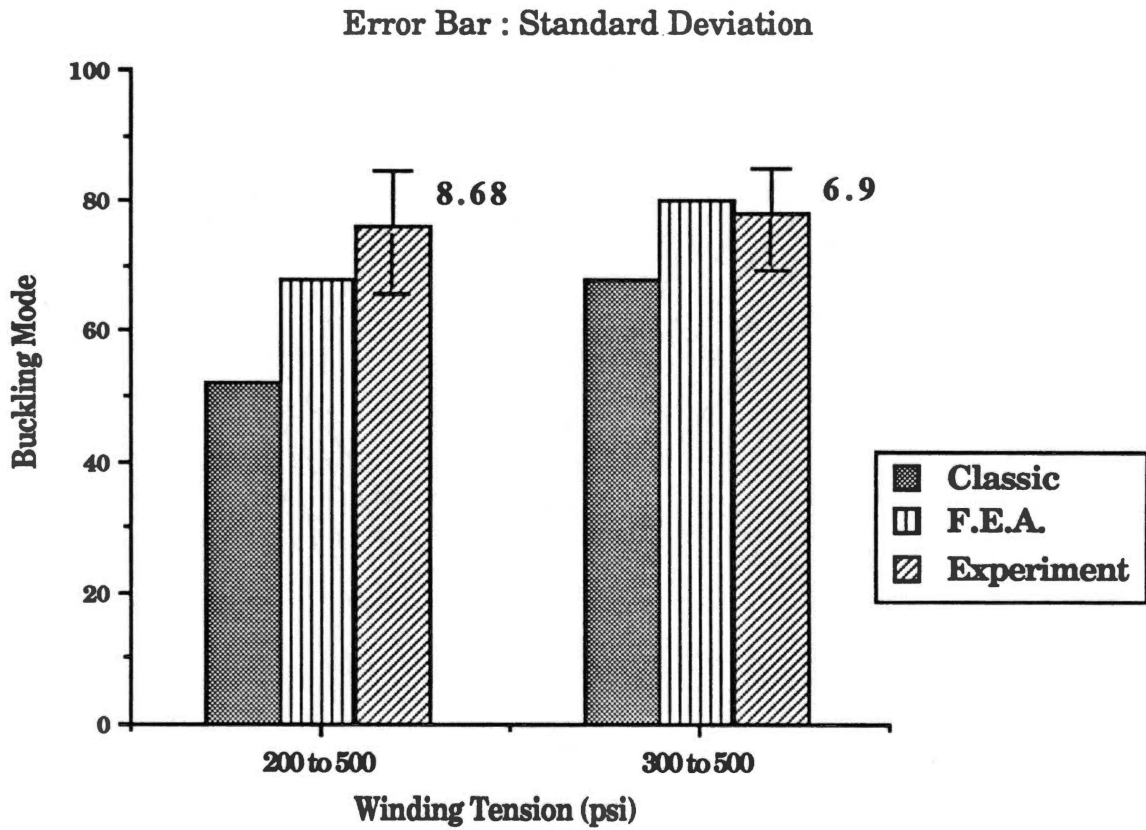


Figure 51. Classic, Numerical and Experimental Buckling Modes at Stepped Tension Windings.

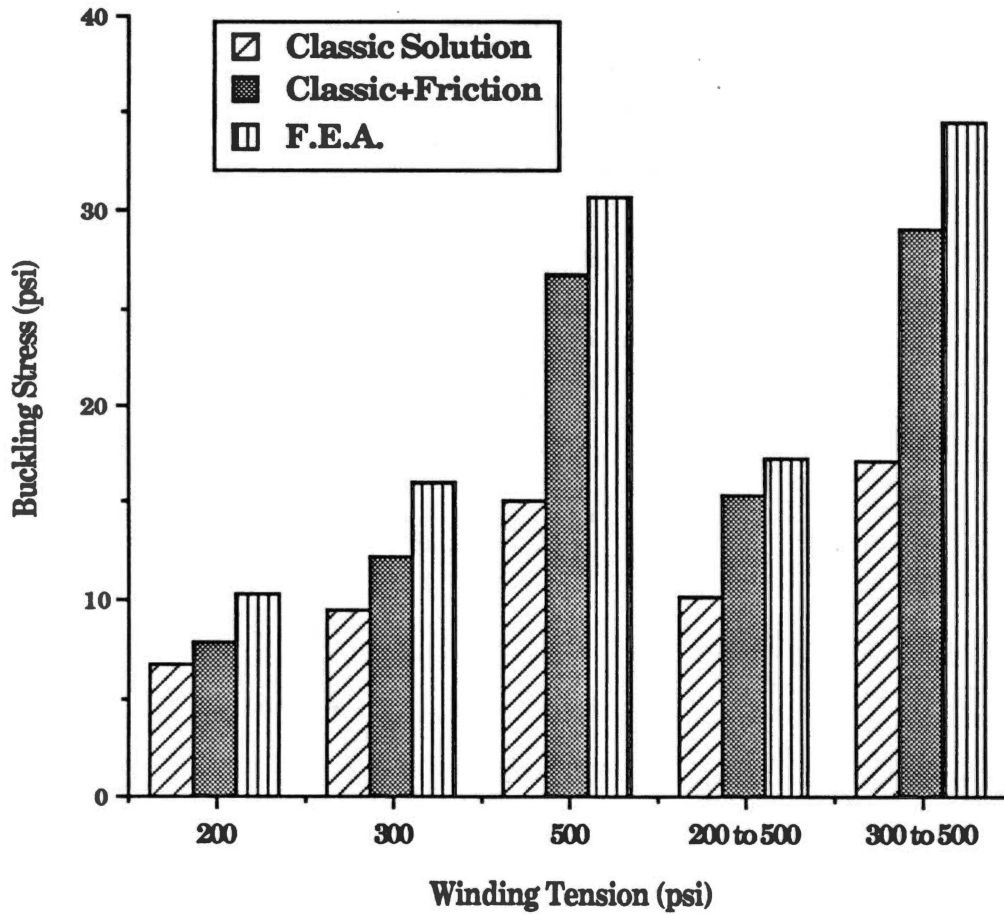


Figure 52. Classic and Numerical Buckling Stresses at Constant Tension Windings

Failure Criterion for Starred Roll Defects

A failure criterion of starred roll defects was obtained by developing a concept of a margin of safety. The margin of safety for a starred roll defect was defined as the difference of the maximum compressive circumferential stress from the buckling stress divided by the maximum circumferential stress or by the buckling stress as follows;

$$\text{Margin of Safety} = \frac{|\sigma_{cr}| - |\sigma_{t(max)}|}{|\sigma_{cr}| \text{ or } |\sigma_{t(max)}|} \quad (4.12)$$

$$\text{where Denominator} = \begin{cases} |\sigma_{t(max)}| & \text{if M.S.} > 0 \\ |\sigma_{cr}| & \text{if M.S.} < 0 \end{cases}$$

The margin of safety is an indicator to determine whether the wound roll may buckle or not for a given winding condition. The larger the margin of safety is, the safer the roll is from starring. If it is around zero, the roll may be buckled by a small perturbing load. When it is negative, the larger the absolute value is, the more easily the starred roll defect may occur.

Table VIII and Figure 53 show the margins of safety for different winding conditions. The margins of safety at the winding conditions of 200 to 500 psi and 300 to 500 psi were -16.69 and -4.86 respectively. The starred roll defect may occur more easily at the former case than at the latter case because the margin of safety is negative and the absolute value is larger.

TABLE VIII
COMPARISON OF BUCKLING STRESSES AND
CIRCUMFERENTIAL STRESSES
FOR CENTER WINDINGS

Winding Tension (psi)	Maximum Circumferential Stress (psi)	Buckling Stress (psi)	Margin of Safety (psi/psi)
200~500	304.21	17.2	-16.69
300~500	202.05	34.5	-4.86
200	1.595	10.31	5.44
300	3.607	16.00	3.43
500	9.810	30.68	2.13

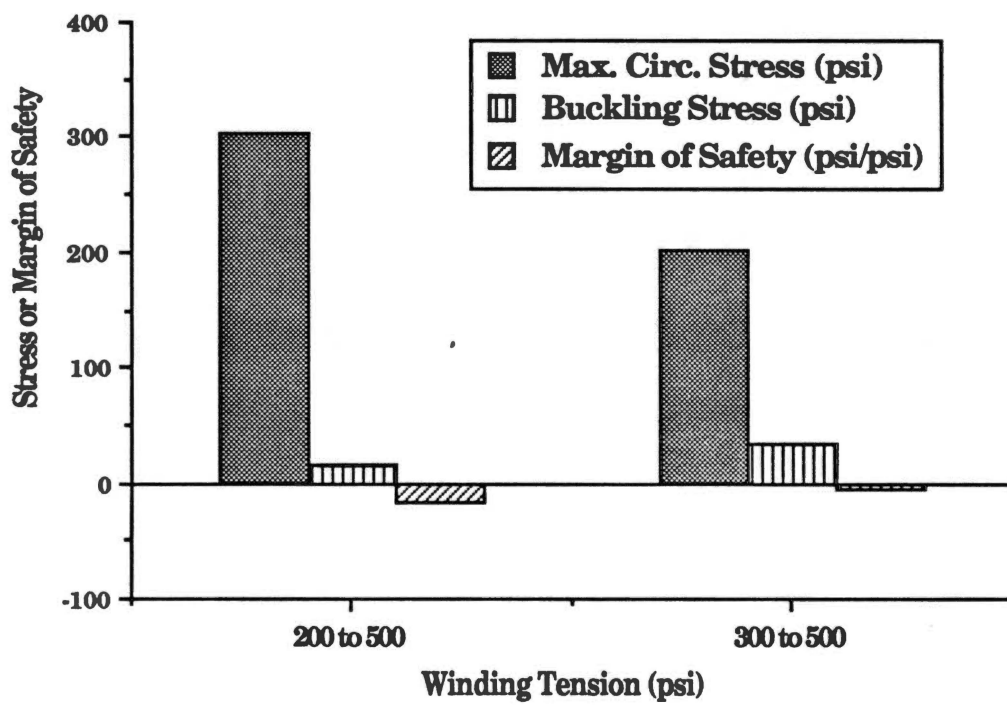


Figure 53. Margin of Safety for Starred Roll Defect at Stepped Tension Windings

Constant Tension Windings

The beam thickness was selected so that the circumferential stress of the beam was larger than 99 % of the maximum compressive circumferential stress.

In Table VII and Figure 52., the classic buckling stresses which included the friction forces were smaller than the numerical solutions within 25 % error. The classic solutions can be used as rough predictions of the numerical solutions.

In Table VII and Figure 54., the classic buckling modes were within 12 % error from the numerical solutions.

The margins of safety for constant tension windings were shown in Table VIII and Figure 55. Because the critical buckling stresses were larger than the maximum circumferential stresses of the rolls, the margins of safety were positive and the rolls were safe from starring. As the winding tension was increased, the margin of safety was decreased, i.e., the roll became less safe from starring.

Even if the circumferential stress is below the buckling stress, the roll may buckle if an additional perturbing load is encountered, which yields the total circumferential stress to be larger than the buckling stress. Examples of perturbing loads might be cases where the roll is dropped or impacted.

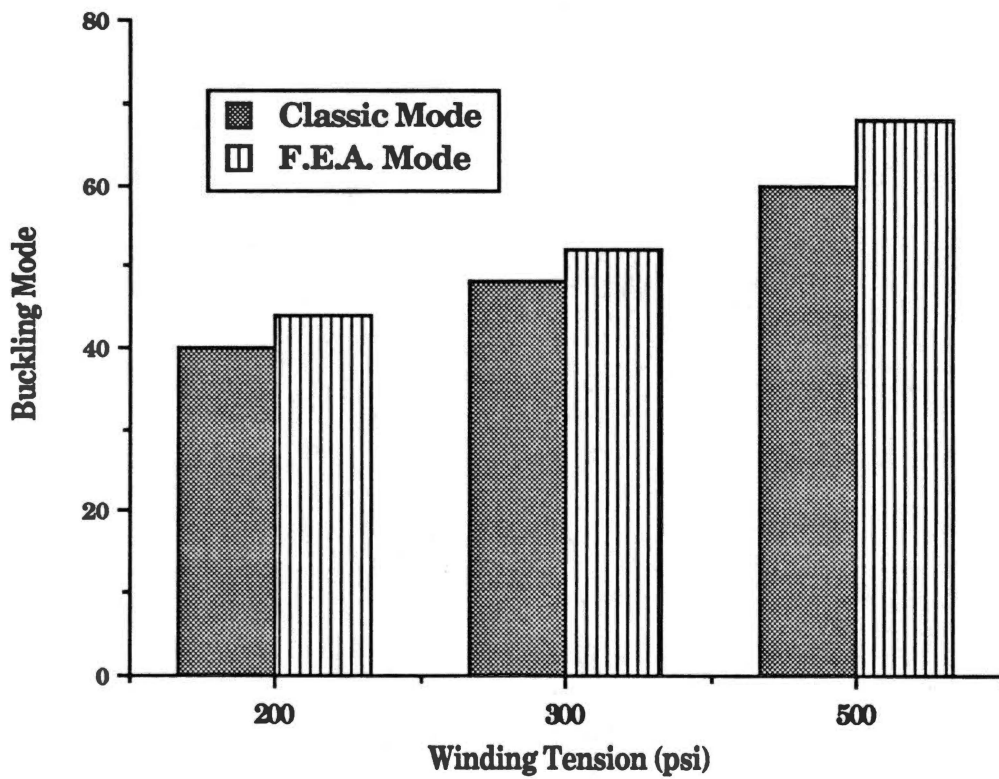


Figure 54. Classic and Numerical Buckling Modes at Constant Tension Windings

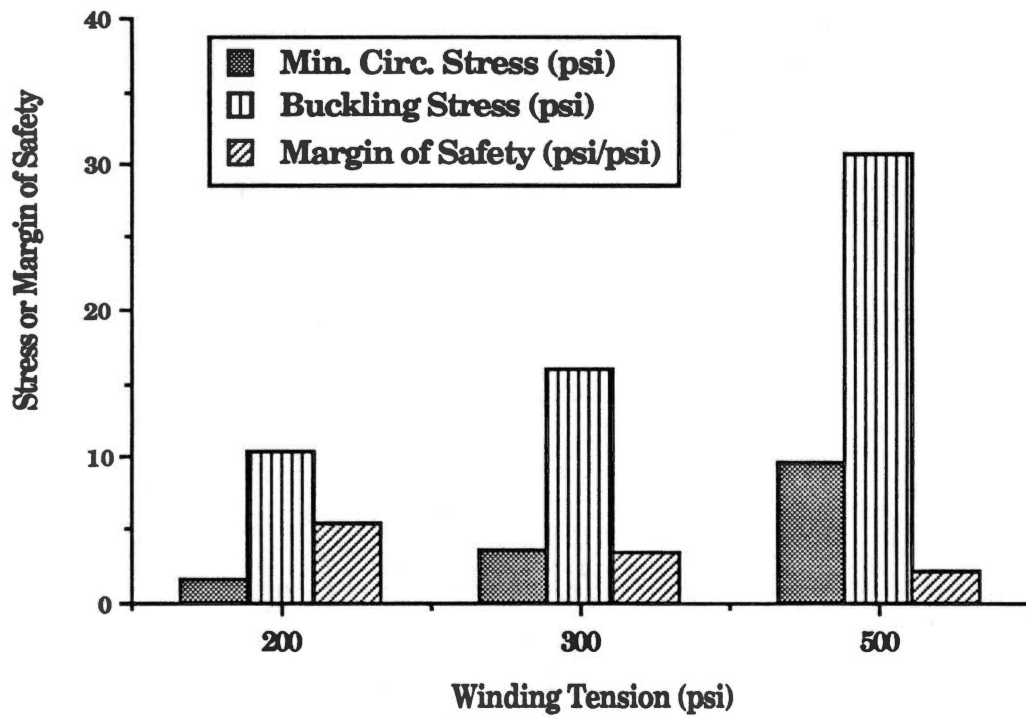


Figure 55. Margin of Safety for Starred Roll Defect at Constant Tension Windings

Experimental Analysis

Winding experiments were performed to validate the variable radial modulus model, which used polypropylene and polyester films with the 3M Splicer Winder in the WHRC at OSU.

The drawing of the winder is shown in Figure 56. The winding conditions and the material properties were discussed in the finite element analysis part and presented in Table VI.

Only the buckling modes were measured after winding because the buckling loads could not be measured during or after winding. The polypropylene and polyester were tested to generate the starred roll defect. The wound roll of polypropylene showed severe edge deformation at high winding tensions and the starred roll defect could not be generated. Clear starred roll defects were generated with polyester film by stepping the winding tension. A focus was on the polyester film for the winding experiments.

Radial Modulus of Polyester Film

The INSTRON machine [22] was used to measure the radial modulus of the polyester film in conjunction with a 2248 lb load cell. The output signal from the INSTRON was collected by the IBM-AT compatible computer through a GPIB board and a data acquisition program accompanied by the INSTRON. The radial modulus was obtained by the least-squares curve fitting method.

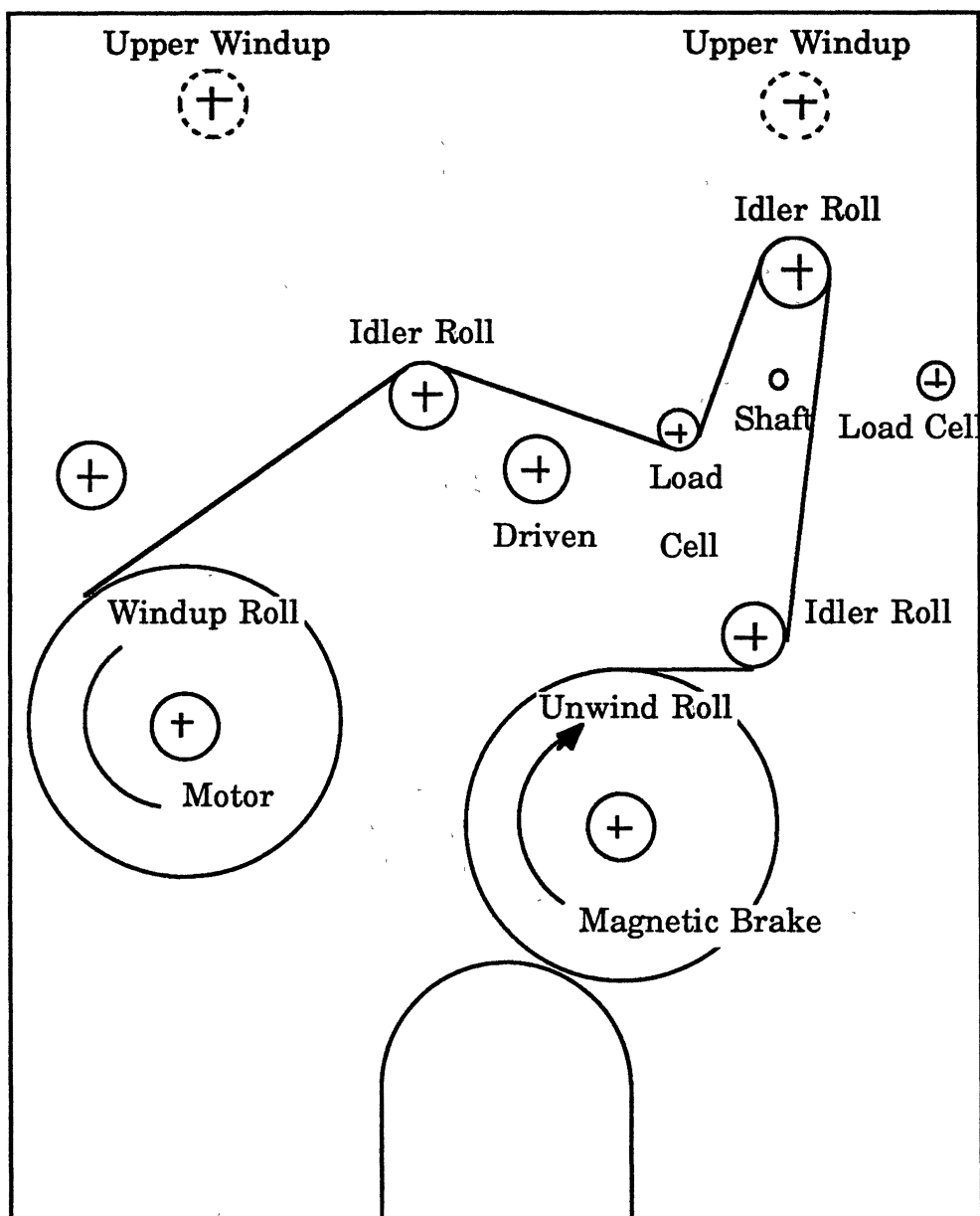


Figure 56. Layout of 3M Splicer Winder

The specimen area of the stack of polyester film was 3.00" by 4.25" and the initial height was 3.86". The pressure vs strain curve is shown in Figure 57. A third order polynomial function was obtained by least squares curve fitting of the pressure vs strain data.

The radial modulus was obtained as a function of strain by differentiating the polynomial function of pressure.

The radial moduli were tabulated as a function of the experimental strain. Several modulus functions were obtained for different pressure ranges by least-squares curve fittings with respect to the radial pressures. The modulus functions were overlapped and divided by several linear functions as shown in Figure 58 and Table IX . These linear functions are used to let the Hakiel's model run faster.

$$P_r = -1.2033 + 143.21\epsilon_r - 5492.1\epsilon_r^2 + 1.066E5\epsilon_r^3 - 8.4364E5\epsilon_r^4 + 3.8713E6\epsilon_r^5$$

$$E_r = 143.21 - 1.0982E4\epsilon_r + 3.198E5\epsilon_r^2 - 3.3746E6\epsilon_r^3 + 1.93565E7\epsilon_r^4$$

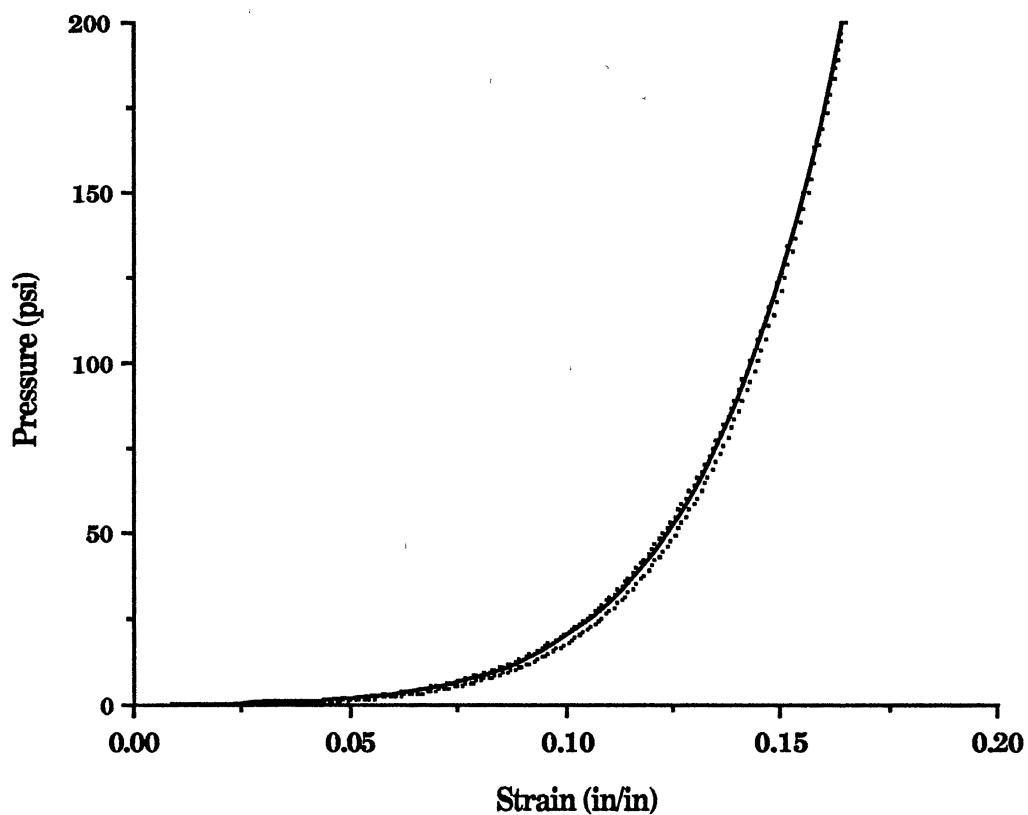


Figure 57. Pressure vs Strain Curve of Polyester Film
(Type 377/ Grade 92)

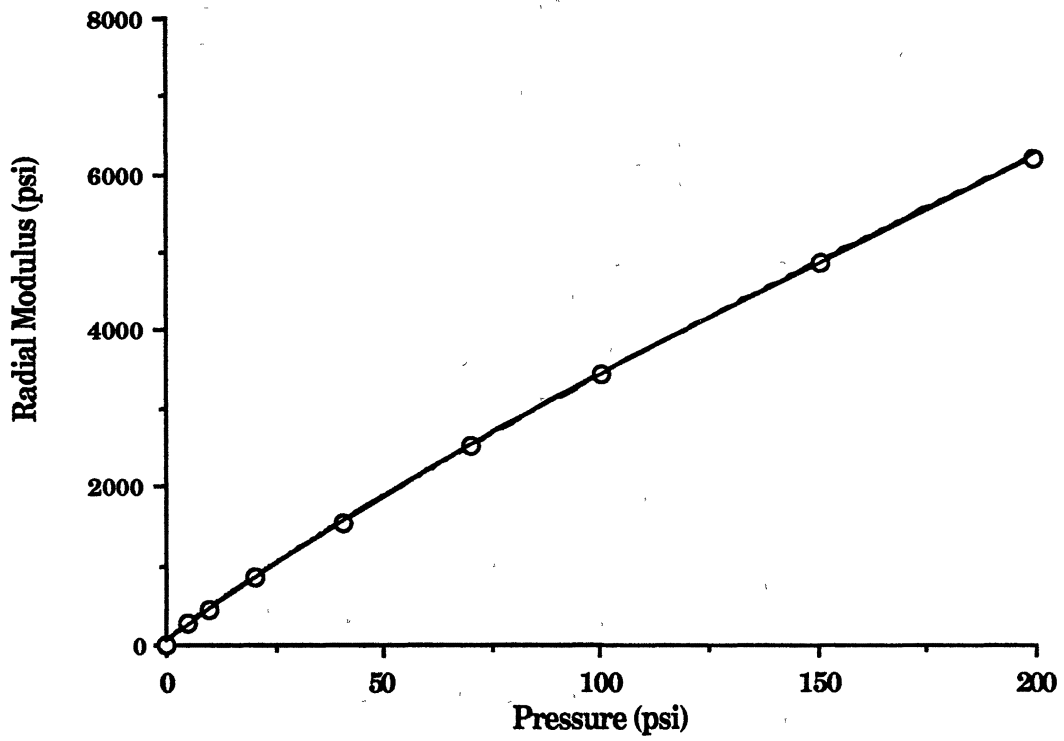


Figure 58. Radial Modulus of Polyester Film
(Type 377/ Grade 92)

TABLE IX
 RADIAL MODULUS OF POLYESTER FILM
 AS A FUNCTION OF PRESSURE
 (Type 377/Grade 92)

Pressure(psi)			Radial Modulus(psi)	
0.0	to	5.0	51.244 p	
5.0	to	10.0	40.427 p	- 54.081
10.0	to	20.2	37.257 p	+ 84.836
20.2	to	40.5	34.698 p	+ 137.505
40.5	to	70.5	32.336 p	+ 233.088
70.5	to	100.4	30.505 p	+ 362.051
100.4	to	150.8	28.846 p	+ 528.648
150.8	to	199.1	27.381 p	+ 749.474

Experimental Procedure

A chart, which tabulated the rotating speed of the windup roll versus the roll radius, should be prepared before the windings to maintain a certain winding speed. The experimental procedure was as follows:

1. Mount the unwind roll and place the web upon the winding machine in a proper path in which the load cell was calibrated. Different path may cause incorrect reading of the load;
2. Tape the edge of the web on the windup roll. Wind a few wraps and realign the web path on the windup roll if there is any misalignment;
3. Run the machine by monitoring the rotating speed of the windup roll. Adjust the rotating speed of windup roll frequently by a chart which tabulates the rotating speed vs radius for a certain winding speed;
4. For a stepped winding tension, increase the winding tension continuously by counting the number of revolutions of the windup roll;
5. During the winding, paint the sides of the wound roll using a black permanent marker, which will show clear buckling mode after buckling occurred;
6. After a roll was wound, place the wound roll upon a flat surface and rotate the roll several times while pressing it down to generate the starring;
7. Count the number of half sine wave of the wound roll, which is the buckling mode.

Results of Experimental Analysis

Stepped Tension Windings. In stepped tension windings, the circumferential stresses were larger than the buckling stresses as shown in Figure 53. The margins of safety were -16.69 and -4.86 for two different

winding conditions as shown in Table VIII and Figure 53. The starred roll defects were generated by rotating the wound rolls upon a flat surface while pressing them down. Figure 59 shows a typical starred roll defect generated at a stepped tension winding .

The starring did not occur during or after winding because the radial pressure and the friction force inside the roll prevented the roll from buckling. This means that the roll could not be buckled without any perturbing load. This is the reason why good looking wound rolls frequently encounter starred roll defects during transportation or in stock or in use.

Figures 60 and 61 show the experimental buckling modes at the stepped tension windings. The horizontal lines are the averaged buckling modes. The sides 1 and 2 are the cross machine directional ends of the wound roll. Figure 62 shows the average buckling modes with standard deviations.

The classic, numerical and experimental buckling modes in winding experiments are shown in Table VII and Figure 51. The classic and numerical buckling modes were multiplied by four to be compared to the experimental values because a quarter of the circumferential length of the wound roll was modeled.

For the stepped winding tension from 200 psi to 500 psi, eleven windings tests were performed. The average experimental buckling mode was 76 and the standard deviation was 8.68. The classic and numerical buckling mode was 52 and 68 respectively. The numerical buckling mode was within one standard deviation of the experiments.

For the stepped winding tension from 300 psi to 500 psi, eleven windings tests were performed. The classic, numerical and experimental

buckling modes were 68, 80 and 78 respectively. The standard deviation of the experiments was 6.9. The numerical and experimental buckling modes were very close in this winding condition.

Constant Tension Windings. In constant tension windings, the numerical buckling stresses were much larger than the circumferential stresses of the wound rolls as shown in Figure 54. Because the margins of safety were larger than 2.13 for three constant tension windings, they were safe from starring. Clear starred roll defects could not be generated at these constant winding tensions. Only dim starred roll defects were generated.

By comparing the numerical and experimental buckling modes, it was proven that the finite element model could predict the buckling stresses and modes of center wound rolls for given winding conditions.

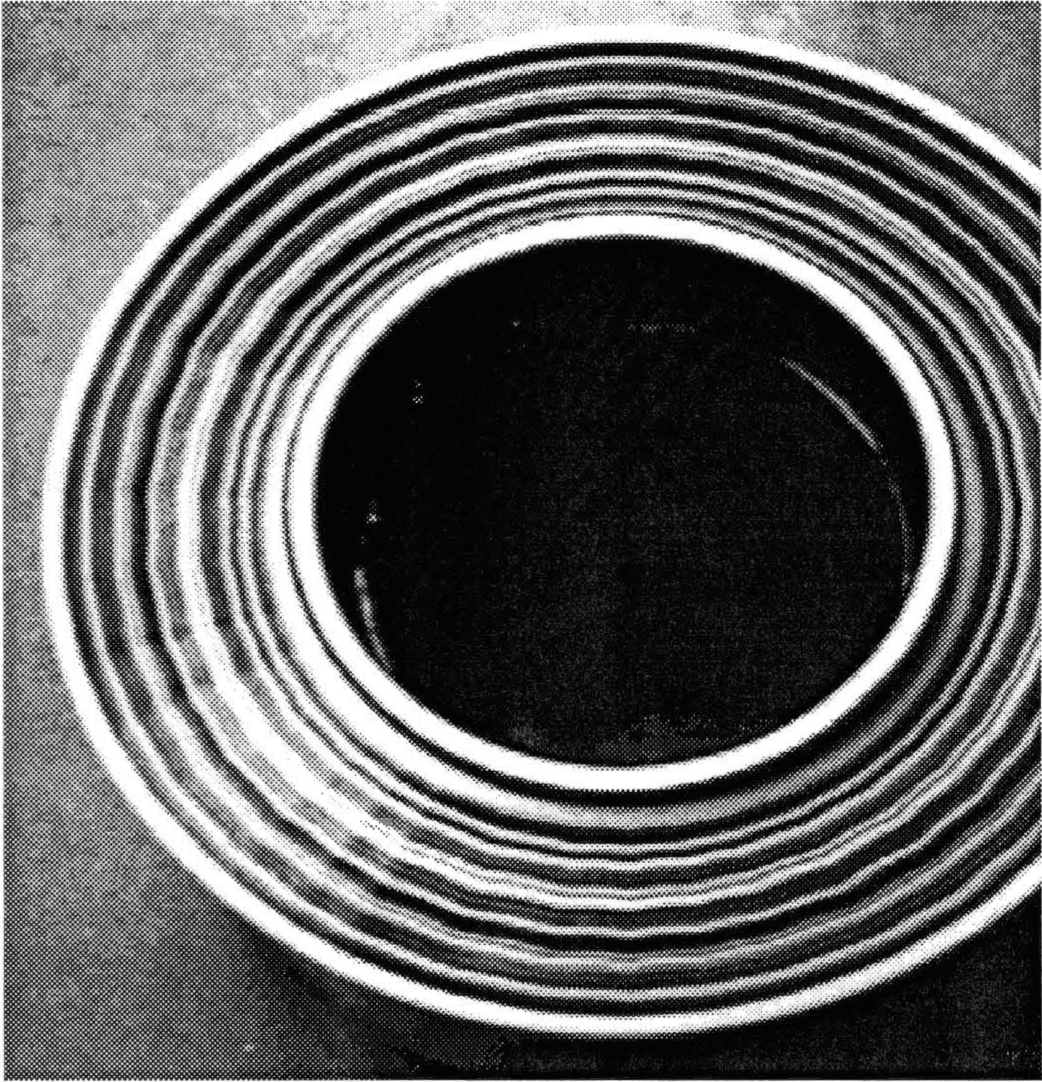


Figure 59. Starred Roll Defect at Stepped Tension Winding

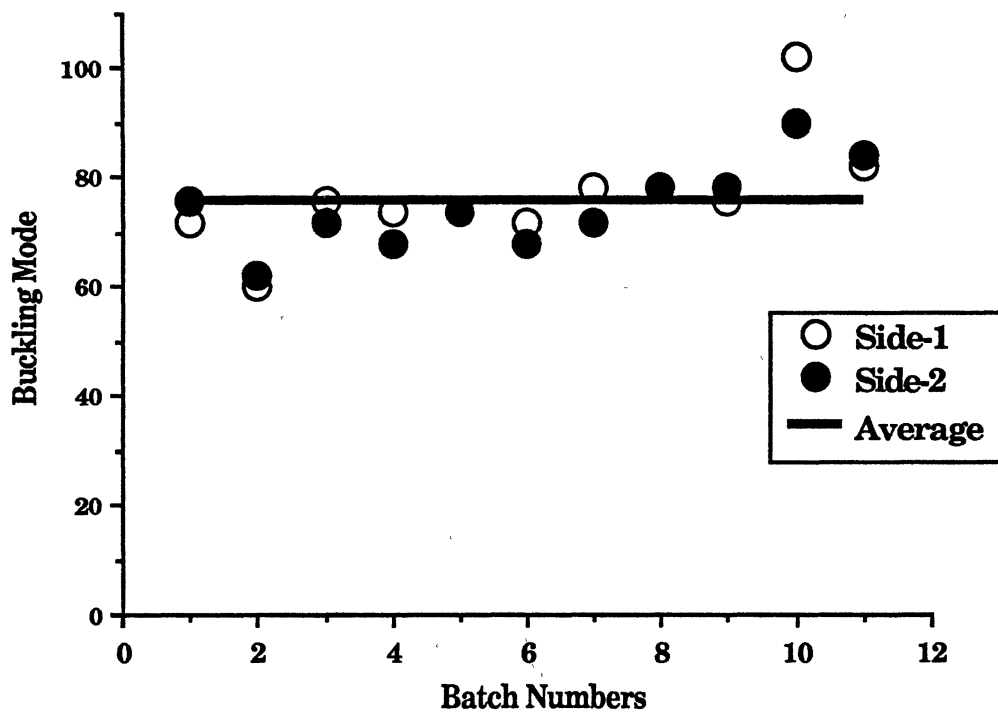


Figure 60. Buckling Modes at Stepped Tension Windings (200 to 500 psi)

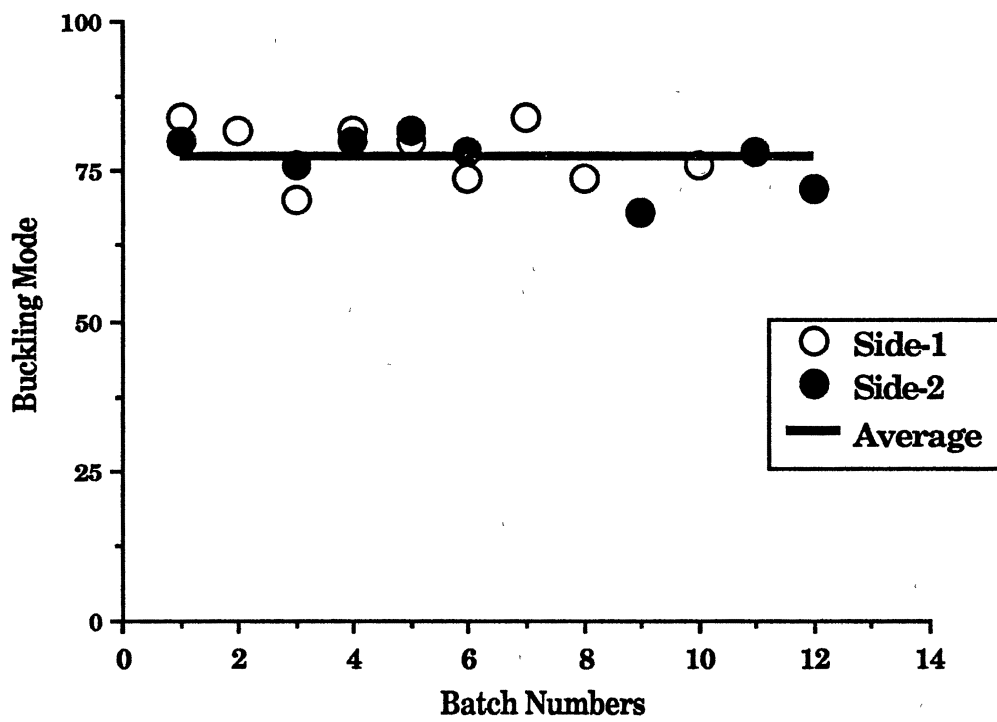


Figure 61. Buckling Modes at Stepped Tension Windings (300 to 500 psi)

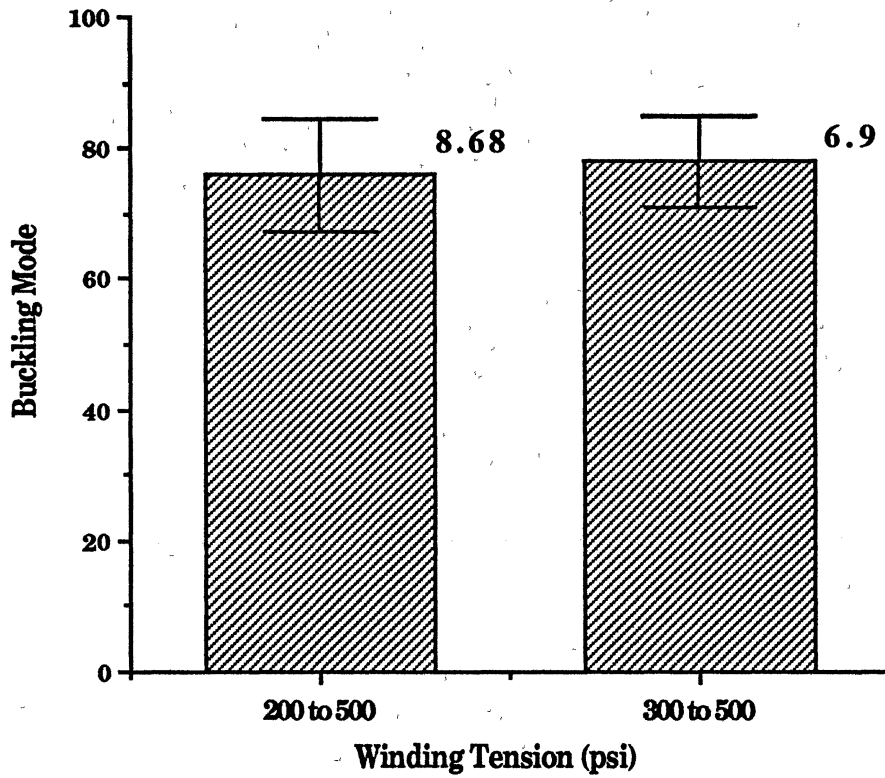


Figure 62. Experimental Buckling Modes at Stepped Tension Windings with Standard Deviations

CHAPTER V

SUMMARY AND RECOMMENDATIONS

Summary

A finite element model was developed which can predict the buckling stress of a center wound roll for a given winding condition. The model was based on the stress distribution calculated by Hakiel's nonlinear winding model.

The first model assumed the radial pressure and modulus as constant throughout the wound roll. The model was validated by the finite element analyses using ANSYS program and the buckling experiments using stacks of reproduction paper on the MTS machine.

The second model implemented the variable radial pressure and modulus in a wound roll. The model was validated by the finite element analyses and the center winding experiments using polyester films on the 3M Splicer Winder.

Classic solutions were obtained by the energy method based upon Winkler's foundation model [18, 19, 42]. The classic buckling load was modified by adding the friction force between the beam and the foundations as follows;

$$F_{crm} = F_{cr} + \mu P_r A/2$$

A margin of safety for a starred roll defect was defined as an indicator of starring for a given winding condition as follows;

$$\text{Margin of Safety} = \frac{|\sigma_{cr}| - |\sigma_{t(max)}|}{|\sigma_{cr}| \text{ or } |\sigma_{t(max)}|}$$

The larger the margin of safety is, the safer the roll is from starring. When it is around zero, the roll may be buckled by a small perturbing load. When it is negative, the larger the absolute value is, the more easily the starred roll defect may occur.

By comparing the results from the classic, numerical and experimental analyses, the following conclusions were obtained:

1. The numerical buckling loads of stacks of reproduction paper represented the initial buckling loads for given stack pressures.
2. The numerical buckling modes of the wound rolls could predict the experimental values.
3. A concept of the equivalent moment of inertia of a beam was valid to represent a series of webs.
4. The modified classic buckling loads were good predictions of numerical values within a 25 % error.
5. The margin of safety of starred roll defect was useful indicator to determine the starring of the wound roll for a given winding condition.

Recommendations

The following are recommended for further study;

1. If the computer memory is large enough, model the whole roll instead of modeling a quarter of the roll and use finer mesh for the foundations to represent the pressure distribution more accurately.
2. Develop a more accurate winding model than Hakiel's to calculate the stress distributions in wound rolls.
3. Perform a parametric study for a wide range of constant winding tensions with different web materials and roll dimensions.
4. If the roll is wide in the cross machine direction, plane strain condition should be assumed in the winding model and the finite element analysis.
5. To perform winding experiments to validate the numerical model, use computerized winding machine to apply accurate winding conditions consistently and find better method to generate the starred roll defect from the wound roll.
6. Find better classic solution to predict the numerical solution and the starred roll defect more accurately.

REFERENCES

1. Altmann, H. C. (1968), "Formulas for Computing the Stresses in Center Wound Rolls.", Tappi, Vol. 51, No. 4, pp.176-179.
2. ANSYS (1989), User's Manual Revision 4.4, Swanson Analysis Systems, Houston, PA 15342.
3. ASTM (1988), "Standard Test Method for Static and Kinetic Coefficients of Friction of Plastic Film and Sheeting.", Annual Book of ASTM Standards, Vol. 08.02, pp. 129-133.
4. Carnahan, B., Luther, H. A. and Wilkes, J. O. (1969), "Applied Numerical Methods", John Wiley & Sons, Inc., pp. 441-442.
5. Catlow, M. G. and Walls, G. W. (1962), "A Study of Stress Distribution in Pirns", J. of Textile Institute Part 3, pp. T410-429.
6. Connor, J. and Morin, N. (1970), "Perturbation Techniques in the Analysis of Geometrically Non-linear Shells.", IUTAM on High Speed Computing of Elastic Structures, Aug., U. of Liege, pp. 23-28.
7. Daly, D. A. (1967), "Study of Defects in Wound Rolls leads to Better Winding Control.", Paper Trade Journal, Dec. 4, pp. 46-48.
8. Ericksson, L. G., Lydig, C., Viglund, J. A. and Lomulainen, P. (1983), "Measurement of Paper Roll Density During Winding.", Tappi, Vol. 66, No. 1, pp. 63-66.
9. Ericksson, L. G. and Rand, T. (1973), "Physical Properties of Newsprint Rolls During Winding.", Tappi, Vol. 56, No. 6, pp. 153-156.
10. Fikes, M. (1990), "The Use of Force Sensing Resistors to Measure Radial Interlayer Pressures in Wound Rolls.", Master's Thesis, Department of Mechanical and Aerospace Engineering, Oklahoma State University

11. Filonenko-Borodich, M. M. (1940), "Some Approximate Theories of the Elastic Foundation.", (in Russian) Uchenyie Zapiski Moskovskogo Gosudarstvennogo Universiteta Mehanika, U.S.S.R., No. 46, pp. 3-18.
12. Frye, K. G. (1967), "Winding Variables and Their Effect on Roll Hardness and Roll Quality.", Tappi, Vol. 50, No. 7, pp. 81A-86A.
13. Gallety, G. D. (1959), "Circular Plates on a Generalized Elastic Foundation.", J. of Applied Mechanics, Vol. 26, pp. 55-58, ASME, Vol. 81, Series E, p. 297.
14. Gilmore, W. J. (1973), "Report on Roll Defect Terminology.", Tappi Finishing and Converting Conference Proceedings (Tappi CA 1228), pp. 59-66.
15. Haisler, W. E., Stricklin, J. A. and Riesemann, W. A. (1971), "Geometrically Nonlinear Analysis by the Direct Stiffness Method.", J. of the Structural Division, ASCE, Vol. 97, No. ST9, pp. 2299-2314.
16. Haisler, W. E., Stricklin, J. A. and Stebbins, F. J. (1972), "Development and Evaluation of Solution Procedures for Geometrically Nonlinear Structural Analysis.", AIAA, Vol. 10, No. 3, pp. 264-271.
17. Hakiel, Z. (1987), "Nonlinear Model for Wound Roll Stresses.", Tappi, Vol. 70, No. 5, pp. 113-117.
18. Hetenyi, H. (1945), "A Beam on Elastic Foundations.", Ann Arbor, The U. of Michigan Press.
19. Hetenyi, H. (1950), "A General Solution for the Bending of Beams on an Elastic Foundation of Arbitrary Continuity.", J. of Applied Physics, Vol. 21, pp. 55-58.
20. Hussain, S. M. and Farewell, W. R. (1977), "Roll Winding-Causes, Effects and Cures of Loose Cores in Newsprint Rolls.", Tappi, Vol. 60, No. 5, pp. 112-114.
21. Hussain, S. M., Farewell, W. R. and Gunning, J. R. (1968), "Most Paper in the Roll is in Unstable Condition.", Canadian Pulp and Paper Industry, Aug., pp. 52-54.
22. Instron (1988), Instruction Manual, Manual No. M11-98500-1(B), Instron Dynamic Testing Instruments.

23. Jones, R. and Xenophontos, J. (1977), "The Vlasov Foundation Model", Int. J. of Mechanical Sciences, Vol. 19, No. 6, pp. 317-323.
24. Kerr, A. D. (1964), "Elastic and Viscoelastic Foundation Models.", ASME, J. of Applied Mechanics, Sept., pp. 491-498.
25. Marcal, P. V. (1967), "Effect of Initial Displacement on Problem of Large Deflection and Stability.", Tech. Report ARPA E54, Brown Univ.
26. Monk, D. W., Lautner, W. K. and McMullen, J. F. (1975), "Internal Stresses Within Rolls of Cellophane.", Tappi, Vol. 58, No. 8, pp. 152-155.
27. MTS (1988), Operational Manual, MTS 810 Material Testing Machine, MTS Systems Corporation.
28. Oden, J. T. (1969), "Finite Element Applications in Nonlinear Structural Analysis.", Proc. Symp. on Application of Finite Element Methods in Civil Eng., ASCE, Vanderbilt U., Tenn.
29. Pasternak, P. L. (1954), "On a New Method of Analysis of an Elastic Foundation by Means of Two Foundation Constants.", Gosudarstrennoe Izdatelstvo Literaturipo Stroitelstvu i Arkhitekture, USSR.
30. Perrone, N. and Kao, R. (1970), "Large Deflection Response and Buckling of Partially and Fully Loaded Spherical Caps.", AIAA, Vol. 8, No. 12, pp. 2130-2136.
31. Pfeiffer, J. D. (1966), "Internal Pressures in a Wound Roll of Paper.", Tappi, Vol. 49, No. 8, pp. 342-347.
32. Pfeiffer, J. D. (1968), "Mechanics of a Rolling Nip on Paper Webs", Tappi, Vol. 51, No. 8, pp. 77A-85A.
33. Pfeiffer, J. D. (1977), "Nip Forces and Their Effect on Wound-In Tension.", Tappi, Vol. 60, No. 3, pp. 115-117.
34. Pfeiffer, J. D. (1979), "Prediction of Roll Defects from Roll Structure Formulas.", Tappi, Vol. 62, No. 10, pp. 83-85.
35. Pfeiffer, J. D. (1981), "Measurement of the k_2 Factor for Paper.", Tappi, Vol. 64, No. 4, pp. 105-106.
36. Pfeiffer, J. D. (1987), "An Update of Pfeiffer's Roll-Winding Model.", Tappi, Vol. 70, No. 10, pp. 130-131.

37. Ressler, E. (1958), "A Note on Deflections of Plates on a Viscoelastic Foundation.", J. of Applied Mechanics., Vol. 25, ASME, Vol. 80, pp. 144-145.
38. Roark, R. J. and Young, W. C. (1975), "Formulas for Stress and Strain.", 5th ed., McGraw-Hill.
39. Roisum, D. R. (1987), "Paper Stresses During Winding. Advances and Trends in Winding Technology.", Proceedings of the First Winding Technology Conference, March 16, Stockholm Sweden, pp. 7-23.
40. Roisum, D. R. (1988), "How to Measure Roll Quality.", Tappi, Vol. 71, No. 10, pp. 91-103.
41. Roisum, D. R. (1990), "The Measurement of Web Stresses During Roll Winding", Ph.D Thesis, Department of Mech. and Aero. Engn., Oklahoma State University.
42. Timoshenko, S. and Gere, J. (1961), "Theory of Elastic Stability", New York, McGraw-Hill.
43. Vlasov, V. Z. and Leont'ev, U. N. (1966), "Beams, Plates and Shells on Elastic Foundations.", (Translated from Russian), Israel Program for Scientific Translation.
44. Willett, M. S. and Poesch, W. L. (1988), "Determining the Stress Distributions in Wound Reels of Magnetic Tape Using a Nonlinear F.D. Approach.", J. of Applied Mechanics, Vol. 55, June, pp. 365-371.
45. Winkler, E. (1867), "Die Lehre von der Elastizitat und Festigkeit.", Prag, pp. 182-184.
46. Wissmann, J. W. (1965), "Nonlinear Structural Formulation: Tensor Formulation.", Proc. of the Conference on Matrix Methods in Structural Mechanics, Wright-Patterson Air Force Base, Ohio
47. Yagoda, H. P. (1980), "Resolution of a Core Problem in Wound Rolls.", ASME, J. of Applied Mechanics, Vol. 47, No. 12, pp. 847-854.
48. Zhaohua, F. and Cook, R. D. (1983), "Beam Elements on Two-Parameter Elastic Foundations", ASCE, Vol. 109, No. 6, pp. 1390-1402.
49. Zienkiewicz, O. C. (1977), "The Finite Element Method.", 3rd ed., McGraw-Hill., Chap. 9., pp. 500-526.

APPENDIX A

BUCKLING OF A BEAM UPON AN ELASTIC FOUNDATION

When a beam is subjected to the elastic foundation, the energy method can be used to calculate the critical value of the compressive force. The work done by the axial load is equal to the strain energy of the beam and the foundation.

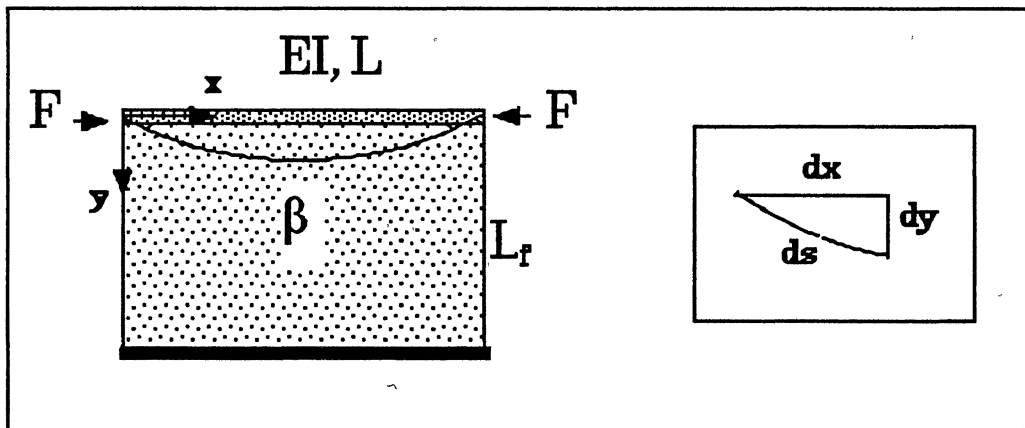


Figure 63. A Beam with Axial Load upon Elastic Foundation

The general expression for the deflection curve of a beam with hinged ends can be represented by a series summation such as:

$$y = \sum_{n=1}^{\infty} a_n \sin \frac{n\pi x}{L} \quad (\text{A.1})$$

The strain energy due to the bending of the beam is:

$$U_1 = \frac{EI}{2} \int_0^L \left(\frac{d^2 y}{dx^2} \right)^2 dx \quad (\text{A.2})$$

Differentiating Equation (A.1) twice and substituting it into Equation (A.2) gives:

$$U_1 = \frac{\pi^4 EI}{4L^3} \sum_{n=1}^{\infty} (a_n^2 n^4) \quad (\text{A.3})$$

The strain energy due to the deformation of the foundation is:

$$U_2 = \frac{\beta}{2} \int_0^L y^2 dx \quad (\text{A.4})$$

Substituting Equation (A.1) into Equation (A.4) gives:

$$U_2 = \frac{\beta L}{4} \sum_{n=1}^{\infty} a_n^2 \quad (\text{A.5})$$

The work done by the axial load F is:

$$T = \int_0^L F(ds-dx) \quad (\text{A.6})$$

The axial deformation of the beam can be approximated by Taylor's series expansion:

$$ds = \sqrt{dx^2 + dy^2} = dx \sqrt{1 + \left(\frac{dy}{dx}\right)^2} \quad (\text{A.7})$$

$$ds = dx \left[1 + \frac{1}{2} \left(\frac{dy}{dx}\right)^2 \right] \quad (\text{A.8})$$

Substituting Equation (A.8) into Equation (A.6) gives:

$$T = \frac{F}{2} \int_0^L \left(\frac{dy}{dx}\right)^2 dx \quad (\text{A.9})$$

Differentiating Equation (A.1) and substituting it into Equation (A.9) gives:

$$T = \frac{\pi^2 F}{4L} \sum_{n=1}^{\infty} (a_n^2 n^2) \quad (\text{A.10})$$

The work done by the axial load is equal to the strain energy obtained by the beam and the foundation:

$$U_1 + U_2 = T \quad (\text{A.11})$$

Substituting Equations (A.3), (A.5) and (A.10) into Equation (A.11) gives:

$$\frac{\pi^4 EI}{4L^3} \sum_{n=1}^{\infty} (a_n^2 n^4) + \frac{\beta L}{4} \sum_{n=1}^{\infty} a_n^2 = \frac{\pi^2 F}{4L} \sum_{n=1}^{\infty} (a_n^2 n^2) \quad (\text{A.12})$$

Solving Equation (A.12) for F gives:

$$F = \frac{\pi^2 EI}{L^2} \left(\frac{\sum_{n=1}^{\infty} (a_n^2 n^4) + \frac{\beta L^4}{\pi^4 EI} \sum_{n=1}^{\infty} a_n^2}{\sum_{n=1}^{\infty} (a_n^2 n^2)} \right) \quad (\text{A.13})$$

Let all terms except one be equal to zero, i.e., the buckling mode will have a simple sine wave.

$$y = a_m \sin \frac{m\pi x}{L} \quad (\text{A.14})$$

The critical buckling load can be expressed as follows:

$$F_{cr} = \frac{\pi^2 EI}{L^2} \left(m^2 + \frac{\beta L^4}{m^2 \pi^4 EI} \right) \quad (\text{A.15})$$

The critical load depends not only on the properties of the beam but also on the integer m that represents the buckling mode. By gradually increasing β , a point will be reached where the critical load (F_{cr}) for mode $m+1$ is smaller than that for mode m . This means that the buckling mode must be changed from m to $m+1$ for values for the modulus of the foundation (β) which are larger than this point. The critical value of β can be found as follows:

$$m^2 + \frac{\beta L^4}{m^2 \pi^4 EI} \leq (m+1)^2 + \frac{\beta L^4}{(m+1)^2 \pi^4 EI} \quad (\text{A.16})$$

Arranging Equation (A.16) gives simple expression as:

$$\frac{\beta L^4}{\pi^4 EI} \leq m^2(m+1)^2 \quad (\text{A.17})$$

The minimum integer that satisfies Equation (A.17) is the buckling mode. The corresponding buckling load can be obtained by substituting the buckling mode (m) into Equation (A.15).

APPENDIX B

HAKIEL'S NONLINEAR WINDING MODEL

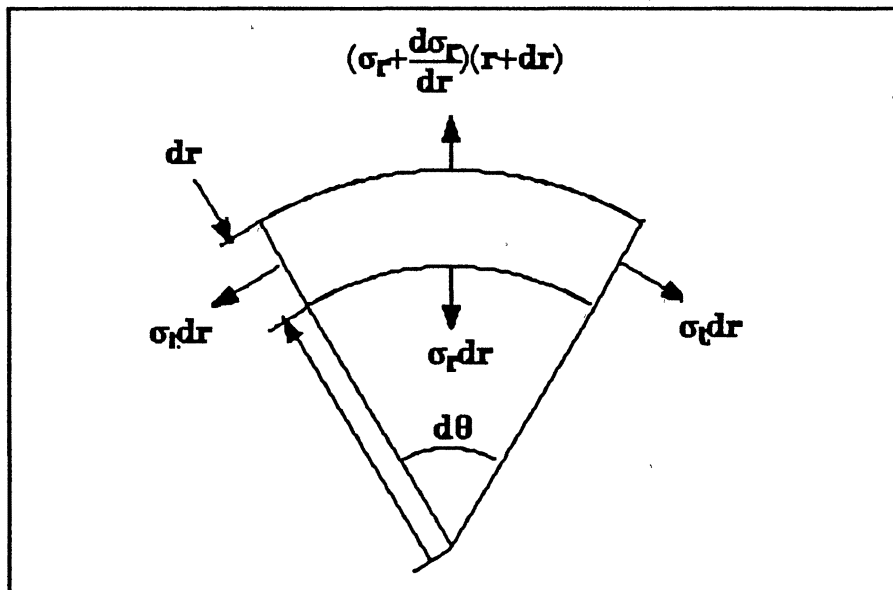


Figure 64. Free Body Diagram of a Segment of a Ring

Basic Assumptions

Hakiel's winding model assumed the followings.

1. The wound roll is a geometrically perfect cylinder: The web has uniform thickness and width throughout the winding,

2. The roll is made of a collection of concentric hoops of web not a spiral. The elastic constants including the radial modulus (E_r) are constant in a single hoop,
3. The roll is an orthotropic elastic cylinder: It is linear elastic in the circumferential direction and nonlinear elastic in the radial direction. The radial modulus is a function of pressure,
4. The stresses are functions of radius but not of axial or circumferential position,
5. The plane stress condition is assumed.

Basic Linear Equation

The equilibrium equation for plane stress in cylindrical coordinates in absence of shear is:

$$r \frac{d\sigma_r}{dr} + \sigma_r - \sigma_t = 0 \quad (\text{B.1})$$

The linear orthotropic constitutive equations are:

for the radial direction:

$$\epsilon_r = \frac{\sigma_r}{E_r} - \nu_{rt} \frac{\sigma_t}{E_t} \quad (\text{B.2})$$

for the tangential direction:

$$\epsilon_t = \frac{\sigma_t}{E_t} - \nu_{tr} \frac{\sigma_r}{E_r} \quad (\text{B.3})$$

The strain energy constraint is:

$$\frac{\nu_{tr}}{E_r} = \frac{\nu_{rt}}{E_t} \quad (\text{B.4})$$

Define the simple symbols as:

$$\nu \equiv \nu_{rt} \quad (\text{B.5})$$

and

$$g^2 \equiv \frac{E_t}{E_r} \quad (\text{B.6})$$

where g^2 is constant during the winding of any one lap.

Equations (B.2) and (B.3) can be rewritten as:

$$\varepsilon_r = \frac{1}{E_t}(g^2\sigma_r - \nu\sigma_t) \quad (\text{B.7})$$

and

$$\varepsilon_t = \frac{1}{E_t}(\sigma_t - \nu\sigma_r) \quad (\text{B.8})$$

The strain compatibility equation is:

$$r \frac{d\varepsilon_t}{dr} + \varepsilon_t - \varepsilon_r = 0 \quad (\text{B.9})$$

By substituting Equations (B.1), (B.7) and (B.8) into (B.9) and eliminating σ_t , a second order ordinary differential equation (ODE) can be obtained in terms of the radial stress.

$$r^2 \frac{d^2\sigma_r}{dr^2} + 3r \frac{d\sigma_r}{dr} - (g^2 - 1)\sigma_r = 0 \quad (\text{B.10})$$

This ODE can be represented by the incremental radial pressure as:

$$r^2 \frac{d^2\delta P}{dr^2} + 3r \frac{d\delta P}{dr} - (g^2 - 1)\delta P = 0 \quad (\text{B.11})$$

where $\delta P = -\sigma_r$

Boundary Conditions

The second order ODE is subject to two boundary conditions: One is at the outside of the winding roll and the other is at the core boundary.

The incremental interlayer pressure caused by the winding of the last lap is equal to the pressure given by the hoop stress formulation:

$$\delta P = -\frac{T_w t}{r} \text{ at } r = s \quad (\text{B.12})$$

The radial deflection of the core outer surface must be equal to that of the inside of the roll.

$$w = \frac{\delta P}{E_c} \text{ at } r = 1 \quad (\text{B.13})$$

Because the strain ϵ_t is w at $r = 1$, Equation (B.8) becomes:

$$w = \frac{\delta T + \nu \delta P}{E_t} \text{ at } r = 1 \quad (\text{B.14})$$

where $\delta T (= \sigma_t)$ is incremental circumferential stress.

By substituting σ_t in Equation (B.2) into δT in Equation (B.14) and equating Equations (B.13) and (B.14), the second boundary condition at the core will be:

$$\frac{d\delta P}{dr} = \left[\frac{E_t}{E_c} - 1 + \nu \right] \delta P \text{ at } r = 1 \quad (\text{B.15})$$

Finite Difference Method

The term g^2 in the second order ODE in Equation (B.11) is a function of radial modulus, consequently a function of radial pressure that is the independent variable, i.e., Equation (B.11) is nonlinear. If g^2 is assumed as constant at one layer, a finite difference method can be used to solve the equation. By applying the central difference approximation, a set of algebraic equations can be obtained as follows:

$$A_i \delta P_{i+1} + B_i \delta P_i + C_i \delta P_{i-1} = 0 \quad (i=2, \dots, n) \quad (\text{B.16})$$

where

$$A_i = 1 + \frac{3t}{2r_i}$$

$$B_i = \frac{t^2}{r_i^2} (1 - g_i^2) - 2$$

$$C_i = 1 - \frac{3t}{2r_i} \quad (\text{B.17})$$

The boundary conditions can be represented as:

$$\delta P_{n+1} = - \frac{T_{w,n+1} t}{r_{n+1}} \quad (\text{B.18})$$

and

$$\frac{\delta P_2 - \delta P_1}{t} = \left[\frac{E_t}{E_c} - 1 + \nu \right] \delta P_1 \quad (\text{B.19})$$

Finally Equations (B.17) to (B.19) constitute a set of $n+1$ linear algebraic equations with $n+1$ unknowns. This set of equations consists of a tri-diagonal system. This can be solved easily by Thomson's algorithm which can solve tri-diagonalized matrix equations [4]. The solutions are the radial pressures caused at $n+1$ locations in the roll by the winding of the lap $n+1$. The total stresses will be obtained by adding all the incremental stresses due to the winding of each lap.

$$P_i = P_1 + \sum_{j=i+1}^n \delta P_{ij} \quad (\text{B.20})$$

The circumferential stress can be calculated by solving Equation (B.1) for σ_t :

$$T_i = P_i - r_i \frac{dP_i}{dr} \quad (\text{B.21})$$

APPENDIX C

PROGRAMS FOR HAKIEL'S WINDING MODEL AND CLASSIC SOLUTION

```
#include <string.h> /* Main Program for Hakiel's model */
#include <stdio.h>
void Initialize();
void hakiel();
void mesh();
void buckle();
char finp[20];
extern char fdel[50];
extern char fn1[20],fn2[20],fn3[20],fn4[20],fn5[20];
extern int section,nline,leng,part;
extern double rmin,rmax,percent,R1,R2;
extern int itw[10],nh;
extern double tww[10],H,hh,ec,et,nyu,tw,rk;
extern int nlayer,ntw,mat,norm; /* IBM-RT */

main(argc,argv)
int argc;
char *argv[];
{
    FILE *f1;
    strcpy(finp,argv[1]);
    Initialize();
    if (!strcmp("yes",argv[2])) hakiel();
    else {
        int line = 0;
        char c[80];
        f1 = fopen(fn3,"r");
        while(!feof(f1)) {
            fgets(c,80,f1); line++;
        }
        nline = --line;
        fclose(f1);
    }
    mesh();
} /* main */
```


/* Hakiel's Winding Model */

```

#define      Max      3000      /* IBM-RT */
#include     "variable.h"
void      Initialize();
void      Tw_pick();
void      Constant_Tri();
void      Result();
double    Er();
extern char    finp[20];
char      fdel[50]="rm ";
int       section,nline,leng,part;
double    rmin,rmax,percent,R1,R2;
int       itw[10],nh;
double    tww[10],H,hh,ec,et,nyu,tw,rk;
int       nlayer,ntw,mat,norm; /* IBM-RT */
double    dp[Max],p[Max],T[Max],r[Max], /* IBM-RT */
          a[Max],b[Max],c[Max],d[Max],beta[Max],gama[Max];

void      hakiel()
{
    int          i,k,n1;
    double       a2,b2,c2;
    k = 0;
    rk = 1.0+H*(et/ec-1.0+nyu)/r[0];
    while (k < nlayer) {
        Tw_pick(k);
        if ((k+1) % 50 == 0)
            printf(" Winding ... %4d-th layer, Tw = %.1f\n",k+1,tw);
        dp[k+1] = H*tw/r[k];
    /*** Calculate dp[i]      ***/
        if (k == 0); /*      first layer      */
        else if (k == 1) /*      second layer     */
            dp[1] = dp[2]/rk;
        else if (k == 2) { /*      third layer     */
            a2 = 1.0-1.5*H/(1.0+H);
            b2 = H/(1.0+H)*H/(1.0+H)*(1.0-et/Er(p[2]))-2.0;
            c2 = 1.0+1.5*H/(1.0+H);
            dp[1] = c2*dp[3]/(-b2*rk-a2);
            dp[2] = rk*dp[1];
        }
        else { /*      4th - nlayer     */
            Constant_Tri(k);
        }
    /*** Calculate p[i] & T[i] from dp[i]      ***/
        for (i=1; i <= k+1; i++)
            p[i] = p[i] + dp[i];
        if (k == nlayer-1) {
            T[k+1] = tw;
        }
    }
}

```

```

        for (i=k; i >= 2; i--)
            T[i] = -p[i]-r[i-1]*(p[i+1]-p[i-1])/(2*H);
        T[1] = -p[1]-r[0]*(p[2]-p[1])/H;
        Result(k);
    }
    k++;
} /* while */
printf("\n k = %d !! Everything is wound.\n",k);
} /* hakiel */
void Initialize()
{
/***** INPUT NOMENCLATURE *****/
    mat      : Material Identification
    norm     : Option for Normalization of the radius
    ntw      : Number of Junction of Winding Tension
    section  : Number of section of a circumferential length of a roll
    part     : Beam Selection by percentage or specified radii
    percent  : Percentage of Max. Stress for Beam Part Selection

    nh      : No. of Layers for one Element
    hh      : Caliper of Web Material
    ec      : Core Stiffness
    et      : Tangential Young's modulus
    nyu     : Poison's Ratio
    rmin    : Initial Radius
    rmax    : Final Radius
    B       : Beam Length(if it is zero, it will be calculated at middle)

    itw[i]  : No. of Layers at Junction Point
    tww[i]  : Winding Tension at Junction Point
*****/
    int      i,fp;
    dinp('r','p');
    leng = strlen(finp);
    f1 = fopen(finp,"r");
    fgets(head,100,f1);
    fscanf(f1,"%d%d%d%d%d %lf",
        &mat,&norm,&ntw,&section,&part,&percent);
    fscanf(f1,"%d %lf%lf%lf%lf%lf%lf %lf%lf %lf",
        &nh,&hh,&ec,&et,&nyu,&rmin,&rmax,&R1,&R2,&B);
    for (i=0; i < ntw; i++) {
        fscanf(f1,"%d%lf",&itw[i],&tww[i]);
        itw[i]/=nh;
    }
    fclose(f1);
    dinp('w','p');
    H = hh*nh;
    nlayer = (rmax-rmin+1e-10)/H;
    for (i=0; i < nlayer+1; i++) {

```

```

    dp[i]=p[i]= 0.0;
    r[i] = rmin + H*i;
}
strcpy(fn1,fnp);
strcat(fn1,".d");      /* fn1.d ... input data to mesh.c      */
strcpy(fn3,fnp);
strcat(fn3,".f");      /* fn3.f ... input data redisplay      */
strcpy(fn4,fnp);
strcat(fn4,".b");      /* fn4.b ... output from buckle.c      */
strcpy(fn5,fnp);
strcat(fn5,".a");      /* fn5.a ... input data to ansd.c      */
for (fp=0; fp < 2; fp++) {
    if (fp == 0)
        f3 = stdout;
    else
        f3 = fopen(fn3,"w");
    fprintf(f3," %s\n",head);
    fprintf(f3," Material I.D. ... %d\t",mat);
    switch (mat) {
    case 1:
        fprintf(f3,"*Hakiel's Paper * \n");          break;
    case 2:;
    case 3:
        fprintf(f3,"*Polypropylene (linear function)* \n");          break;
    case 4:
        fprintf(f3,"*Polypropylene (3rd polynomial function)* \n");          break;
    case 5:
        fprintf(f3,"*ICI film Polypester (377/92) * \n");          break;
    default:
        printf("mat = %d !!          Check Material I.D !\n",mat);
        exit(1);
    }
}

fprintf(f3," Thickness (hh) = %12.5f\n",hh);
fprintf(f3," No. of layer (nh) = %12d\n",nh);
fprintf(f3," Core Modulus (Ec) = %12.5e\n",ec);
fprintf(f3," Tan. Modulus (Et) = %12.5e\n",et);
fprintf(f3," Posson Ratio (nyu)= %12.5e\n",nyu);
fprintf(f3," Min. Radius (rmin)= %12.5e\n",rmin);
fprintf(f3," Max. Radius (rmax)= %12.5e\n",rmax);
fprintf(f3," No. of section          = %2d\n",section);
fprintf(f3," Beam part Selection(1/0) = %2d\n",part);
fprintf(f3," Normalization(1/0)      = %2d\n\n",norm);
fprintf(f3," \n Output File \"%s\" ... input informations ",fn3);
fprintf(f3," \n          \"%s\" ... input to mesh.c",fn1);
fprintf(f3," \n          \"%s\" ... input to buckle.c\n",fn4);
fprintf(f3," \tLayer\tRadius\tTension\n");
for (i=0; i < ntw; i++)
    fprintf(f3," \t%6d\t%6.3f\t%6.3f\n",itw[i],r[itw[i]],tww[i]);

```

```

    fprintf(f3, "\n Total layers    ... %8d\n", nlayer);
}
    fclose(f3);
} /* Initialize */
void Result(k)
int k;
{
    int i, line = 0;

    f1 = fopen(fn1, "w");
    fprintf(f1, "* Radius\tRadial Pressure\tCircumferential Stress\n",
            tw, r[k+1], tw, r[k+1]);
    line++;
    for (i=1; i <= k; i+=2) {
        fprintf(f1, "%.4f\t%.4e\t%.4e\n",
                r[i-1], p[i], T[i]);
        line++;
    }
    fprintf(f1, "%.4f\t%.4e\t%.4e\n", rmax, 0.0, T[k+1]);
    line++;
    nline = line;
    fclose(f1);
}
void Tw_pick(k)
int k;
{
    int i;
    k = k+1;
    for (i=0; i < ntw; i++) {
        if (k == itw[i]) {
            tw = tww[i];
            break;
        }
        else if (k > itw[i] && k <= itw[i+1]) {
            if (tww[i] == tww[i+1]) {
                tw = tww[i];
                break;
            }
            else {
                tw = tww[i] + (tww[i+1] - tww[i]) /
                    (itw[i+1] - itw[i]) * (k - itw[i]);
                break;
            }
        }
    }
    /* for i < ntw */
} /* Tw_pick */

```

```

void Constant_Tri(n)
int n;
{
    int i,n1;
    double h_r,gi2;
    n1 = n+1;
    a[1] = 0.0;
    b[1] = -rk;
    c[1] = 1.0;
    d[1] = 0.0;
    for (i=2; i <= n; i++) {
        h_r = H/r[i];
        gi2 = et/Er(p[i]);
        a[i] = 1.0-1.5*h_r;
        b[i] = h_r*h_r*(1.0-gi2)-2.0;
        c[i] = 1.0+1.5*h_r;
        d[i] = 0.0;
    }
    d[n] = -dp[n+1]*c[n];
    c[n] = 0.0;
    beta[1] = b[1];
    gama[1] = d[1]/b[1];
    for (i=2; i <= n; i++) {
        beta[i] = b[i]-a[i]*c[i-1]/beta[i-1];
        gama[i] = (d[i]-a[i]*gama[i-1])/beta[i];
    }
    dp[n] = gama[n];
    for (i=n-1; i >= 1; i--)
        dp[i] = gama[i]-c[i]*dp[i+1]/beta[i];
}

```

/* Radial Modulus Function */

```

#include <math.h>
extern int mat;
double Er(p)
double p;
{
    switch (mat) {
    case 1: return(450.0*p);
    case 2: return(1060.0*p-0.513*p*p);
    case 3: /* polypropylene (linear functions) */
    if ( p <= 11.0) return(82.93*p);
    else if (p > 11.0 && p <= 50.0) return(325.42*p-2671.8);
    else if (p > 50.0 && p <= 70.0) return(275.44*p-172.8);
    else if (p > 70.0 && p <= 110.0) return(289.46*p-1154.2);
    else if (p > 110 && p <= 150.0) return(272.05*p+760.5);
    else if (p > 150.0 && p <= 300.0) return(231.83*p+6793.0);
    else {
        printf("\nCaution !!! Out of range of \"layer_er Table\"\n");
        exit(1);
    }
    case 4 :/* polypropylene (3rd polynomial functions) */
    if (p <= 20)
        return(81.823+128.04*p+6.8096*p*p-0.17355*p*p*p);
    else if (p > 20.0 && p <= 100.0)
        return(-444.98+176.54*p+2.5333*p*p-1.6321e-2*p*p*p);
    else if (p > 100.0 && p <= 330.0)
        return(-4.4852e4+972.39*p-3.1059*p*p+3.7733e-3*p*p*p);
    else {
        printf("Caution !!! Out of range of \"layer_er Table\"\n");
        exit(1);
    }
    case 5: /* polyester(ICI 377/92) */
    if ( p <= 5.0) return(51.2436*p);
    else if (p > 5.0 && p <= 10.0164) return(40.4274*p+54.081);
    else if (p > 10.0164 && p <= 20.1897) return(37.2571*p+84.8356);
    else if (p > 20.1897 && p <= 40.4648) return(34.6979*p+137.5052);
    else if (p > 40.4648 && p <= 70.4554) return(32.3358*p+233.0884);
    else if (p > 70.4554 && p <= 100.377) return(30.5054*p+362.0507);
    else if (p > 100.377 && p <= 150.796) return(28.8457*p+528.6479);
    else if (p > 150.796 && p <= 199.079) return(27.3813*p+749.4736);
    else {
        printf("\nCaution !!! Out of range of \"layer_er Table\"\n");
        exit(1);
    }
    default ;;
    } /* switch */
}

```

```
/* Buckling of a Beam upon Elastic Foundation */
```

```
#include <stdio.h>
#include <math.h>
#include "variable.h"
extern double et,hh;
int i,m;
double iz,L2, L3, L4,Pe,
beta0,beta1,pe,Beta,Alpa;

buckle() /* BUCKLE.H */
{
    printf("\n... calculating buckling mode and load...\n");
    f1 = fopen(fn4,"w");
    iz = W*hh*hh*t1/12;
    L2 = B*B;
    L3 = L2*B;
    L4 = L3*B;
    beta0= L4/(pow(M_PI,4.0)*et*iz);
    beta1= 3*beta0/16;
    fprintf(f1," Young's modulus = %12.5e\n",et);
    fprintf(f1," Moment of inertia = %12.5e\n",iz);
    fprintf(f1," Width of the plate = %12.5f\n",W);
    fprintf(f1," Length of the plate = %12.5f\n",B);
    fprintf(f1," Foundation = %12.5f %12.5f\n",a1,a2);
    fprintf(f1," Thickness of the sheet = %12.5f\n",hh);
    fprintf(f1," Orig. Th. of the stack = %12.5f\n",t1);
    fprintf(f1," Equiv. Th. of the stack = %12.5f\n\n",t);
    Alpa = k1;
    pe= M_PI*M_PI*et*iz/L2;
    fprintf(f1," \tk1\tmode Fcr(lb)\t Pcr(psi)\t Pe(lb)\n");
    Beta=beta0*Alpa/B;
    for(m=1;m < 50;m++) {
        if((m*m*(m+1)*(m+1)-Beta) > 0.0) {
            Fc = pe*(m*m+Beta/(m*m));
            Pc = Fc/t1/W;
            Pe = pe*m*m;
            mode_b = m;
            fprintf(f1,"%12.4e\t%3d\t%8.3f\t%8.3f\t%8.3f\n",
                Alpa,m,Fc,Pc,Pe);
            break;
        }
    }
    fclose(f1);
} /* buckle */
```

```
/* Header File "variable.h" */
```

```
#include <stdio.h>
#include <string.h>
#define NMAX 100
#define FMAX 100
FILE *f1, *f2, *f3, *f4, *f5;
char fn1[20],fn2[20],fn3[20],fn4[20],fn5[20];
int ii,jj,kk,ll,ie,na,nc,nt,nb1,ne,nac,nae;
int db1,db2,nfx[50],fs;
int niter,nprn,nstep;
int n1[10],e1[10],n[10];
double a1,a2,B,W,ks,k1,area,t,t1,MU,Ey,cnvr,
pr[50],Dav,fr[50],X[50],Ex,Pav,Fs,Ps;
double df,fx,h,areah,areat,Iz1,Iz2,rate;
double x[NMAX],y[2],z;
/* ansd.inp */
double fc1,fc2,fc3,Fc,Pc;
int restart,slope,mode,mdiv,mode_b,nb,nf,nd,ifc;
char head[6][100],ansdin[10];
void dinp(rw,N)
char rw,N;
{
    int i;
    if (N == 'c')
        strcpy(ansdin,fn5);
    else
        strcpy(ansdin,"ansd.inp");
    switch(rw) {
    case 'r' :
        f1=fopen(ansdin,"r");
        for (i=0; i < 6; i++)
            fgets(head[i],100,f1);
        fscanf(f1,"%lf %lf %lf",&fc1,&fc2,&fc3);
        fscanf(f1,"%d %d %d %d %d %d %d",
            &ifc,&restart,&slope,&mode,&mdiv,&nf,&nd);
        nb = mode*mdiv;
        fscanf(f1,"%lf %lf %lf %lf %lf %lf %lf %lf %lf",
            &a1,&t,&a2,&B,&W,&t1,&Ey,&MU,&df);
        fscanf(f1,"%lf %d %d %d %d %d %lf",
            &rate, &na,&ne,&nt,&niter,&nprn,&cnvr);
        fscanf(f1,"%lf %d %lf %lf %lf %lf %lf %lf",
            &k1,&mode_b,&Fc,&Pc,&Fs,&Ps,&Pav,&Ex);
        nae = na + ne + 1;
        if (N == 'p')
            for (i=0; i <= nae; i++)
                fscanf(f1,"%lf",&X[i]);
        break;
    }
```



```

case 'w' :
    fl=fopen(ansdin,"w");
    for (i=0; i < 6; i++)
        fprintf(f1,"%s",head[i]);
    fprintf(f1,"%0.3f\t%0.3f\t%0.3f ",fc1,fc2,fc3);
    fprintf(f1,"%03d\t%03d\t%03d\t%03d\t%03d\t%03d\t%03d\n",
        ifc,restart,slope,mode,mdiv,nf,nd);
    fprintf(f1,"%0.4f\t%0.5e %0.4f\t%0.4f\t%0.3f\t%0.4f\t%0.3e %0.2f\t%0.4f\n",
        a1,t,a2,B,W,t1,Ey,MU,df);
    fprintf(f1,"%0.2f\t%d\t%d\t%d\t%d\t%0.4f\n",
        rate,na,ne,nt,niter,nprn,cnvr);
    fprintf(f1,"%0.5e\t%02d\t%0.3f\t%0.3f\t%0.3f\t%0.3f\t%0.3f\t%0.3f\n",
        k1,mode_b,Fc,Pc,Fs,Ps,Pav,Ex);
    nae = na + ne + 1;
    for (i=0; i <= nae; i++) {
        fprintf(f1,"%010.8f\n",X[i]);
    }
break;
default ::
}
fclose(f1);
}

```

/* Data File "ansd.inp" */

polyester(377/92) (h = 0.00092", Tw = 200psi) Beam = center L=(R1+R2)/2

fc1	fc2	fcr	ifc	restart	slope	mode	mdiv	nf
a1	t	a2	b	w	t1	Ey	MU	df
fac	na	ne	nt	niter	nprn	cnvr		
k1	mode	Fc	Pc	Fs	Ps	Pav	Ex	
x[i]								
-23.750	-23.800	-23.800	10	1	20	14	4	10
0.5637	5.02600e-03	0.5637	2.8000	6.000	0.1500	6.534e+0	0.28	0.0050
1.75	7	7	2	-20	20	0.0005		
3.48786e+03		6	22.014	24.460	1.738	1.931	1.724	88.355
0.00000000								
0.24651137								
0.38737501								
0.46786852								
0.51386481								
0.54014840								
0.55516760								
0.56375000								
0.56877600								
0.57735840								
0.59237759								
0.61866119								
0.66465748								
0.74515099								
0.88601463								
1.13252600								

/* Data File "finp" */

fname	fg1	fg2	ncheck	div	mode	mdiv	restart
c200.1_17.00	-20	-40	4	10	17	4	0

APPENDIX D

PROGRAMS FOR NONLINEAR BUCKLING ANALYSIS

```
#include      "variable.h"
main()              /* main.c */
{
    char        line[120],fname[20],ansys[50],ansp[50],ansys1[50],
                file3[50],keep3[50],fetch3[50],
                file16[50],keep16[50],fetch16[50];
    double      fg1,fg2,fi,Df;
    int         ncheck,div,i,j,leng,nfile;
    FILE        *f1,*f2;
    dinp('r','p');
    f1 = fopen("finp","r");
    fgets(line,120,f1);
    fscanf(f1,"%s %lf%lf %d%d%d%d%d",fname,&fg1,&fg2,
           &ncheck,&div,&mode,&mdiv,&restart);
    fclose(f1);
    leng = strlen(fname);
    strncpy(file3,fname,leng-2);
    strncpy(file16,fname,leng-2);
    strcat(file3,"f3");
    strcat(file16,"f16");
    strncpy(ansys,fname,leng-1);
    strcat(ansys,"a");
    strcpy(keep3,"cp file03.dat ");
    strcat(keep3,file3);
    strcpy(keep16,"cp file16.dat ");
    strcat(keep16,file16);
    strcpy(fetch3,"cp ");
    strcat(fetch3,file3);
    strcat(fetch3," file03.dat");
    strcpy(fetch16,"cp ");
    strcat(fetch16,file16);
    strcat(fetch16," file16.dat");
    Df = (fg2-fg1)/ncheck;
    fi = Df/div;
    nfile=0;
```

```

for (i=0; i < ncheck; i++) {
    fc1 = fg1+Df*i;
    fc2 = fc1 + Df;
    nf = div;
    j = 0;
do {
    nfile++;
    slope = 1;
    dinp('w','p');
if(!restart) {
    system("ansd");    /* make ansys input "ansd.1" */
        /* ansd < ansd.inp > ansd.1+node */
    system("ansys < ansd.1 > /dev/null ");
system(keep3);
system(keep16);
    system("cp ans.out ans.out11");
    restart = 1;
    system("date >> finp");
} /* !restart */
for(ifc=0; ifc <= nf; ifc++) {
fcr = fc1+(fc2-fc1)/nf*ifc;
    dinp('w','p');
    system(fetch3);
    system(fetch16);
    system("ansd");    /* make ansys input "ansd.2" */
    system("ansys < ansd.2 > /dev/null ");
    system("cat pre2 >> pre");
    system("cat ans.out2 >> ans.out");
}

        /*** Examine the displacements ***/
system("ansp");
        /* ansp < ans.out+ansd.inp+node > ansp.o */
dinp('r','p');
        /*** Update load ranges ***/
system("ansq");
        /* ansq < ansp.o+ansd.inp > ansd.inp */
strcpy(ansys1,"mv ans.out ");
strcat(ansys1,ansys);
system(ansys1);    /* cp ans.out > file##.#a */
ansys[leng-1]='b';
strcpy(ansys1,"mv ans.dsp ");
strcat(ansys1,ansys);
system(ansys1);    /* cp ans.out > file##.#b */
fname[leng-1]++;
strcpy(ansp,"cat ansp.o st1 > ");
strcat(ansp,fname);
system(ansp);    /* cat ansp.o st1 > file##.#1 */
f3 = fopen(fname,"a");
fprintf(f3,"\nFile name = %s\n",fname);

```

```
fclose(f3);
    j++;
    dinp('r','p');
if (slope == 1)
    restart=0;
else if (slope == 2)
    system("cp ans.out11 ans.out");
else if (slope > 2){
    system("rm file* core");
    exit();
}
} while (slope==2 && nfile<9);    /* end do*/
}
    system("rm file* core");
}
```

```
/* Input Data generation to ANSYS program */
```

```
#include      "variable.h"
void  constants();
void  mesh();
void  boundary();
void  resume();
double x_y();
double h2,areah2,ks2;
main()
{
    /* ansd.c */
    {
        dinp('r','p');
        constants();
        if (!restart) {
            mesh();
            boundary();
        }
        else      resume();
    }
}
void  constants()
{
    int      i;
    char      temp[100];
    Dav=Pav*a1/Ex;
    if (MU != 0.0)      fs=0;
    else                fs=1;
    area = W*B;
    h = B/nb;
    areah = W*h;
    areat = W*t;
    Iz1 = W*h*h*h/12;
    Iz2 = W*t*t*t/12;
    ks = k1/nb;
    sprintf(temp,"%0.9e %0.9e %0.9e",h/2,areah/2,ks/2);
    sscanf(temp,"%lf %lf %lf",&h2,&areah2,&ks2);
    h = h2*2;
    areah = areah2*2;
    ks = ks2*2;
    nb1 = nb+1;
    nac = nae+3;
    y[0] = 0;
    y[1] = B;
    z = 0.0;
    /* Node generation */
    n1[0] = 1;
    n1[1] = nb1*na+1;
    n1[2] = n1[1]+nb1;
    n1[3] = n1[2]+nb1*nt;
}
```

```

n1[4] = n1[3]+nb1;
n1[5] = n1[4]+nb1*ne;
nc = n1[2]+nb1;
e1[0] = 1;
e1[1] = na+1;
e1[2] = e1[1]+2;
e1[3] = e1[2]+5;
e1[4] = e1[3]+2;
e1[5] = e1[4]+ne;
db1 = mdiv/2;
db2 = mdiv;
}
void mesh()
{
    int i,j,m,pick,half;
    double xin;
    f3 = fopen("ansd.1","w");
    fprintf(f3,"/OUTPUT,pre\n/PREP7\n/TITLE ");
    fprintf(f3,
" MU=%4.2f,t=%7.5f,t1=%7.5f,Ey=%9.3e,m=%2d,F=%8.3f,%8.3f\n",
    MU,t,t1,Ey,mode,fc1,fc2);
    fprintf(f3,"KAY,6,1 \t * Large Deflection Option\n");
    fprintf(f3,"CNVR,,,%4f,,1 \t * Convergent Bound\n\n",cnvr);
    fprintf(f3,"ET,1,42,0,1,3 \t * Plane stress\n");
    fprintf(f3,"R,1,%7.3f \t * Thickness\n\n",W);
    fprintf(f3,"EX,%2d,%4e $EY,%2d,%4e $NUXY,%2d,0\n",
    1,Ex,1,Ey,1);
    fprintf(f3,"\nET,2,12,%d,,1,,3 \t\t *** Gap Element\n",fs);
    fprintf(f3,"R,2,-90,%10e,,1",ks);
    fprintf(f3," \t \t * theta,stiffness,interfernce,status\n");
    fprintf(f3,"MU,2,%2f \t\t * Friction Coefficient\n",MU);
    fprintf(f3,"\nET,6,12,%d,,1,,3 \t\t *** Gap Element\n",fs);
    fprintf(f3,"R,6,-90,%9e,,1",ks2);
    fprintf(f3," \t \t * theta,stiffness,interfernce,status\n");
    fprintf(f3,"MU,6,%2f \t\t * Friction Coefficient\n\n",MU);
    fprintf(f3,"ET,4,3 \t \t \t * Center Beam Element\n");
    fprintf(f3,"EX,4,%4e\nNUXY,4,0\n",Ey);
    fprintf(f3,"R,4,%6e,%6e,%6e\t* Area,Izz,Thickness\n",areat,Iz2,t);
    fprintf(f3,"ET,3,3 \t \t \t * Lateral Beam Element\n");
    fprintf(f3,"EX,3,%4e\nNUXY,3,0\n",Ex);
    fprintf(f3,"R,3,%10e,1.0E1,%10e\t* Area,Izz,Thickness\n",areah,h);
    fprintf(f3,"ET,5,3 \t \t \t * Top_Bottom Beam Element\n");
    fprintf(f3,"EX,5,%4e\nNUXY,5,0\n",Ex);
    fprintf(f3,"R,5,%9e,1.0E1,%10e\t* Area,Izz,Thickness\n",
    areah2,h2);
    for (i = 0; i <= nae; i++)
        if (i < na)
            x[i] = X[i];
        else if (i == na){

```

```

        x[i] = X[i];
        x[i+1]=X[i];
        x[i+2]=(X[i]+X[i+1])/2;
        x[i+3]=X[i+1];
    }
    else if (i > na)
        x[i+3] = X[i];
    for (i=0; i <= nac; i++) {
        n[0] = nb1*i+1;
        n[1] = n[0]+nb;
        for (j = 0; j <= 1; j++)
            fprintf(f3, "$N,%4d,%10.8f,%10.8f  ",n[j],x[i],y[j]);
        fprintf(f3, "$FILL\n");
    }
}
/** Node Generation **/
for (ie = 0; ie < 5; ie++){
    ii = n1[ie];
    jj = ii+1;
    kk = jj+nb1;
    ll = kk-1;
    switch (ie) {
    case 0 :
        fprintf(f3, "\nTYPE,1 $MAT,%2d $REAL,1  ",1);
        fprintf(f3, "\n$E,%4d,%4d,%4d,%4d",ii,jj,kk,ll);
        fprintf(f3, "\t \t $EGEN,%2d,%2d,%2d",na,nb1,1);
        fprintf(f3, "\t \t * Element %2d-%2d\n",1,na);
        break;
    case 1 ;;
    case 3 :
        fprintf(f3, "TYPE,6 $MAT, 6 $REAL,6  ");
        fprintf(f3, "$E,%4d,%4d\n",ii,ll);
        fprintf(f3, "TYPE,2 $MAT, 2 $REAL,2  ");
        fprintf(f3, "$E,%4d,%4d  ",jj,kk);
        fprintf(f3, "\t \t * Element %2d-%2d\n",e1[ie],e1[ie]+1);
        break;
    case 2 :
        fprintf(f3, "TYPE,5 $MAT, 5 $REAL,5  ");
        fprintf(f3, "$E,%4d,%4d  ",ii,ll);
        fprintf(f3, "$E,%4d,%4d  ",nc,nc+nb1);
        fprintf(f3, "* Element %2d-%2d\n",e1[ie],e1[ie]+1);
        fprintf(f3, "TYPE,4 $MAT, 4 $REAL,4  ");
        fprintf(f3, "$E,%4d,%4d",nc,nc+1, ' ');
        fprintf(f3, "\t \t * Element %2d\n",e1[ie]+2);
        fprintf(f3, "TYPE,3 $MAT, 3 $REAL,3  ");
        fprintf(f3, "$E,%4d,%4d  ",jj,kk);
        fprintf(f3, "$E,%4d,%4d  ",jj+nb1,kk+nb1);
        fprintf(f3, "* Element %2d-%2d\n",e1[ie]+3,e1[ie]+4);
        break;
    case 4 :

```



```

        fprintf(f3, "\nTYPE,1 $MAT,%2d $REAL,1 ",1);
        fprintf(f3, "\n$E,%4d,%4d,%4d,%4d",ii,jj,kk,ll);
        fprintf(f3, "\t \t$EGEN,%2d,%2d,%2d",ne,nb1,e1[ie]);
        fprintf(f3, "\t \t * Element %2d-%2d\n",e1[ie],e1[ie+1]-1);
        break;
default :
        break;
}
}
fprintf(f3, "\n");
for (ie = 0; ie < 5; ie++){
    ii = n1[ie];
    jj = ii+1;
    kk = jj+nb1;
    ll = kk-1;
    if((ie == 0) || (ie == 4))
        fprintf(f3, "$EGEN,2,1,%2d,%2d ",e1[ie],e1[ie+1]-1);
    else if((ie == 1) || (ie == 3))
        fprintf(f3, "$EGEN,2,1,%2d ",e1[ie]+1);
    else if (ie == 2){
        fprintf(f3, "$EGEN,2,1,%2d\n",e1[ie]+2);
        fprintf(f3, "$EGEN,2,1,%2d,%2d ",e1[ie]+3,e1[ie]+4);
    }
}
fprintf(f3, "\t * Element %d-%d\n",e1[5],e1[5]+na+ne+4);
fprintf(f3, "$EGEN,%2d,1,%2d,%2d",nb-2,e1[5],e1[5]+na+ne+4);
fprintf(f3, "\t \t \t \t * Element %d-%d\n",
    e1[5]+na+ne+5,nb*(na+ne+5)+4-e1[5]);
fprintf(f3, "$EGEN,%d,%2d,%2d,%2d ",2,nb-1,e1[0],e1[0]+na-1);
fprintf(f3, "$EGEN,%d,%2d,%2d ",2,nb,e1[1]);
fprintf(f3, "$EGEN,%d,%2d,%2d,%2d\n",2,nb,e1[2],e1[2]+1);
fprintf(f3, "$EGEN,%d,%2d,%2d ",2,nb-1,e1[2]+2);
fprintf(f3, "$EGEN,%d,%2d,%2d ",2,nb,e1[3]);
fprintf(f3, "$EGEN,%d,%2d,%2d,%2d ",2,nb-1,e1[4],e1[5]-1);
fprintf(f3, "\t * Element %d-%d\n",
    nb*(na+ne+5)+5-e1[5],nb*(na+ne+5)+4);
/**/ Element Generation /**/
f4 = fopen("node","w");
pick = mode % 4;      half = nb/2+1;
switch(pick) {
    case 0 : pick = half-db1;      break;
    case 1 : pick = half;          break;
    case 2 : pick = half+db1;      break;
    case 3 : pick = half;          break;
    default ;;
}
fprintf(f4, "%d %d %d %d\n",nc,nc+pick-1,nc+nb-db1,nc+nb);
fclose(f4);
} /* mesh */

```

```

void boundary()
{
    int i,j,m,pick,half;
    fprintf(f3,"\nITER,%d,%d,%d",niter,nprn,-1);
    fprintf(f3,"\n$PRNF,-1 $PRDI,-1 $PRST,-1 $KRF,-1");
    fprintf(f3,"\n$PRDI,,%4d,%4d,%4d \t \t * Loading Points",
        nc,nc+nb,1);
    /* Equivalent Displacement corresponding to Radial Pressure */
    nstep=0;
    fprintf(f3,"\nD,%4d,UX,%15.10f,,%4d,%4d",1,Dav,nb1,1);
    fprintf(f3,"\nD,%4d,UX,%15.10f,,%4d,%4d",n1[5],-Dav,n1[5]+nb,1);
    fprintf(f3,"\nD,%4d,UY,,,, \t \t * Left Center ",nb/2+1);
    fprintf(f3,"\nD,%4d,UY,,,, \t \t * Right Center ",n1[5]+nb/2);
    fprintf(f3,"\nCE,%3d,0,%3d,UX,1,%3d,UX,-1 ",1,nc,nc+nb2);
    fprintf(f3,"\nRP%-d,1, , , ,%3d \t \t * Mode Constraints\n",
        mode,db2);
    /* Perturbing Load */
    for (m = 0; m < 2; m++){
        for (j = 0; j < mode; j++){
            if (j % 2) fx = -df;
            else fx = df;
            nfx[j] = nc + db1+db2*j;
            fprintf(f3,"\nF,%4d,FX,%10.6f",nfx[j],fx);
        }
        fprintf(f3,"\n$LWRI \t\t \t STEP %4d",++nstep);
        fprintf(f3,"\t * Perturbing Load *\n");
    /* Assumed Buckling Load */
    if (!m) {
        fprintf(f3,"FDEL,%4d,FX,%4d,%2d\n",
            nc+db1,nc+nb-db1,db2);
        fprintf(f3,"F,%4d,FY,%10.4f",nc,-fc1);
        fprintf(f3," $F,%4d,FY,%10.4f",nc+nb,fc1);
        fprintf(f3,"\n$LWRI \t\t \t STEP %4d",++nstep);
        fprintf(f3,"\t * Axial Load *\n");
        fprintf(f3,"\nFDEL,%4d,FY,%4d,%4d",nc,nc+nb,nb);
    }
    }
    fprintf(f3,"\nAFWRITE \nFINISH\n\n");
    fprintf(f3,"/OUTPUT,ans.out\n/INPUT,27 \nFINISH\n");
    fclose(f3);
} /* mesh */
void resume()
{
    f3 = fopen("ansd.2","w");
    fprintf(f3,"/OUTPUT,pre2\n/PREP7\n/TITLE ");
    fprintf(f3,
        " MU=%4.2f,t=%7.5f,t1=%7.5f,Ey=%9.3e,m=%2d,F=%8.3f,%8.3f\n",
        MU,t,t1,Ey,mode,fc1,fc2);
}

```

```

    fprintf(f3,"RESU\n");
    fprintf(f3,"/GOLI\n");
    fprintf(f3,"/GOPR\n");
    fprintf(f3,"\nITER,%d,%d,%d",niter,nprn,-1);
    fprintf(f3,"\n$PRNF,-1 $PRDI,-1 $PRST,-1 $KRF,-1");
    fprintf(f3,"\n$PRDI,,%4d,%4d,%4d \t \t * Loading Points",
            nc,nc+nb,1);
/* Check the buckling load */
    fprintf(f3,"\n\nFDEL,%4d,FX,%4d,%2d",
            nc+db1,nc+nb-db1,db2);
    fprintf(f3,"\nF,%4d,FY,%10.4f",nc,-fcr);
    fprintf(f3,"\nF,%4d,FY,%10.4f",nc+nb,fcr);
    fprintf(f3,"\t\t $LWRI\tSTEP %4d\n",++nstep);
    fprintf(f3,"\nSLOAD,1\nAFWRITE \nFINISH\n\n");
    fprintf(f3,"/LOAD\n/OUTPUT,ans.out2\n/INPUT,27 \nFINISH\n");
    fclose(f3);
}
double x_y(q,r)
double q;
int r;
{
    int i;
    double x1;
    if (r == 0) return(1.0);
    else {
        x1 = 1.0;
        for (i=0; i < r; i++)
            x1=x1*q;
        return(x1);
    }
}

```

```
/* Pick up Displcements from "ans.out" */
```

```
#include      "variable.h"
main()
{
    char      line[120],ln[30],li[60],fout[9],n1[9],n2[9],n3[9],n4[9];
    char      st0[8],st1[5],st2[5];
    int       i,icc,nstep,istep,ip,c;
    int       iprint=0;
    double    f,af;
    dinp('r','p');
    f1 = fopen("node","r");
    fscanf(f1,"%s%s%s%s",n1,n2,n3,n4);
    fclose(f1);
    f2 = fopen("ansd.2","r");
    for (i=0; i < 3; i++)
        fgets(line,120,f2);
    fclose(f2);
    f4 = fopen("ansp.o","w");
    fprintf(f4,"%s",head[0]);
    fprintf(f4,"%s",line+7);
    fprintf(f4," %s(Ux)\t %s(Ux)\t %s(Ux)\t %s(Uy)\tStep\tForce\n",
        n1,n2,n3,n4);
    nstep = -nd-1;
    icc = 0;
    af =(fc2-fc1)/nf;
    f3 = fopen("ans.out","r");
    f5 = fopen("ans.dsp","w");
    while (!feof(f3)){
        fgets(line,120,f3);
        if(strlen(line) > 30){
            if(!strncmp(line," SOLUTION NOT CONV",18)) {
                slope = 99;
                dinp('w','p');
                exit();
            }
            if (line[3] == ' '){
                if (line[4] == ' '){
                    strncpy(st0,line+5 ,2);
                    st0[2]='\0';
                }
                else {
                    strncpy(st0,line+4 ,3);
                    st0[3]='\0';
                }
            }
            else
                strncpy(st0,line+3 ,4);
        }
    }
}
```

```

        st0[4]='\0';
        strncpy(st1,line+8,4);
        strncpy(st2,line+58,4);
if (!strcmp(st1," ") && !strcmp(st2," 4.4"))
        for (i=0; i<13; i++)
                fgets(line,120,f3);
if(!strcmp(st0,n1)) {
        iprint=1;
        nstep++;
        if (nstep<0)          f = 0;
        else                  f = fc1+af*nstep;
        strncpy(li+52,line+69,3);
        li[55] = '\0';
        strncpy(li,line+11,12);
        li[12] = '\t';
}
else if(!strcmp(st0,n2)) {
        strncpy(li+13,line+11,12);
        li[25] = '\t';
}
else if(!strcmp(st0,n3)) {
        strncpy(li+26,line+11,12);
        li[38] = '\t';
}
else if(!strcmp(st0,n4)) {
        strncpy(li+39,line+27,12);
        li[51] = '\t';
        fprintf(f4,"%s %.3f\n",li,f);
}
if(iprint) fprintf(f5,"%s",line);
if(!strcmp(st0,n4)) iprint=0;
}          /* end if(strlen(line) > 30)*/
}          /* end while */
fclose(f3);
fclose(f4);
fclose(f5);
}

```

```
/* Check Buckling Status from "ansp.o" */
```

```
#include      "variable.h"
#include      <math.h>
double      abs();
double      min();
double      max();
main()
{
    char      line[120],fcr[50],ff1[10],ff2[10];
    FILE      *f1,*f2,*f3;
    int       i,j,nn;
    int       incr,decr,inc,dec;
    double    eps,fi,ux1,ux2,ux3,uy,step,fc[30],ux[30],uxx;
    dinp('r','p');
    f2 = fopen("ansp.o","r");
    for (i=0; i < nd+2; i++) {
        fgets(line,120,f2);
        if (i==1) {
            strncpy(ff1,line+50,8);
            strncpy(ff2,line+59,8);
            sprintf(fcr,"%s %s ",ff1,ff2);
        }
    }
    sscanf(fcr,"%lf %lf",&fc1,&fc2);
    fi = (fc2-fc1)/nf;
    eps=1E-10;
    incr=decr=inc=dec = 0;
    f3 = fopen("st1","w");
    fscanf(f2,"%lf %lf %s %s %s %s",&ux1,&ux2);
    uxx = abs(ux1-ux2);
    for (i=1; i<nf+2 ; i++) {
        fscanf(f2,"%lf %lf %s %s %s %lf",&ux1,&ux2,&fc[i]);
        ux[i] = abs(ux1-ux2);
        if (ux[i] > (uxx+eps)) {
            incr = 1;          if (!inc) inc=i;
        }
        if (ux[i] < (uxx-eps)) {
            decr = 1;
            dec = i;
        }
        if (decr && !incr)      slope = 1;
        else if (decr && incr)  slope = 2;
        else if (!decr && incr) slope = 3;
        fprintf(f3,"%2d= %.3e ",i,uxx);
        fprintf(f3,"%9.3e dec=%d inc=%d ",ux[i],decr,incr);
        fprintf(f3,"f=%.3f\n",fc[i]);
    } /* for i */
    fclose(f2);
}
```

```
if (slope == 2) {
    fc1 = fc[dec];
    fc2 = fc[inc];
    slope = (fi < -0.1) ? 2 : 20;
}
fprintf(f3,
    "\nfc=(%.2f,%.2f) Pc=(%.2f,%.2f) slope=%2d,df=%.4f,cnvr=%.4f\n",
    -fc1,-fc2,-fc1/W/t1,-fc2/W/t1,slope,df,cnvr);
fclose(f3);
dinp('w','p');
} /** ansq.c ***/
double abs(x)
double x;
{
    return(x>0 ? x : -x);
}
double min(x,y)
double x,y;
{
    return(x>y ? x : y);
}
double max(x,y)
double x,y;
{
    return(x<y ? x : y);
}
```

APPENDIX E

PROGRAM FOR PFEIFFER'S K_1 AND K_2

```
/* Pfeiffer's Radial Modulus Function. */
/*      Pr = -k1 + k1*exp(k2*e)
      log(Pr+k1) = log(k1) + k2*e
      Er = k1*k2 + k2*Pr      */
#include <stdio.h>
#include <string.h>
#include <math.h>
#include <stdlib.h>
void least();
main()
{
    char  data[20],out1[20],out2[20];
    int   i,N,ok,iter,Max=1000;
    double *p,*e,*pr,*Pr,k1,kp,logk1,k2,ei;
    FILE  *f1,*f2,*f3;

    printf("Input File Name ?\t");
    scanf("%s",data);  strcpy(out1,data);  strcpy(out2,data);
    strcat(out1,".1");  strcat(out2,".2");
    f1 = fopen(data,"r");
    f2 = fopen(out1,"w");
    f3 = fopen(out2,"w");
    i = 0;
    p = malloc(Max*sizeof(double));
    e = malloc(Max*sizeof(double));
    pr = malloc(Max*sizeof(double));
    Pr = malloc(Max*sizeof(double));
    while(!feof(f1)) {
        fscanf(f1,"%lf %lf",&pr[i],&e[i]);
        i++;
    }
    fclose(f1);
    N = i-1;
    kp = ok = 0;
    fprintf(f2,"* Iteration \t k1 \t k2\n");
    iter = 0;
```



```

while (!ok) {
    for(i=0; i<N; i++)      p[i]=log(pr[i] + kp);
    least(p,e,&logk1,&k2,N);
    k1 = exp(logk1);
    if(fabs(k1-kp) < 1E-5)  ok = 1;
    else kp = k1;
    iter++;
    fprintf(f2,"%5d\t%10.4e\t%10.3f\n",iter,k1,k2);
}
fprintf(f2,"\n\nPr = (%10.3e) + (%10.3e)exp(%10.3f*e)\n",-k1,k1,k2);
fprintf(f2,"Er = %10.3e + %10.3f*Pr\n",k1*k2,k2);
fclose(f2);
free(p);      free(e);      free(pr);      free(Pr);
printf("\tk1,k2 \t==> %s\n\te,Pr,Er\t==> %s\n\n",out1,out2);
} /* main */

```

```

void least(y,x,a0,a1,N)
double *y,*x,*a0,*a1;
int N;
{
    int i;
    double sx,sy,sx2,sxy,det;

    sx = sy = sx2 = sxy = 0;
    for(i=0; i<N; i++) {
        sx += x[i];
        sy += y[i];
        sx2 += x[i]*x[i];
        sxy += x[i]*y[i];
    }
    det = N*sx2 - sx*sx;
    *a0 = (sy*sx2 - sx*sxy)/det;
    *a1 = (N*sxy - sx*sy)/det;
}

```

2

VITA

Bang-Eop Lee

Candidate for the Degree of

Doctor of Philosophy

**Thesis: BUCKLING ANALYSIS OF STARRED ROLL DEFECTS
IN CENTER WOUND ROLLS**

Major Field: Mechanical Engineering

Biographical:

**Personal Data: Born in Taejon, Korea, the son of Mr. Seong-II Lee and
Mrs. Ji-Ja Kim.**

**Education: Graduated from the Taejon High School, Taejon, Korea,
in February, 1975;**

**Received Bachelor of Science Degree in the Department of
Mechanical Design and Production Engineering in the Seoul
National University in February, 1980;**

**Received Master of Science Degree in the Department of
Mechanical Design and Production Engineering in the Seoul
National University in February, 1982;**

**Completed the requirements for the Doctor of Philosophy degree
at Oklahoma State University in May, 1991.**

**Professional Experience: Research Associate, Web Handling
Research Center, Oklahoma State University, January 1989 to
May 1991;**

**Teaching Assistant, School of Mechanical and Aerospace
Engineering, Oklahoma State University, August 1988 to
December 1988;**

**Research Engineer at the Agency for Defense Development in
Korea, January 1982 to August 1987.**